REPORT DOCUMENTATION PAGE

Form Approved
OMB No. 0704-0188

1. AGENCY USE ONLY *(Leave blank)*

2. REPORT DATE
11 JUL 97

3. REPORT TYPE AND DATES COVERED

4. TITLE AND SUBTITLE
DIURNAL CYCLE OF TROPICAL DEEP CONVECTION EXAMINED USING HIGH SPACE AND TIME RESOLUTION SATELLITE DATA

5. FUNDING NUMBERS

6. AUTHOR(S)
TIMOTHY J. HALL

7. PERFORMING ORGANIZATION NAME(S) AND ADDRESS(ES)
COLORADO STATE UNIVERSITY
FORT COLLINS, COLORADO

8. PERFORMING ORGANIZATION REPORT NUMBER
97-085

9. SPONSORING/MONITORING AGENCY NAME(S) AND ADDRESS(ES)
DEPARTMENT OF THE AIR FORCE
AFIT/CI
2950 P STREET
WRIGHT-PATTERSON AFB OH 45433-7765

10. SPONSORING/MONITORING AGENCY REPORT NUMBER

11. SUPPLEMENTARY NOTES

12a. DISTRIBUTION AVAILABILITY STATEMENT

12b. DISTRIBUTION CODE

13. ABSTRACT *(Maximum 200 words)*

14. SUBJECT TERMS

15. NUMBER OF PAGES
110

16. PRICE CODE

17. SECURITY CLASSIFICATION OF REPORT	18. SECURITY CLASSIFICATION OF THIS PAGE	19. SECURITY CLASSIFICATION OF ABSTRACT	20. LIMITATION OF ABSTRACT

THESIS

DIURNAL CYCLE OF TROPICAL DEEP CONVECTION EXAMINED USING HIGH SPACE AND TIME RESOLUTION SATELLITE DATA

Submitted by

Timothy J. Hall

Department of Atmospheric Science

In partial fulfillment of the requirements
for the Degree of Master of Science
Colorado State University
Fort Collins, Colorado
Spring 1997

COLORADO STATE UNIVERSITY

WE HEREBY RECOMMEND THAT THE THESIS PREPARED UNDER OUR SUPERVISION BY TIMOTHY J. HALL ENTITLED DIURNAL CYCLE OF TROPICAL DEEP CONVECTION EXAMINED USING HIGH SPACE AND TIME RESOLUTION SATELLITE DATA BE ACCEPTED AS FULFILLING IN PART REQUIREMENTS FOR THE DEGREE OF MASTER OF SCIENCE.

Committee of Graduate Work

Paul W. Mielke

William M. Gray

Thomas H. Vonder Haar

Adviser

Wayne Schubert /acting Head

Department Head

ABSTRACT OF THESIS

DIURNAL CYCLE OF TROPICAL DEEP CONVECTION EXAMINED USING HIGH SPACE AND TIME RESOLUTION SATELLITE DATA

Infrared (IR) and visible (VIS) satellite data from GMS-4 with 5-km spatial and 1-hr temporal resolution was used to examine the diurnal cycle of deep convection over a sector of the tropical west Pacific warm pool (WP) bounded by 140°-180°E, 0°-20°N. Data were analyzed for 45 days of summer from 22 June 1994 - 5 August 1994 (JJA) and for 65 days of winter between 28 November 1994 - 31 January 1995 (NDJ).

The synoptic backdrop for JJA was characterized by the monsoon trough, oriented northwest to southeast through the WP. Convection was largely focused along the trough. During NDJ, convection was concentrated within 5° latitude of the intertropical convergence zone (ITCZ) which was oriented east to west near the equator. December 1994 was characterized by an active phase of the intraseasonal oscillation (ISO) while January 1995 coincided with an inactive phase.

Deep convective cloud was identified in IR imagery using brightness temperature (T_{BB}) threshold techniques. Cloud forms associated with deep convection showed two distinct diurnal modes representing deep convection ($T_{BB} \leq -60°C$) and stratiform cirrus ($-52°C \leq T_{BB} \leq -23°C$). Clouds with T_{BB} warmer than -60°C and colder than -53°C comprised a mixed deep convection and cirrus anvil regime from the satellite's perspective with a diurnal cycle reflecting both modes of variability. The diurnal variation of cloud in these regimes was consistent for all time periods and for two tropical storms which occurred in the WP during December 1994. Based on these results and on previous studies, a -65°C cloud-top T_{BB} threshold was chosen to isolate pixels containing active, deep convection. Spectral analysis of time series constructed from hourly cold cloud ($\leq -65°C$) pixel counts revealed a powerful diurnal cycle of deep convection significant at the 95% confidence level during JJA and NDJ. Composited hourly statistics of fractional areal cloud cover documented a 0500-0600 LST maximum with a 1500-1900 LST minimum of convection for both seasons. The ratio of maximum to minimum areal cold cloud coverage was greater than 2:1. A significant bi-diurnal cycle was evident in both JJA and January 1995. The bi-diurnal peak was strongest in the near-equatorial region during JJA. No semi-diurnal (spectral) peak occurred during

either season. This suggests that semi-diurnal atmospheric tides do not strongly influence convection in the WP.

Three objective analysis techniques were developed to analyze the relation of tropical cloud cluster structure to the daily spatial and temporal variation of deep convection. The first technique identified cold cloud intervals, called *line clusters*, in each image. These line clusters represented a characteristic horizontal dimension for cloud clusters of various sizes. Results showed that the diurnal cycle of convective rainfall with an early morning maximum was disproportionately dominated by the largest ~ 10% of clusters for each time period. While the number of large clusters increased only slightly throughout nocturnal hours, the area of cold cloud associated with these systems expanded dramatically. An algorithm called *threshold initiation* showed that all scales of organized, intensifying deep convection existed at all times of day and night. In addition, the early morning peak was composed primarily of building convection. Conditional recurrence probabilities of line clusters were computed at 24 and 48 hour intervals. Results for JJA and December 1994 revealed that when early morning convection occurred at any location, the same region contained convection the next morning nearly half the time. Convection was less likely at the 48 hour point. These results do not support diurnal theories based on sea surface heating, afternoon initiation of convection and nocturnal evolution of mesoscale convective systems.

Findings indicate that the diurnal cycle of deep convective cloud is driven by the internal variation of large clusters. Clusters that exist into or form during the night, grow spatially larger and more intense. Some results support direct radiative forcing of clouds and large scale clear region radiative destabalization as possible contributors to diurnal convective variability. However, all findings are consistent with the work of Gray and colleagues that emphasizes the role of day-night variations in net tropospheric cooling in clear and longwave cooling in cloudy versus clear regions as an explanation of the observed daily variation of tropical convective rainfall.

ACKNOWLEGDEMENTS

I would like to express my deepest appreciation to my advisor, Dr. Thomas H. Vonder Haar, for allowing me to pursue this research and for his dedication to the successful timely completion of this work. Also, I would like to thank my other committee members, Dr. William Gray and Dr. Paul Mielke. Dr. Gray was instrumental in my choice of research topic and made resources available to me which were invaluable in the completion of the study.

Several individuals gave selflessly of their own time to help my research efforts. John Forsythe provided endless technical support and programming advice in my efforts to process over 50 gigabytes of raw satellite data. With Don Reinke, he also helped focus my analysis techniques in the project's initial stages. I am indebted to John Sheaffer for acting as a sounding board and critic for a year's worth of great and not-so-great ideas. Our scientific and at times philosophical discussions played a key role in the research process. Finally, I would like to thank Dr. Clara Deser for providing the computer code and expert tutelage for the spectral analysis presented in chapter 6.

Most of all, I would like to thank my wife Courtney. Without her willingness to give up a career, raise our kids and follow me around the world, my graduate studies at Colorado State would not have been possible. I love her more than she will ever know. Financially, my program of study was sponsored by the Air Force through the Air Force Institute of Technology.

Research for this thesis was funded by the Center for Geosciences, Phase II at CIRA/CSU under grant #DAAH04-94-G-0420.

TABLE OF CONTENTS

TERMS AND ACRONYMS

brightness temperature	see equivalent blackbody temperature
Cb	cumulonimbus
CEM	cloud ensemble model
CNC	cloud/no cloud; type of binary image array in CHANCES database
dateline	180°E
diurnal dancing	day-to-day local spatial variation of organized deep convection whereby MCSs are disfavored to occur on two consecutive days and so tend to occur every other at any particular geographic location
equivalent blackbody temperature	the temperature a theoretical blackbody must be to register the same amount of energy at the sensor
off-equatorial region	5°-20°N
GATE	GARP (Global Atmospheric Research Program) Atlantic Tropical Experiment
GCM	general circulation model
GMS	Japanese Geostationary Meteorological Satellite, located 35,800 km above the equator at 140°E longitude
IR	infrared
ISCCP	International Satellite Cloud Climatology Project
ISO	intraseasonal oscillation; 30-60 day timescale eastward propagation of anomalous equatorial westerlies and easterlies in the lower and upper troposphere accompanied by a large-scale region of anamalously deep convection
ITCZ	intertropical convergence zone; transition between the northeast and southeast trades characterized by strong upward motion and heavy rainfall
JJA	summer portion of data set spanning 45 days from 22 June 1994 - 5 August 1994
LH	latent heat
line cluster	connected segments of cold cloudiness with $T_{BB} \leq -65^{\circ}C$ found within each line (latitude row) of the data array containing one satellite image
LST	local standard time
LW	longwave radiation; term used to describe terrestrial radiation which peaks in the infrared portion of the spectrum near 10 μm
MCS	mesoscale convective system

near-equatorial region	0^{o}-5^{o}N
NDJ	winter portion of data set spanning 65 days from 28 November 1994 - 31 January 1995
PBL	planetary boundary layer; roughly the lowest 1 km of the atmosphere
pixel	single element of digital image array
SH	sensible heat
SSM/I	Special Sensor Microwave Imager
SST	sea surface temperature
SW	shortwave radiation; term used to describe solar radiation which peaks in the visible portion of the spectrum near 0.48 μm
$\mathbf{T_{BB}}$	equivalent blackbody temperature or brightness temperature
TD	tropical depression
TOGA COARE	Tropical Ocean Global Atmosphere Coupled Ocean-Atmosphere Response Experiment
VIS	visible
WP	west Pacific warm pool sector of present study bounded by 140^{o}-180^{o}E, 0^{o}-20^{o}N

Chapter 1

Introduction

Deep convection plays a key role in global climate. In the tropical west Pacific, latent heat released in organized tropical convection drives planetary circulations such as the Walker circulation and the Madden-Julian oscillation. Changes in deep convection on various time scales are associated with dramatic latitudinal and longitudinal variations in cloud cover, precipitation and sea surface temperature (SST). For this thesis I investigated the diurnal cycle of deep convection in the tropical west Pacific warm pool.

The study of the diurnal cycle of tropical convection is "one of the most important areas of research in the history of our science" (Gray 1997, personal communication). First, diurnal changes in deep convective cloudiness affect incoming shortwave (SW) and outgoing longwave (LW) radiation and hence influence the earth radiation budget (Hendon and Woodberry 1993; Duvel 1989). Second, modelers require knowledge of the daily spatial and structural variation of convection to validate the diurnal cycle produced by general circulation models (GCMs, Randall et al. 1985; Slingo et al. 1987). Finally, the diurnal cycle encompasses a critical time scale for tropical air-sea interactions. Webster et al. (1996) describe these short time scale interactions. Because of the high SSTs and the Clausius-Clapeyron relationship, diurnal surface temperature variations can have a substantial impact on interfacial fluxes on sensible and latent heat. Rainfall and wind associated with deep convection cools SSTs and creates a well mixed fresh surface layer. Also, a key feedback between clouds and SSTs occurs on the fractional cloudiness-damping time scale of ~ 0.6 day.

Until a landmark paper by Gray and Jacobson (1977) based on island rain gauge and rawinsonde data sets, the meteorological community generally inferred only a small diurnal variation in oceanic, deep cumulus convection. Since 1977, many atmospheric scientists have studied the problem and yet the mechanism responsible for the diurnal cycle of oceanic, tropical deep convection remains a subject of much investigation and debate. Studies of the diurnal cycle have used data from many sources: rainfall measurements taken on atolls or small islands, shipboard measurements of rainfall, photographs, radar, satellite microwave measurements, and satellite IR observations.

Due to the paucity of surface-based observing sites in the tropics, various intensive field projects such as the GARP (Global Atmospheric Research Program) Atlantic Tropical Experiment (GATE) and the

Tropical Ocean Global Atmosphere Coupled Ocean-Atmosphere Response Experiment (TOGA COARE, Webster and Lukas 1992) have been undertaken to observe tropical weather. However, space-based platforms offer the only hope of adequately detailing convective properties throughout large regions of the tropics (Hendon and Woodberry 1993). Satellite data interpreted in light of insights gained from observational and modelling studies motivated by the major field projects offer the best hope of defining the driving mechanism(s) of the oceanic diurnal convective cycle. Results of previous projects have yielded no less than six theories about the driving mechanism(s) of the tropical diurnal cycle:

(1) Atmospheric Tides (AT)

(2) Day versus Night Radiation-Subsidence (DNS)

(3) Direct Radiative Cloud Forcing (RCF)

(4) Large Scale Radiative Destabilization (LRD)

(5) Boundary Layer - MCS Lifecycle (BLML)

(6) Remote Continental Effect (RC)

Tropical deep convective clouds are easily identified on IR satellite pictures (Mapes and Houze 1993). In the present study, I analyzed the temporal and structural characteristics of deep convection for a west Pacific warm pool sector spanning from approximately 140^{o}-180^{o}E and 0^{o}-20^{o}N (Fig. 1.1). This sector was extracted from the new Climatological and Historical ANalysis of Clouds for Environmental Simulations (CHANCES, Vonder Haar et al. 1995) database. CHANCES has 1-hr temporal and 5-km spatial resolution. This is the highest resolution satellite data set (to date) used to study convection for a major portion of the WP, and the only one to focus specifically on the northern hemisphere. This study was investigative. The hypothesis was that analysis of a unique high space and time resolution satellite database would provide new results to define daily structural and temporal characteristics of tropical deep convection and to evaluate various current theories about the mechanism(s) driving the diurnal cycle.

In chapter 2, I put the diurnal problem into physical and historical context. Discussion topics include the role of tropical convection in atmospheric processes, and the nature of deep convection in the west Pacific warm pool. Chapter 3 details previous work related to six theories of the mechanism(s) driving the diurnal cycle. This is the first comprehensive summary of work on the diurnal cycle since Gray and Jacobson (1977). The CHANCES satellite database used for the present study is discussed in chapter 4. Deep convective cloud was analyzed using various IR temperature thresholds. In the last half of chapter 4, thresholds used in many other tropical studies are summarized. Based on previous work, -65^{o}C was chosen as the primary threshold to identify deep convection in CHANCES IR imagery.

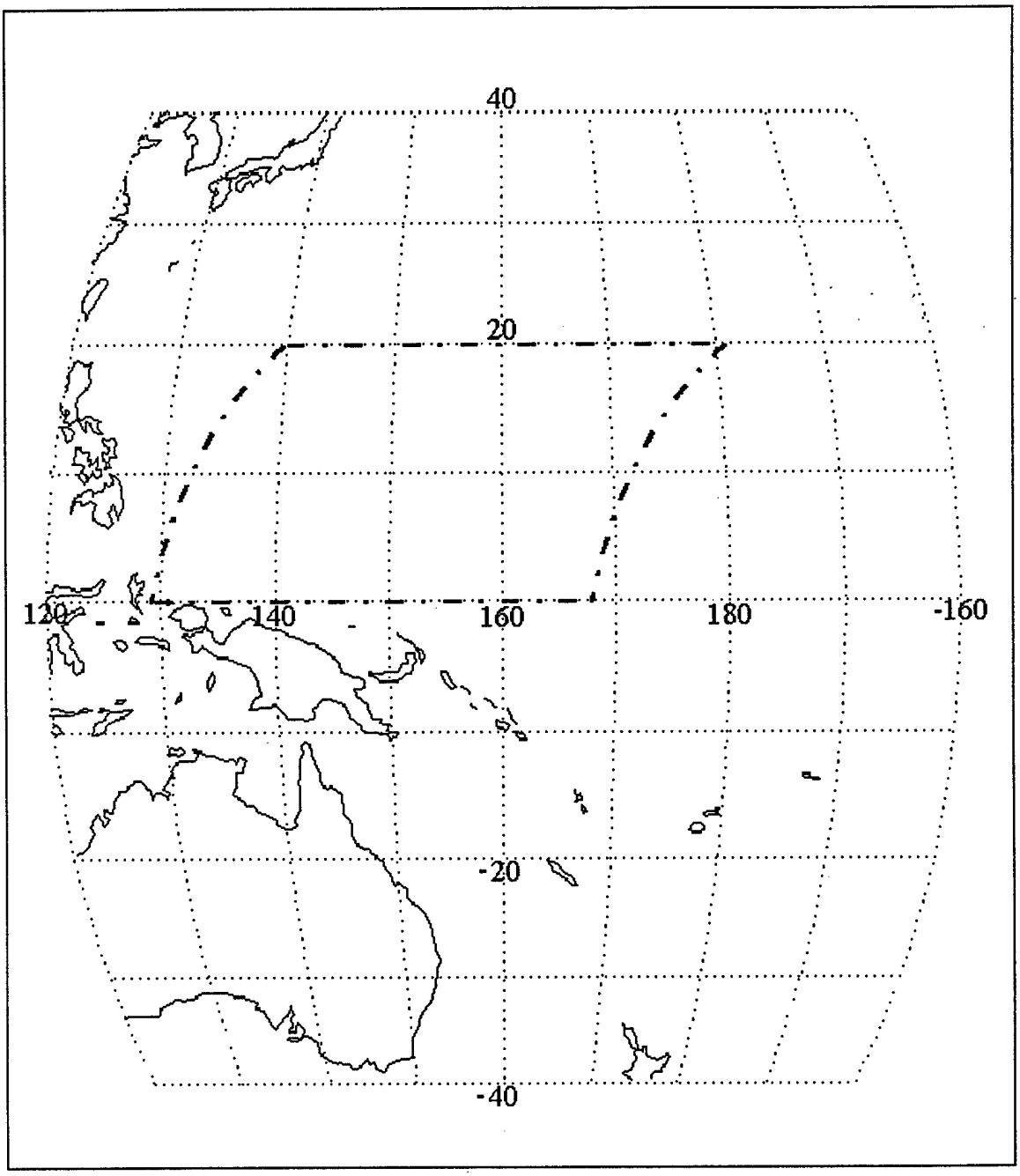

Figure 1.1 Map of west Pacific warm pool with region analyzed in this study framed by the dot-dashed line.

Chapters 5-7 contain the methods, results and discussion of original research for this thesis. Chapter 5 presents a qualitative overview of convection during summer 1994 (JJA) and winter 1994/95 (NDJ). 1994 was a weak El-Nino year. During JJA, convection was largely concentrated along the monsoon trough within the 29°C sea surface temperature isotherm. NDJ consisted of two distinct phases of the intraseasonal oscillation (ISO). A convectively active phase occurred during November 1994 through December 1994. An inactive phase occurred through January 1995. Loops of IR imagery revealed that convection on all spatial scales existed at all times of day and night in the WP with individual organized weather systems building, reaching maturity and dissipating seemingly at random. There was a tendency for systems to become spatially larger at night. These observations were quantified in results presented in chapters 6 and 7.

Chapter 6 presents a quantitative assessment of short time scale convective variability. Spectral analysis revealed a powerful diurnal cycle of deep convection for JJA and NDJ significant at the 95% confidence level. For JJA and January 1995, there was a strong suggestion of bi-diurnal variability. The strongest diurnal and bi-diurnal spectral peaks occurred in the near equatorial region in JJA. No significant spectral power was evident on the semi-diurnal time scale.

To document the phase of daily variability associated with convective cloud, fractional coverage of cloud from IR digital images was computed during each time period for every hour of the day. Consistent with many other studies, deep convective cloud peaked around 0500-0600 LST with a late afternoon to evening minimum between 1500-1900 LST during winter and summer. This same cycle occurred in both active and inactive phases of the ISO, and for two tropical storms that occurred during December 1994. For all time periods, there was a greater than 2:1 ratio of morning to evening areal coverage of convective cloud. Cloud associated with deep convection showed two distinct diurnal modes representing deep convection and stratiform cirrus regimes. The coldest regime included all clouds with cloud-top brightness temperature colder than -60°C and validated -65°C as an effective threshold to isolate deep tropical convection. The stratiform cirrus regime had a single daily maximum in the late afternoon. Convective and cirrus anvil cloud in the mixed regime peaked in the early morning in phase with deep convection and again in the afternoon. This modal phase propagation of diurnal peaks was interpreted to represent the general expansion of the tropical cloud shield following each days early morning peak of deep convection.

After quantifying the diurnal cycle, the final goal was to investigate its relation to the satellite observed morphology of convective cloud clusters (chapter 7). Several objective image analysis techniques were applied to document variability relative to cluster size. During each time period, clusters of various sizes were characterized by compiling statistics of cold cloud intervals, called *line clusters*, of

adjacent pixels colder than -65°C. An extension of this technique called *threshold initiation* separated building from dissipating convection.

Line clusters were grouped into size categories according to their intrinsic diurnal cycle expressed in terms of the morning to afternoon/evening ratio of deep convective cloud. The results revealed that the diurnal cycle during JJA and NDJ was dominated disproportionately by the largest 10% of mesoscale convective systems (MCSs) embedded within tropical cloud clusters. The diurnal cycle for all scales of convection during JJA and both active and inactive phases of the ISO in NDJ contained an early morning peak with a late afternoon to evening minimum. The threshold initiation algorithm verified that these peaks were composed primarily of deepening convection.

A similar technique to line cluster detection was used to analyze the diurnal cycle of clear regions. The results showed a substantial relative diurnal cycle in fractional cloud-free area with a late morning maximum. The diurnal cycle was dominated by clear intervals between 875-1500 km in horizontal dimension.

The final step was to look at the daily spatial variability of cloud clusters. Some previous studies indicate a preference for clusters to form in relatively clear regions and return to the same location every other day. To analyze spatial variation for JJA and NDJ, I computed 24 and 48 hour conditional recurrence probabilities of line clusters. Given deep convection associated with a large cluster on any particular morning during JJA and December 1994, convection occurred in the same geographic location the next morning nearly 50% of the time. There was a smaller recurrence of deep convection every other day in a location. The probability of convection recurring on two consecutive days in a particular location at any hour of the day was about one in three. Nearly one third of the time, convection recurred in the same location three mornings in a row.

My findings document the diurnal cycle of convective cloud for the WP sector during summer 1994 and winter 1994/95. Throughout this thesis, I present the results in detail and discuss them in relation to previous work. This study provides new evidence to enhance understanding of the mechanism driving the diurnal cycle of tropical, oceanic deep convection.

Chapter 2

Deep Convection in the West Pacific Warm Pool

Deep, tropical convective clouds around the globe are the "firebox" of the atmospheric heat engine (Simpson 1990). This engine drives the atmospheric general circulation and motivates the global hydrologic cycle. Organized deep convection in the west Pacific warm pool provides the primary fuel for the fire. In this chapter I discuss the role of deep convection in local, regional and global scale processes, reasons the deepest convection (globally) occurs in the tropics and why a disproportionate amount of this convection occurs in the west Pacific.

2.1 Role of Deep Convection in Local , Regional, and Global Scale Processes

It is well documented that the troposphere, on average, is continually cooling at a rate of about 1-1.5^{o}C day^{-1} (Cox and Griffith 1979; Dopplick 1972; London 1957; Rogers 1967; Smith 1980). Since the global mean temperature is not continually cooling, we know compensating warming occurs. In a global sense the daily cooling is balanced by latent heating (LH) from condensation (70-80%) and by surface-to-air sensible heat (SH) transfer through conduction (20-30%) (London 1952; Sellers 1965; Peixoto and Oort 1992; Webster 1994). Over the oceans, however, sensible heat transfer is negligible and latent heat released by precipitation makes up most of the vertical energy deficit. This is a particularly important at tropical latitudes where there is very little land.

The fuel for latent heating in the tropics is locked up in water vapor that evaporates from the ocean surface. The release of latent heat requires condensation, which implies upward motion. Significant upward motion in the tropics only occurs within the cores of deep cumulus clouds in organized weather systems. Therefore, deep convection is the most effective means of transporting heat from the planetary boundary layer to the free troposphere (Riehl and Malkus 1958, Riehl and Simpson 1979). Organized weather systems exist primarily as environments conducive to copious heavy precipitation, and hence latent heat release to balance vertical atmospheric energy deficits.

Webster (1994) postulates that the ultimate forcing mechanism of atmospheric motions is the pole-to-equator gradient of radiative heating of the planet. The gradient of radiant flux with more surface heating at the equator and less at the poles requires a net meridional flux of energy to the poles. Therefore, organized tropical systems must exist to release latent heat for subsequent transport to the poles. However,

at tropical latitudes net tropospheric horizontal energy divergences (~ 0.1°C day^{-1}) (Oort and Rasmusson 1971; Peixoto and Oort 1992) are much smaller than the net local tropospheric radiational cooling (~ 1°C day^{-1}). Therefore, meridional fluxes in the tropics can be largely neglected in comparison with net tropospheric radiational losses and the tropical region must closely meet its own energy budget requirements (Gray 1972). The sum total required heating from tropical precipitation drives a vigorous hydrologic cycle with more deep convection than anywhere else on the planet.

2.2 Deep Cumulus Convection - An Indirect Warming Mechanism

As stated above, LH and SH balance the troposphere's net radiational cooling of ~ 1°C day^{-1}. Cumulus clouds, however, do not directly warm the troposphere (through sensible temperature gain). In fact, they directly cool their immediate environment through the evaporation of residual liquid particles on cloud edges or droplets left behind as the cumulus dissipates (Gray 1973, Grube 1979).

So, how does tropical convection act to warm the environment? Tropical convection is organized into mesoscale convective systems (MCSs) of 100-300 km in width which are usually embedded in broad scale cloud clusters of up to 700 km width (Houze 1992; Gray 1995). Within these disturbances, latent heat released by condensation goes primarily into potential energy gains through increasing the temperature of rising parcels relative to the environment (Williams and Gray 1973, Fingerhut 1978). These buoyant parcels continue to rise to an equilibrium level where they mix into the environment.

As a whole, this process takes mass at low and middle levels and transports it to high altitudes. The atmosphere responds dynamically through compensating dry adiabatic sinking (Lopez 1973; Webster 1994). This compensating sinking and warming of air occurs on the mesoscale in relatively cloud-free areas around MCSs and (Foltz and Gray 1979; Gray 1976; Lopez 1973), and on a synoptic scale (Dewart 1978; Foltz and Gray 1979; Hendon and Woodberry 1993; McBride and Gray 1980; Deser 1994,1997) between clear zones and large scale disturbed regions such as the ITCZ. From a large scale point of view, the net effect of this entire convective feedback process is a net heating of the environment (Gray 1972; Yanai et al. 1973). Warming created through forced subsidence near convection and gentle subsidence far removed from convection balances large scale radiational cooling. Subsidence variation in the subtropical highs and expansive clear zones along the equator (Deser 1994, 1997) are evidence of this convective feedback and the atmosphere's efforts to keep the troposphere in radiative balance.

2.3 The West Pacific Warm Pool

The intertropical convergence zone (ITCZ) lies in the equatorial trough where the trade winds converge to form a zone of increased mean convection, cloudiness, and precipitation (Waliser and Gautier

1993). The warm pools of the Pacific and Indian oceans are characterized by anomalously high SSTs in excess of 27°C (Fig. 2.1) and the most intense, widespread convection on the planet (Webster and Lukas 1992). This section considers the existence of the warm pools, the relation of high SSTs to organized disturbances and the significance of the warm pools to the general circulation.

Webster (1994) attributes the exceptionally warm water in the eastern Indian and western Pacific oceans to the existence and distribution of the continents. If there were no tropical continents, a general equatorial SST maximum would occur with no preferred longitudinal bias. Furthermore, the lack of land asymmetry between the hemispheres would prevent the monsoon circulation. But, with the existing distribution of continents, general wind circulations are more complicated.

For example, the prevailing flow from the southern hemisphere to south Asia during the boreal summer is strongly biased toward the western Indian Ocean. These stronger winds cool the western Indian ocean by mixing and evaporation. Relative to the western half of the ocean, the eastern Indian Ocean stays warm and becomes the focus for more convection. Islands that comprise the Indonesian archipelago enhance heating (LH and SH) of the eastern Indian Ocean. The combined effect of wind and island heating creates a low-pressure regime that produces low-level confluence from both the Indian and Pacific oceans. In the western Pacific, decreased winds reduce equatorial upwelling and surface cooling leaving the region relatively undisturbed. In the eastern Pacific, however, flow toward the western Pacific creates cold upwelling through a comparatively shallow surface layer, leading to a reduction of the eastern basin SST. So, the western Pacific is relatively warm and becomes the primary center of deep convection.

Based on many observations, Riehl (1954) noted that tropical convection tends to occur within the 28°C SST isotherm. Fifty years later the basic processes responsible for this association are still a subject of active research. The predominant theory contends that 28°C is a threshold value at which the stability of the tropical troposphere is sufficiently reduced to allow the onset of large-scale moist convection (Lau and Chan 1988; Waliser and Graham 1993). Results from Zhang (1993) and Fu et al. (1990), however, contain no evidence of a *critical SST*. Gray (1995) states that generally increased instability combined with greater amounts of mid-level moisture left over from previous convection make high SST regimes more conducive to thunderstorms. Greater middle-level humidity lessens the inhibiting effects of entrainment on convection (Gray et al. 1975). According to Gray, since organized weather systems and rainfall is limited to about 10% of the tropics at any one time, these favorable high SST regimes are the focus for deep convection while the remaining 90% of the area is subsident and dry. Another popular theory considers atmospheric moistening in regions of higher SST implied by the Clausius-Clapeyron relationship (Webster 1994; Webster et al. 1996).

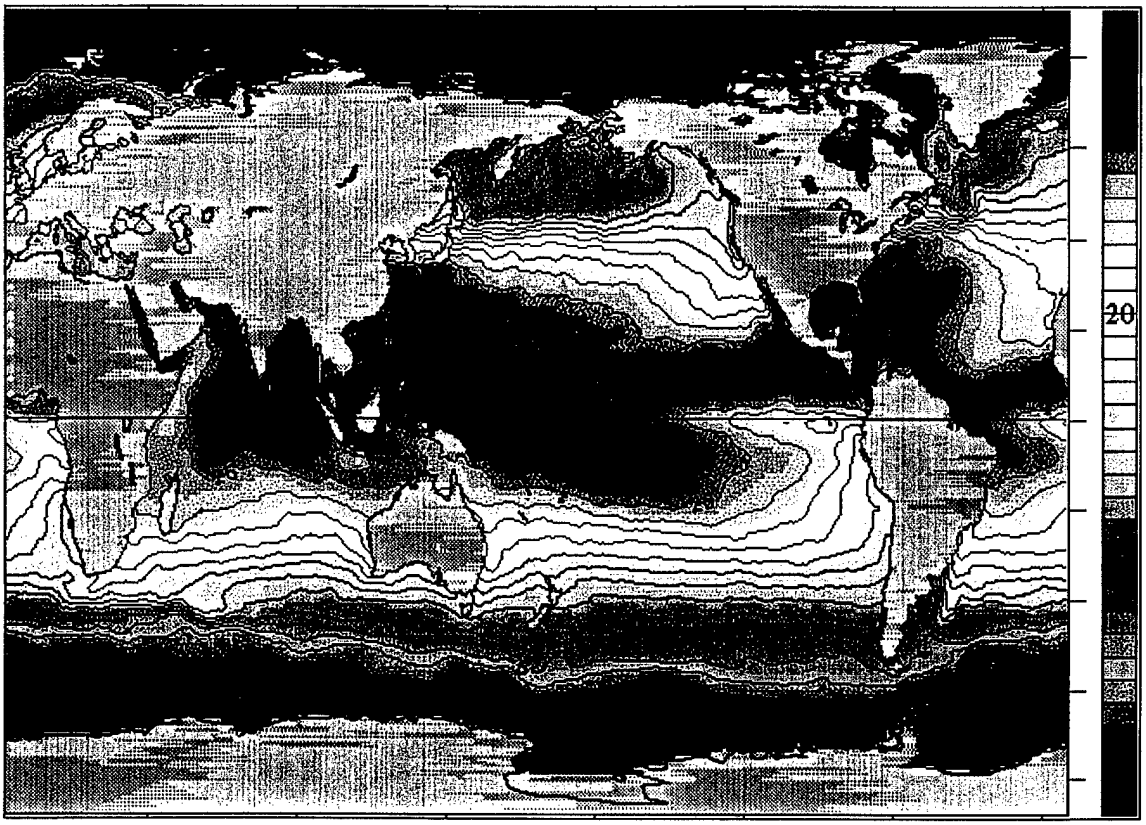

Figure 2.1: July 1994 average satellite derived global SSTs. The approximate west Pacific warm pool region of the present study is indicated by the rectagle near the center of the figure. The equator is indicated by the solid line running horizontally through the middle.

Webster (1994) hypothesizes that the correlation of convection to the warmest SSTs "comes directly from Clausius-Clapeyron moist thermodynamics and the physics of forced dynamic response." Figure 2.2 is the Clausius-Clapeyron saturation vapor pressure curve. The exponential dependence of vapor pressure on temperature makes the absolute humidity very sensitive to small SST changes, especially at temperatures above 23°C. For example, at 28°C an increase of 1°C yields an increase of ~ 6% in vapor pressure (Reid and Gage 1981). Thus in high SST regimes, a favorable heating profile forms which facilitates very deep convection. In response, subsidence zones then form in regions of slightly cooler SST, suppressing convective growth.

A third mechanism theorized to explain the occurrence of deep convection in the regions of highest SST is increased moisture convergence. Lindzen and Nigam (1987) used a model to confirm that pressure gradients produced by the steep SST gradients surrounding the warm pool could enhance moisture convergence in the ITCZ. Increased moisture convergence would facilitate deep convection. Deser and Wallace (1990), however, observed that deep convection in the east Pacific ITCZ is not accompanied by a net increase in surface wind convergence. They suggest that the affect of high SST is to increase the depth of the atmospheric boundary layer and hence increase the total moist static energy. So, the debate over why the highest SSTs and deep convection are juxtaposed rages on. There is no debate, however, over the importance of the warm pool to large scale atmospheric circulations.

The warm pool plays a significant role in setting the atmospheric global-heating gradient and so plays an important role in the general circulation of the atmosphere (Webster and Lukas 1992). The vigorous convection with coincident release of latent heat comprises the ascending branch of the Walker circulation. The Walker circulation is the major tropical ascent occurring over the Pacific-Indian ocean warm pool. The Walker circulation reinforces the meridional Hadley cell. In addition, latent heat released by deep convection is important in the structure and evolution of Kelvin and Rossby waves that propagate the effects of tropical systems into the extratropics, creating teleconnections extending to all portions of the planet (Simpson 1992). Moist processes in the warm pool region also influence the strength of the annual monsoon which has significant effects on major population centers in Asia.

2.4 Organization of Warm Pool Weather Systems

In the tropics, the strongest convective regions are organized by mesoscale processes into cloud clusters. Given the conditionally unstable lapse rates that typify the global tropics, cumulus clouds in these clusters require fairly large mechanically forced low-level convergence (~ 5×10^{-3} s^{-1}) to overcome the low-level gravitational stability of the tropical atmosphere, reach the level of free convection (LFC) and, conditions permitting, develop into intense thunderstorms (Lopez 1973; Matsumoto 1967; Zisper and

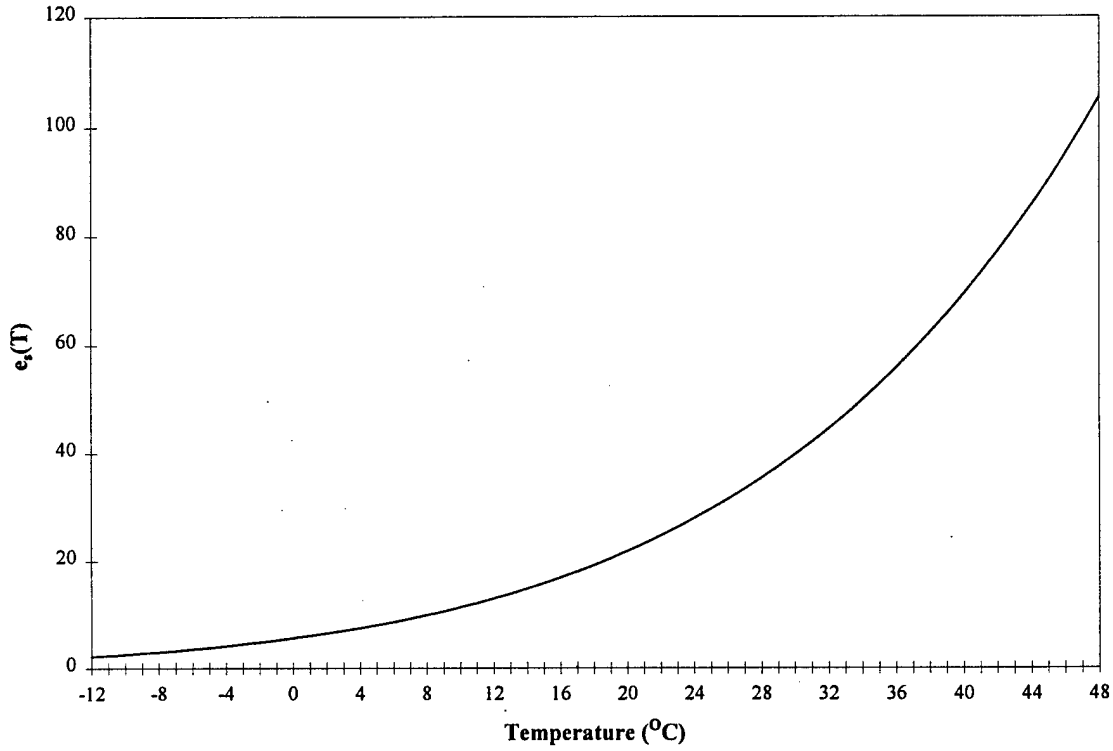

Figure 2.2: Clausius-Clapeyron saturation vapor pressure curve.

Gautier 1978). This required initial convergence is three orders of magnitude greater than typical cluster scale convergence of 10^{-6} s^{-1} (McBride and Gray 1980). Intense, localized low-level convergence can only be sustained by a very large amount of *return flow* mass subsidence into the sub-cloud layer in the downdraft air from cumulus cells (Lopez 1973; Purdom 1976). In this way, intense, widespread cumulonimbus (Cb) activity occurs primarily within organized mesoscale weather systems.

Cloud clusters range in size up to ~ 700 km in diameter. More intense MCSs of up to ~ 250 km in diameter are usually embedded within these clusters. These widespread cloud clusters account for most of the total tropical rainfall (Gray 1973; Hartmann et al. 1984) and typically form along the monsoon trough or in association with the ITCZ (Frank 1969; Ruprecht and Gray 1976; Simpson 1992). Frank (1969) and Martin and Suomi (1972) first defined tropical cloud clusters from satellite data. At about the same time, Williams and Gray (1973) performed an in depth statistical analysis of satellite observed trade wind clusters using a combination of imagery and composite upper-air soundings.

In VIS or IR satellite imagery, a tropical cluster appears as a broad continuous cloud shield (Fig. 2.3). A cloud cluster can typically be tracked in satellite imagery as a coherent entity for about 18-24 hours (Martin and Schreiner 1981; Houze 1989; Mapes and Houze 1993). Mesoscale convective systems within clusters last from 6-12 hours. In special situations, great expanses of convection called *superclusters* (Nakazawa 1988; Mapes and Houze 1993) persist for two days to a week.

Machado and Rossow (1992), Mapes and Houze (1993), Chen et al. (1996) and Chen and Houze (1997) defined a cloud cluster as a region of cold cloud tops surrounded by a single closed contour of a threshold IR brightness temperature in a satellite image. This allowed them to apply objective techniques to identify and track clusters through time. The number distribution of sizes of the cloud shields determined this way in the tropics tends to be lognormal (Houze 1992), which means that the logarithm of the cloud-top size is normally distributed. So, cloud clusters span a wide range of sizes from small single Cb clouds to rare huge clusters with multiple embedded MCSs. Machado and Rossow (1992) noted that cluster frequency decreases as the inverse square of the radius of the disturbance indicating that, in a statistical sense, the warm pools are covered by approximately the same total area of cold cloud at any particular time, irrespective of size.

2.5 Initiation and Maintenance of Mesoscale Tropical Convection

As described above, thunderstorms in the tropics are largely organized into mesoscale convective systems (> 100 km diameter, Houze 1992). The mesoscale processes that drive convection to this level of organization, however, are not satisfactorily understood or modeled (Simpson 1992). Gray (1995) discusses four physically distinct types of convergence forcing for the initiation and maintenance of

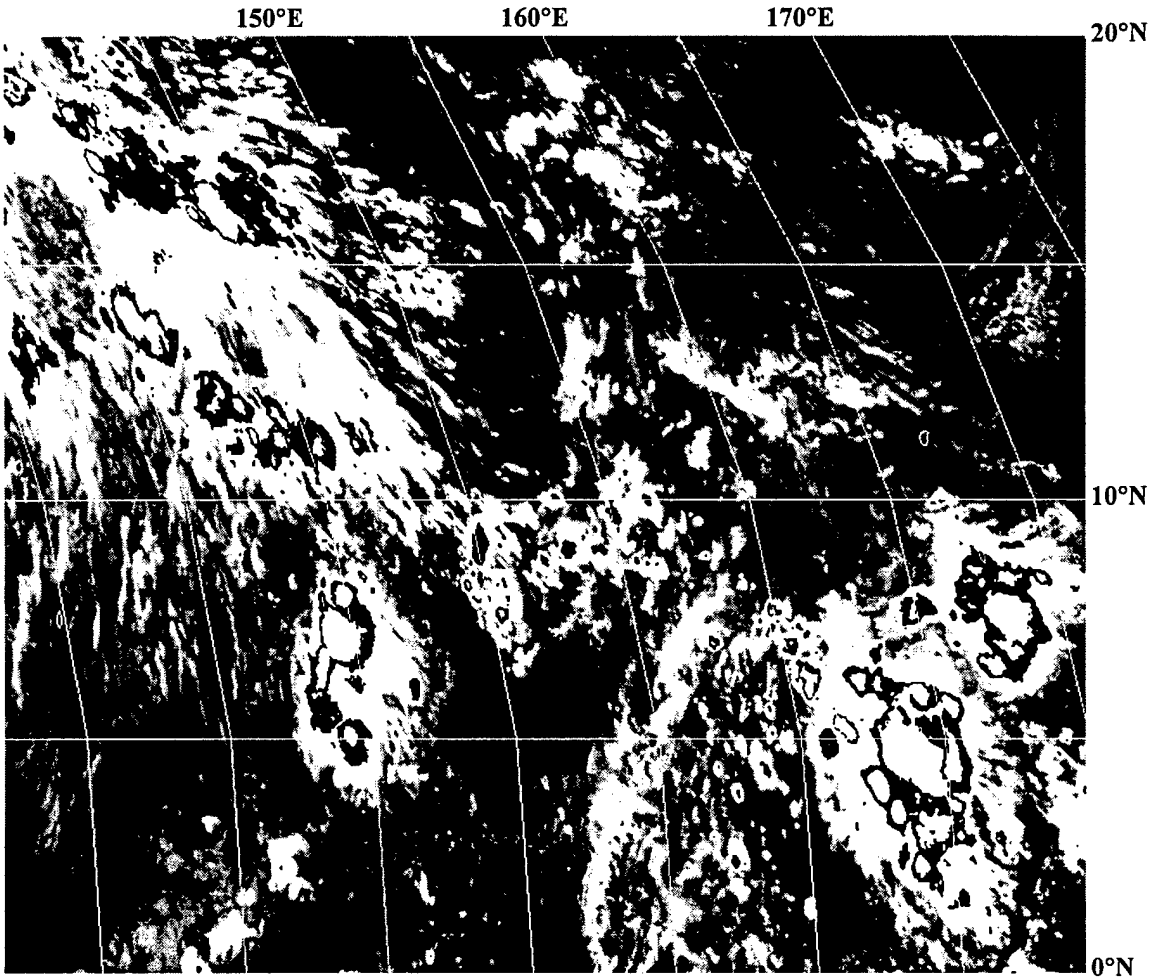

Figure 2.3: GMS-4 IR image derived from CHANCES database for 3 July 1994 valid at 2000 UTC for WP sector of the present study. Cloud-tops with $T_{BB} \leq -65^{o}C$ are enhanced to appear bright white. Cloud tops with T_{BB} between $-65^{o}C$ and $-53^{o}C$ are black. Clouds with T_{BB} between $-53^{o}C$ and $-15^{o}C$ are white. Clouds warmer then $-15^{o}C$ fade gradually from white to black.

mesoscale tropical convection over the oceans. As mentioned in section 2.4, conditionally unstable lapse rates allow organized Cb convection to develop where low-level mass convergence of $\sim 5 \times 10^{-3}$ s^{-1} forces air parcels upward to their level of free convection. Four mechanisms that may provide forcing in the tropics are:

(1) Externally Forced Convergence (EFC)

(2) Frictionally Forced Convergence (FFC)

(3) Radiationally Forced Convergence (RFC)

(4) Internally Forced Convergence (IFC)

Gray suggests that these four forcing mechanisms might be combined into a single equation:

$$\text{(Net Deep Convection Forcing)} = \text{EFC} + \text{FFC} + \text{RFC} + \text{IFC} \qquad (2.1)$$

EFC is wind convergence resulting from forcing processes external to a system. These forces typically result from traveling packets of imbalanced synoptic and mesoscale wind surges that generate deep layer mass convergence. In the current study, the most likely EFC processes at work were surges in the trade winds, southwest monsoon flow or cold front penetration into the tropics during winter. FFC, on the other hand, results from frictional drag at the surface maintaining itself as an Ekman boundary layer (~ 1 km deep) (Holton 1992). Frictional convergence is proportional to the relative vorticity and can extend the depth of the frictional layer to a much higher level. RFC is low-level convergence of mass into cloud areas made available from clear and scattered cloud areas due to net radiation induced subsidence in cloud-free zones. EFC, FFC, and RFC operate continuously in the atmosphere. IFC, however, is a rare, unstable and self-sustaining convergence initiated in areas of extreme convection. In these areas, convection leads to a decrease in pressure at low-levels and draws in ambient air as a result of enhancement of the inward directed pressure gradient.

Conclusion

The fundamental cause of abundant deep convection in the tropics is the need to balance daily net tropospheric LW cooling of about $1^{o}C\ day^{-1}$. Also, the tropics must provide additional heat ($\sim 0.1^{o}C\ day^{-1}$) for transport to the poles. In meeting these vertical and horizontal energy requirements, an immense amount of latent heat is released that drives the general circulation and is associated with a vigorous hydrologic cycle that influences extratropical weather. In this chapter I discussed cumulus as an indirect

heating mechanism of the troposphere, the relation of convection to high SST, the structure and organization of weather systems in the WP and physical mechanisms that initiate and maintain tropical convection. In the next chapter I will build upon the concepts presented above as I discuss the diurnal variation of tropical deep convection.

Chapter 3

Diurnal Variation of Tropical Convection; Previous Studies and Theorized Mechanisms

Tropical convection varies on many time scales. For example, Janowiak and Arkin (1991) and Duvel (1989) document interannual variations whereas Kidder and Vonder Haar (1977) and Kondragunta and Gruber (1996) analyze seasonal variations. Falvey (1992) and Hendon and Liebmann (1994) discuss the thirty to sixty day cycle of convection driven by the Madden-Julian oscillation (Madden and Julian 1972). On shorter times scales Chen et al. (1996), Chen and Houze (1997), Takayabu et al. (1996) and Gray and Sheaffer (1996) have theorized about a possible bi-diurnal or quasi-2-day cycle of deep convection. Of all modes of variability, perhaps the most fundamental is the diurnal cycle. Quantifying and understanding the diurnal cycle is essential to completely understand the role of tropical convection in climate (Hendon and Woodberry 1993).

Over the years, many scientists have inferred a small diurnal cycle of oceanic precipitation due to observation of a lack of significant daily change in low-level tropospheric lapse-rate stability. The paucity of observations over the vast oceans has exacerbated this misunderstanding. Observations from field projects and satellite data over the past 25 years, however, document a significant diurnal variation in deep convection. In many regions, oceanic rainfall is characterized by a late afternoon minimum with an early to mid-morning maximum (Janowiak et al. 1994). Though not widely accepted, this has been known or suspected since the turn of the century (Hann 1901).

More recent papers date to the 1950s. Ramage (1952) documented an early morning maximum over east China, Korea, and Japan and surmised that variations in forcing related to the monsoon flow account for the diurnal cycle over these land areas as well as the nearby open sea. Other studies by Finkelstein (1964), Garstang (1958), Holland (1970), Holle (1968), Inchauspe' (1970), Kraus (1963) and Lavoie (1963) yielded further evidence of a significant oceanic diurnal cycle. In late 1970s the research community at large was finally stimulated into action to study the diurnal cycle of deep tropical convection following a landmark paper published by Gray and Jacobson (1977). Gray and Jacobson used two years of upper air rawinsonde data from twelve Pacific islands combined with twelve years (1961-1973) of hourly precipitation totals from eight of these same stations. Their results documented twice as much rainfall from cloud clusters in the morning (0700-1200 LST) than in the evening (1900-2400 LST). These findings sparked great interest in the diurnal cycle and many papers on the subject have since been published.

Observational studies of the diurnal cycle have utilized data from many sources: from rainfall measurements taken on atolls or small islands, assumed to be representative of the open sea (Finkelstein 1964; Gray and Jacobson 1977; Inchauspe' 1970; Lavoie 1963); from shipboard measurements of rainfall (Garstang 1958; Gray and Jacobson 1977; Kraus 1963; McGarry and Reed 1978; Takeuchi and Nagatani 1974); from lightning discharges (Takeuchi and Nagatani 1974); from photographs (Holle 1968); from radar (Albright et al. 1981; Holle 1968; Rickenbach and Rutledge 1996; Sui et al. 1997); from satellite observations of outgoing longwave radiation (Gruber 1976; Hartmann and Recker 1986; McGarry and Reed 1978; Reed and Jaffe 1981; Riehl and Miller 1978; Schmetz and Liu 1988; Short and Wallace 1980; Wexler 1983); from estimates of rainfall based on satellite IR measurements (Augustine 1984; Janowiak and Arkin 1991; Shin et al. 1990); from estimates of rainfall based on satellite microwave measurements (Chang et al. 1995; Dorman and Bourke 1979; Kidder and Vonder Haar 1977; Nelkin et al. 1996; Sharma et al. 1991); and from satellite IR measurements using various threshold techniques to identify convective cloud (Albright et al. 1985; Browner et al. 1977; Chen et al. 1996; Chen and Houze 1997; Fu et al. 1990; Gray and Sheaffer 1995; Hendon and Woodberry 1993; Janowiak et al. 1994; Lajoie and Butterworth 1984; Mapes and Houze 1993; McGarry and Reed 1978; Murakami 1983; Mesner and Arkin 1987; Steranka et al. 1984; Weickmann et al. 1977; Zehr 1987).

Derived from these observational as well as various modelling studies are no less than six theories about the driving mechanism(s) of day-to-day time scale tropical convective variability. These include the following:

(1) Atmospheric Tides (AT)
(2) Day versus Night Radiation-Subsidence (DNS)
(3) Direct Radiative Cloud Forcing (RCF)
(4) Large Scale Radiative Destabilization (LRD)
(5) Boundary Layer - MCS Lifecycle (BLML)
(6) Remote Continental Effect (RC)

Throughout the rest of this chapter, I discuss these six theories.

3.1 Atmospheric Tides (AT)

A common physical explanation of the diurnal morning rainfall maximum found in many regions of the tropics links oceanic precipitation to the semi-diurnal pressure wave or S_2 oscillation (Brier and Simpson 1969; Malkus 1964). In more recent papers, Augustine (1984), Steranka et al. (1984), Nelkin et

al. (1996), Shin et al. (1990), Xu and Randall (1995) and Rickenbach and Rutledge (1996) all cite S_2 oscillations or atmospheric tides as a possible contributor to the diurnal cycle. The semi-diurnal pressure wave is driven by global scale differential solar heating.

Brier and Simpson (1969) provide a physical explanation of the semi-diurnal pressure wave. During each day, two successive patterns of divergence and convergence are caused by the differential solar heating in the stratosphere. The sun heats only one side of the planet at a time. These divergence patterns constitute a solar tide with pressure maximums near 1000 and 2200 LST with minima around 0400 and 1600 LST. Associated pressure rises at about 0700 and 1900 LST are thought to enhance convection through increased mass convergence, while pressure falls and divergence near 0100 and 1300 LST inhibit convection. Since the late 1970s, various authors have criticized the idea of the atmospheric tides as a driver of the tropical diurnal cycle. Their arguments are as follows:

> (1) Only one maximum and one minimum of deep cumulus convection is observed in the absence of a heat island effect. Specifically, a rainfall minimum occurs at 1900 LST, the time when a maximum is predicted by tidal theory. In addition, convection is often increasing at 0100 LST when tidal theory specifies a minimum. (Gray and Jacobson 1977)
>
> (2) The magnitude of divergence created by the S_2 tides is $\sim 10^{-7}$ s^{-1}. This is much less than the divergence differences documented by Gray and Jacobson (1977) and McBride and Gray (1980).
>
> (3) Convergence of moisture by the atmospheric tide cannot directly account for the observed oscillation in rainfall (Lindzen 1978).
>
> (4) The diurnal component of precipitation variation is generally much larger than the semi-diurnal component whereas in theory the diurnal component of tidal divergence (or vertical motion) variation is much smaller than the semi-diurnal component (Albright 1985).
>
> (5) Even if it were proven that tidal moisture flux convergences are strong enough to balance diurnal or semi-diurnal fluctuations in precipitation, it would not necessarily follow that the fluctuations of the precipitation rate are caused by the tides (Randall et al. 1991).

Foltz and Gray (1979) discuss the possible influence of an S_1 solar tide on tropical convection. They hypothesize that solar warming of the sunlit portion of the atmosphere in comparison with the sun-free portion of the planet produces a hemispheric tidal circulation with increased upper-level divergence in the sun-free hemisphere. Foltz and Gray postulate that this divergence could act to enhance early morning subsidence over broad continental size areas. Enhanced subsidence would lead to increased low-level convergence, and hence more intense convection. The possible effects of these S_1 tides on the diurnal cycle of convection were not directly analyzed in the present study.

In the present study, I attempted to detect any semi-diurnal variations in deep convection through spectral analysis of time series of deep convection. Results yielded observational evidence that semi-diurnal atmospheric tides have no discernible influence on tropical convection.

3.2 Day vs. Night Radiation-Subsidence (DNS)

Ruprecht and Gray (1976) first proposed the DNS mechanism in a study on cloud clusters based on observations from island rain gauges and composited soundings. They noted a *striking* diurnal rainfall variation with twice as much rainfall near 1000 LST than around 2200 LST. They also noted that 1000 LST surface-to-400 mb convergence and upper-tropospheric divergence is twice as large than at 2200 LST. These differences were interpreted to be directly related to the diurnal variation in the net tropospheric radiational cooling and the resulting changes in the clear region sinking between the cloud clusters. If convection is to balance radiational cooling, as stated in chapter 2, then it follows that there must be a variation due to day versus night net cooling. This cluster scale theory was explored in detail by Gray and Jacobson (1977). These papers, combined with subsequent studies by Dewart (1978), Foltz and Gray (1979), Grube (1979) and McBride and Gray (1980) describe a complete theory of the DNS mechanism of the diurnal cycle of tropical convection.

As discussed in chapter 2, the troposphere continually cools at a rate of about $1^{o}C\ day^{-1}$. This cooling is balanced, in a global sense, by a combination of LH and SH and primarily LH over the oceans. Large quantities of latent heat are released in the Cb activity of organized weather systems. In a cumulus cell, latent heating does not cause direct environmental sensible heating, but rather heats rising parcels, making them more buoyant (Fingerhut 1978; Grube 1979; Williams and Gray 1973). These parcels can then ascend to high altitudes where they become neutrally buoyant and mix into the environment. As this high level mass subsides in clear regions away from the active cloud clusters, adiabatic warming directly heats the environment. The amount of isothermal subsidence warming required to balance radiative cooling can be characterized as a required warming to accommodate the vertical energy balance. Foltz and Gray (1979) address an important question about this required warming; "Does it proceed at the same rate through the course of an entire day or does it vary in-phase or out-of-phase with the net radiative cooling?"

To answer this question, they combined data from composite soundings with heating rates calculated using a radiative transfer model. Their results reveal a "maximum required tropical tropospheric warming" of $1^{o}C\ day^{-1}$ near 0600 LST with a minimum around 1500 LST. Conversely, Yanai (1973) and Reynolds et al. (1975) show that heating of the atmosphere during the daylight hours by absorption of solar radiation is large enough to reduce the amount of convective activity necessary to balance SH and LH. These results imply a maximum amount of required subsidence in the early morning with a minimum in the early afternoon. Gray and Jacobson (1977) and McBride and Gray (1980) document vertical motion cycles over the Atlantic and Pacific tropics with a morning maximum of downward motion and an afternoon minimum. Mesoscale day vs.night differential heating between cloudy and clear regions can

enhance the diabatic heating gradient and influence vertical motion (Albrecht and Cox 1975, Fingerhut 1978). So, how does diurnally varying subsidence relate to the diurnal cycle of convection?

This question was addressed by Dewart (1978), Grube (1979), Gray and Jacobson (1977) and McBride and Gray (1980). Their results describe the DNS in terms of two related radiation induced subsidence effects which are superposed causing a significant diurnal cycle in deep convection:

(1) Clear area diurnal subsidence variation driven by day versus night differences in the rate of net tropospheric radiative cooling (McBride and Gray 1980).

(2) Cloudy-clear differential heating/cooling

(a) Synoptic scale ITCZ-subtropical (Hadley Cell) clear vs cloudy radiative-convective heating differences (Dewart 1978; McBride and Gray 1980).

(b) Cluster scale diurnal modulation driven by cluster vs clear area radiative-convective heating differences (Gray and Jacobson 1977; Ruprecht and Gray 1976).

The first DNS effect (Fig. 3.1) is a consequence of day versus night differences in clear area radiative cooling. As stated above, the atmosphere surrounding an organized tropical disturbance accommodates increased radiational cooling at night by greater subsidence. This extra subsidence leads to increased low-level mass convergence, and hence moisture convergence into the adjacent disturbed regions. Enhanced moisture convergence encourages increased convection. During the day atmospheric absorption of incoming SW counteracts LW cooling, hence clear region subsidence rates diminish and cloud region low-level convergence is reduced. This occurs on the local cluster scale (Gray and Jacobson 1977) up to the synoptic ITCZ (active) versus subtropical high or equatorial (suppressed) clear region scale (Deser 1994, 1997; Dewart 1978; McBride and Gray 1980; Hendon and Woodberry 1993). On the synoptic scale, increased nocturnal subsidence in subtropical and equatorial clear zones leads to increased convergence in the ITCZ from two opposing directions. Results presented by Deser and Smith (1997) show that divergence along the clear zones of the equator increases to an early morning maximum each day. The phase and magnitude of this increase implies an early morning increase in ITCZ low-level convergence of 50%. An added feedback is that LW cooling in these clear zones can also increase throughout the night due to drying from increased adiabatic sinking (Smith 1980).

Superposed on the effects of daily varying clear region subsidence, is the additional influence of cloudy-clear differential heating/cooling. Figure 3.2 depicts the DNS on the ITCZ clear versus cloudy radiative forcing scale. In the WP, the ITCZ is generally oriented northwest to southeast. A majority of all tropical cloud clusters occur in the ITCZ as stated in chapter 2. Convergence in the northern hemisphere west Pacific ITCZ occurs along the monsoon trough between the monsoon westerlies and easterly trades. Dewart (1978) documented and explained a large single cycle divergence oscillation in the Atlantic between the ITCZ and surrounding clear regions from GATE data. The same oscillation occurs in the WP

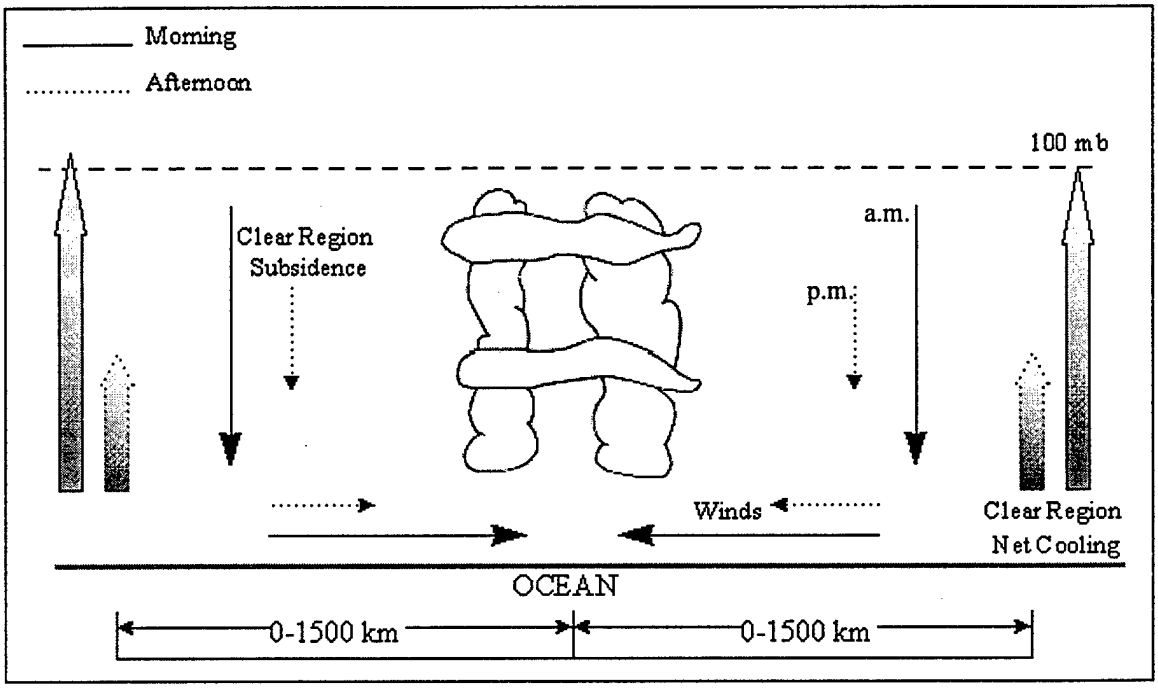

Figure 3.1: (After McBride and Gray 1978, Fig. 10) Idealized illustration of DNS driven by day versus night differences in clear area net radiative cooling. Scale on the bottom implies that the mechanism acts on local cluster scale up to synoptic scale. Solid lines represent morning wind circulation. Dotted lines represent comparative strength of the afternoon/evening circulation.

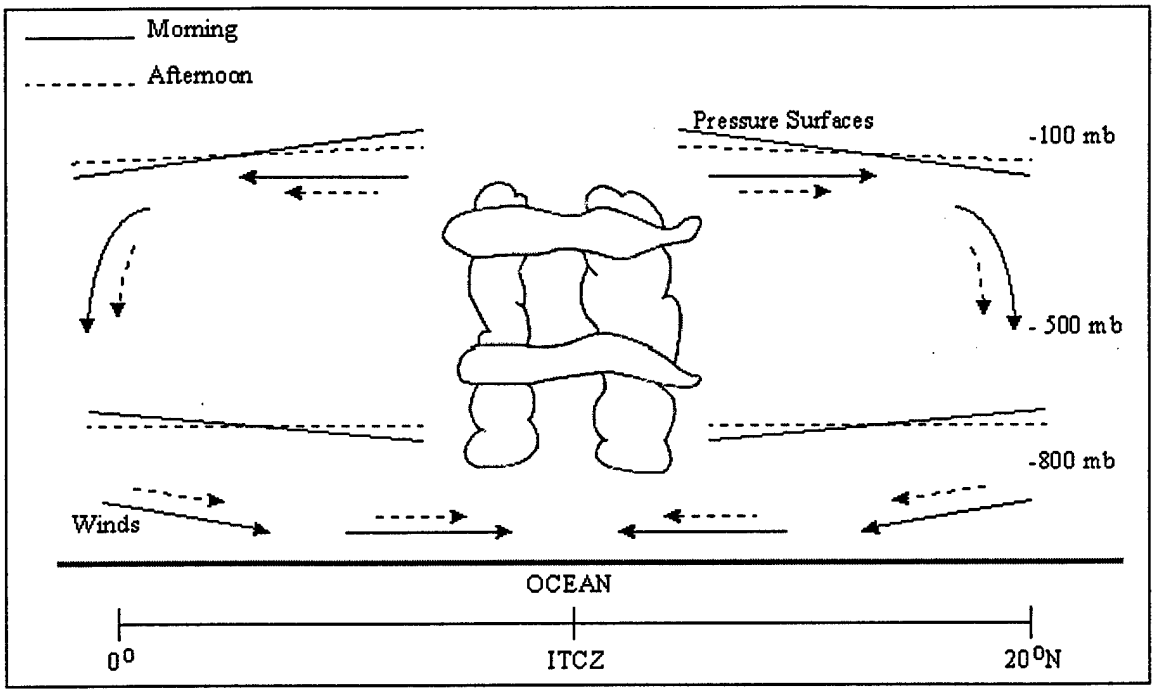

Figure 3.2: (After Dewart 1978, Fig. 21) Idealized model of the diurnal variation of the ITCZ mass circulation with the hypothesized slope of the pressure surfaces and resulting wind circulation. The solid line represents early morning pressure surfaces and winds, and dashed lines the late afternoon.

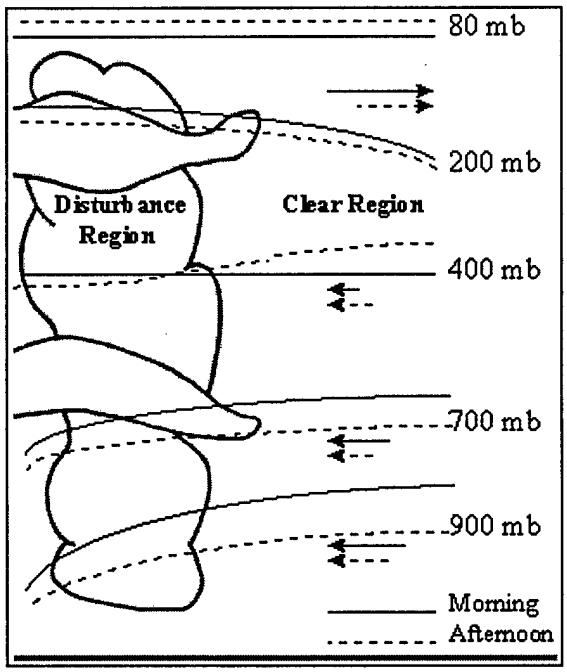

Figure 3.3: (After Gray and Jacobson 1977, Fig. 14) DNS cluster scale clear-cloud differential radiation mechanism. Idealized slope of the disturbance to surrounding clear region pressure surfaces during the day (dashed curve) and at night (solid curve). Also shown are the corresponding down-the-pressure gradient radial wind patterns which are established.

(McBride and Gray 1980). Large scale gradients of radiative and convective heating between the convectively active ITCZ region and the surrounding convectively suppressed regions (Webster and Stevens 1980) may contribute to the convergence. Regardless, these diurnal differences cause a nocturnal enhancement of horizontal pressure gradients which enhances morning and diminishes late afternoon low-level mass convergence into and out of the ITCZ.

Gray and Jacobson (1977) describe an analogous cloudy-clear differential heating/cooling DNS process that occurs on a local cluster scale (Fig. 3.3). They postulate that the vertical convergence profile in a cloud cluster can be modified by diurnal differences in the radiation-condensation heating profiles between thick cirrus shield of the cluster and the immediately surrounding clear area. The stratiform cirrus shield of a cloud cluster is largely opaque to IR radiation. Hence, LW emission from layers below the cirrus do not experience radiative cooling (Albrecht and Cox 1975). The shield radiatively cools more at night and less during the day than the surrounding clear regions. By contrast, cloud-free areas radiatively cool through LW loss at a much higher rate than areas at the same level within the cluster. During the day SW absorption increases the temperature throughout the troposphere, while SW radiation in the disturbance is almost completely absorbed within the upper cloud decks. The end result is that very little diurnal change occurs in the heating profile of the cluster while the surrounding clear regions lose about twice as much energy at night as they do during the day. Energy loss in the clear regions is immediately and continuously balanced by subsidence warming.

The cluster scale horizontal radiational differences described above induce day-night differences in vertical motion. In particular, middle level convergence (and hence upper tropospheric rising motion) is enhanced within clusters during the day and reduced at night. In the lower levels, daytime solar warming of the clear regions leads to a reduction of the clear-cluster pressure gradient and consequent reduction of mass inflow as compared to the inflow at night. Evidence for differential heating/cooling gradients between cluster and clear regions have been documented by Cox and Griffith (1979), Griffith and Cox (1977) and Loranger et al. (1978). A recent modelling study by Guan et al. (1996) has documented an additional radiational forcing that could act to enhance this cluster scale vertical circulation. In their model, cloud side cooling (which could vary diurnally) makes a significant contribution to low-level convergence.

Most observational studies sight the DNS as one possible driver of the diurnal cycle of organized convection (eg; Ackerman and Cox 1981; Anthes 1982; Cox and Griffith 1979; Hendon and Woodberry 1993; Riehl and Miller 1978; Zehr 1987; Gray and Sheaffer 1995; Rickenbach and Rutledge 1996). For example, Hendon and Woodberry (1993) state that the diurnal signal originates near the equator and moves poleward over the course of three to six hours. They suggest this is triggered by DNS with enhanced

nocturnal cooling along the cloud-free equator relative to the cloud covered ITCZ. Modelling studies have yielded mixed results. Byrd and Cox (1984), Fingerhut (1978) and Wong and Stephens (1994) have all modeled the diurnal cycle and documented results supporting the DNS as the primary cause of the observed diurnal cycle. However, modelling studies by Fu et al. (1995), Miller and Frank (1993), Randall et al. (1991) and Xu and Randall (1995) suggest that DNS may be of only secondary importance to the RCF or LRD mechanisms. Chen and Houze (1997) hypothesize DNS is secondary to BLML. A problem with some modelling studies is that the simulations only model the local cluster scale differential heating effect while ignoring the broader scale, general radiative cooling subsidence mechanism that occurs all the time and which does not depend on cloudy-clear heating/cooling gradients. Other problems arise with interpreting possible effects of DNS in areas where regional scale dynamic effects may override radiative forcing such as occurred during GATE (Dewart 1978) and occurs near larger tropical land masses such as Borneo (Houze et al. 1981).

3.3 Direct Radiative Cloud Forcing (RCF)

Early references to the RCF as a driver of the diurnal cycle of clouds date back to 1930 (Refsdal 1930). Meinardus (1941), Riehl (1947), Jeandidier and Rainteau (1957) and Watanabe (1959) theorize that blackbody radiation from the tops of clouds present during the evening will produce cooling and overturning aloft which in time will lead to increased cloudiness. Kraus (1963) modified the theory by noting that absorption of solar energy in high tropical cumulus during the day could evaporate cloud drops and stabilize the lapse rate, thereby reducing precipitation. Ramage (1971) summarizes the theory in his text:

> "At night, radiational cooling from the tops and reduced surface cooling beneath an extensive cloud system presumably increase instability, cloud depth, and rainfall. During the day, radiational warming from the tops and reduced insolation at the surface presumably increase stability and consequently decrease rainfall."

More recent studies emphasize some combination of three possible individual radiative effects that comprise the RCF (Fig 3.4), including:

(1) Solar absorption and hence heating in the upper portion of cloud masses decreases the lapse rate of temperature thus stabilizing the cloud during the day. (stabilizing effect)

(2) LW emission in the absence of SW absorption at night leads to net cooling at cloud top thus destabilizing the lapse rate. (destabilizing effect)

(3) Cloud base warming due to absorption of LW radiation emitted from warmer clouds or the surface below. (destabilizing effect)

Webster and Stevens (1980) used a radiative transfer model to calculate radiative heating rates on spatially extensive decks of middle and high cloud. Their results show substantial heating at cloud base and cooling at cloud top creates a vertical heating differential of nearly $30^{o}C\ day^{-1}$. In their study, diurnal

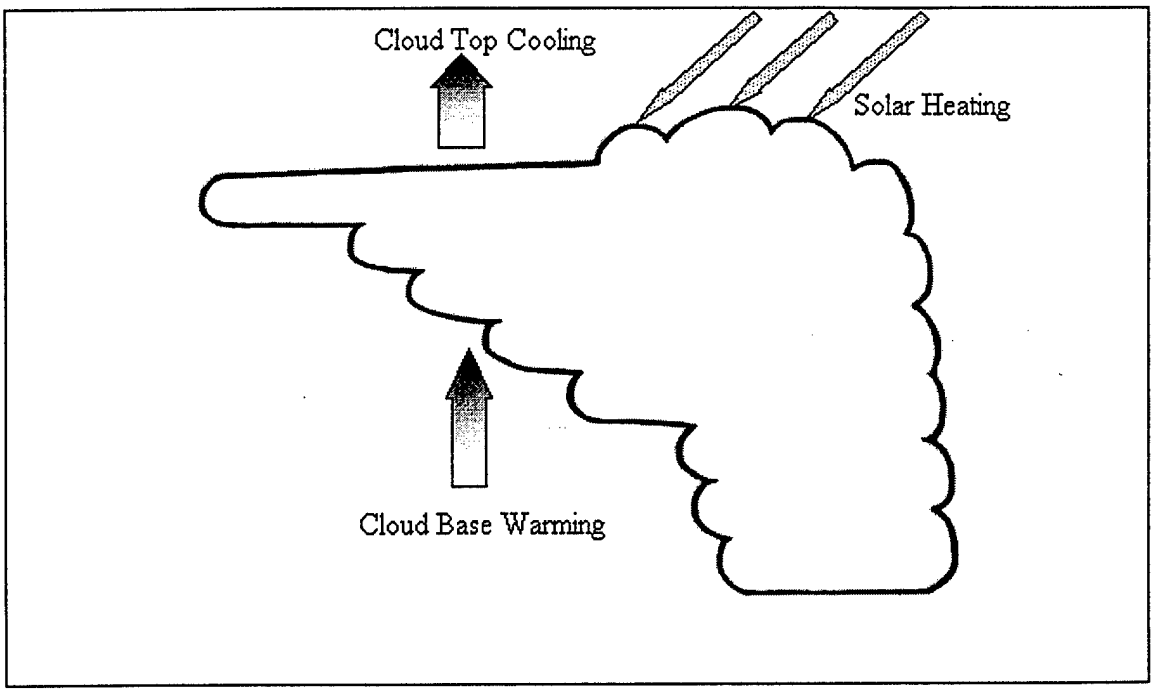

Figure 3.4: Illustration of Direct Radiative Cloud Forcing (RCF) effect on an idealized convective system.

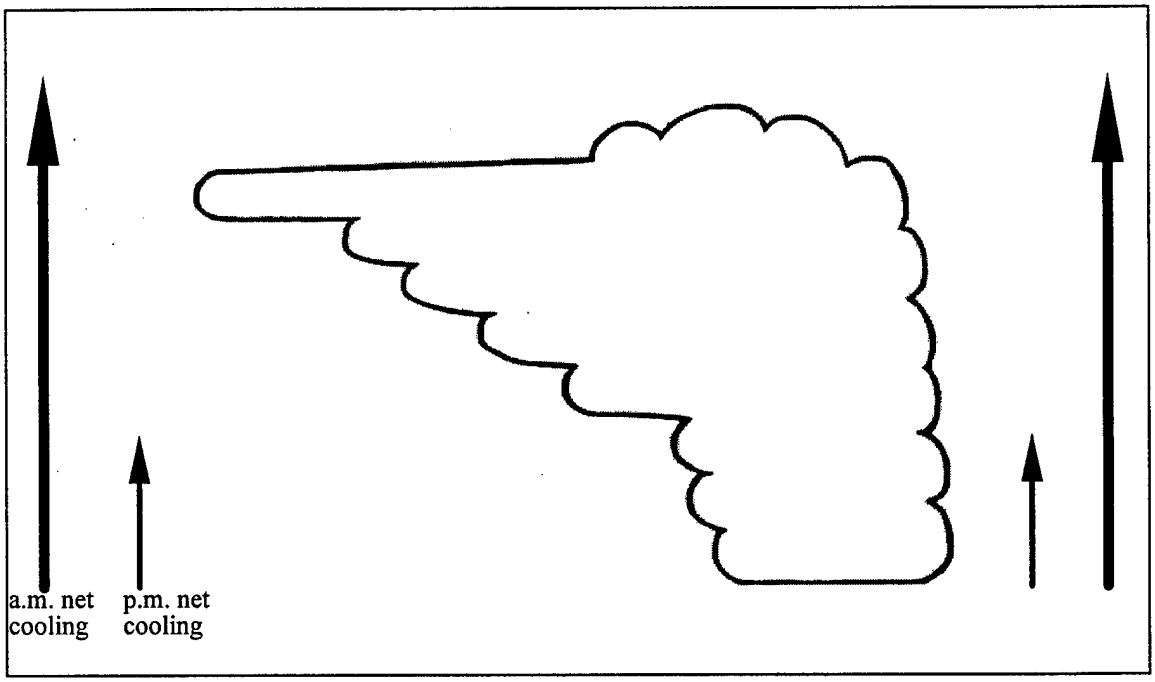

Figure 3.5: Illustration of Large Scale Radiative Destatbilization (LRD) diurnal convective mechanism.

variation of absorption of incoming short wave radiation in the upper portion of the cloud led to a large diurnal variation in net radiation. At cloud base, radiational warming reduced cooling due to evaporation and melting of precipitation.

Ackerman et al. (1988) used an infrared multiple-scattering model to compute heating rates in tropical cirrus anvils. Their results indicate that cloud top solar absorption may be the primary radiative forcing for broad scale cirrus anvils. They theorize that solar heating could impact the diurnal cycle of deep convection in the tropics but point out the need for more sophisticated models to simulate the complex interactions between radiational heating and ice microphysics. In a related paper on cirrus outflow dynamics, Lilly (1988) states that radiative destabilization of large cirrus anvils leads to convectively generated turbulence. This turbulent overturning maintains the cirrus and causes it to grow by entrainment at the top and bottom.

While the above studies suggest a large direct radiative forcing effect on extensive middle cloud decks and upper level cirrus anvils, the question of greatest interest for the present study is the effect on precipitation. Papers by Churchill and Houze (1991), Randall et al. (1991), Machado and Rossow (1993), Miller and Frank (1993), Fu et al. (1995), Xu and Randall (1995), Guichard et al. (1996), Sui et al. (1996), Rickenbach and Rutledge (1996) and Tao et al. (1996) address the problem.

Authors of three of these studies conclude that RCF is the primary mechanism driving the diurnal cycle of precipitation. Randall et al. (1991) found that the observed diurnal cycle can be qualitatively accounted for by direct radiation-convection interactions although the amplitude is weaker than observed (Janowiak et al. 1994). Specifically, the absorption of solar radiation by clouds in their GCM led to a reduction of the precipitation rate in the afternoon. Xu and Randall (1995) come to the same conclusion using the UCLA cumulus ensemble model (CEM). In this model, the greatest diurnal radiative forcing of precipitation occurred in the expansive stratiform region (Xu 1997, personal communication). This idea of the RCF effect on extensive stratiform regions is supported by Bergman and Salby (1996) and Rickenbach and Rutledge (1996). In both Randall et al. and Xu and Randall, DNS was a minor forcing mechanism of the diurnal cycle of precipitation.

An observational study by Machado and Rossow (1993) concluded that the profile of radiative heating-cooling destabilizes the whole anvil layer, destabilizes convection near its top, and stabilizes convection near its base at the top of the planetary boundary layer (PBL). They hypothesize that stabilization of the PBL top could amplify the diurnal cycle of convection. While these studies mentioned above found RCF to be of primary importance, others have reached a different conclusion.

Churchill and Houze (1991) used a two-dimensional, kinematic model to diagnose the thermodynamic, water vapor and hydrometeor fields of the stratiform region of a tropical cloud cluster. In

their model, RCF was limited to a 3 km layer at cloud top and had no effect on the precipitation rates in the stratiform rain region. Stratiform rain regions are typically much deeper than 3 km. Miller and Frank (1993) found RCF to be of secondary importance to LRD in a study of tropical cloud clusters using the Pennsylvania State University-NCAR Mesoscale Model. They also showed that radiative processes are unable to maintain active, precipitating stratiform clouds when the model allows feedback of the heating to the circulation of the cloud. Using a two-dimensional CEM, Fu et al. (1995) found that direct destabilization of clouds via cloud top cooling and cloud base warming contributes to the longevity of anvil cirrus in agreement with Lilly (1988). However, cloud radiative forcing associated with the anvils (a feedback) suppresses deep convection and decreases the total daily surface precipitation by 10%. RCF also inhibited total precipitation in a study by Tao et al. (1996) using the Goddard CEM.

Taken together, studies on the potential impact of RCF on the diurnal cycle of tropical precipitation are inconclusive. Various models imply that RCF may either cause precipitation to increase, decrease, or have no discernible effect. It is significant that the primary radiative impact in these models is on the stratiform rain region. Stratiform rain accounts for only 40-50% of the rain in a tropical cloud cluster (Churchill and Houze 1984; Houze 1977). It is not clear that modelling efforts have yet assessed the impact of RCF on the deep convective cores of tropical cloud clusters, which contribute most of heavy rain (Jacobson 1976, Janowiak et al. 1994, Liu et al. 1995) and probably account for most of the observed diurnal variation (Gray and Jacobson 1977; Machado et al. 1993; Chen and Houze 1996). Some modelling studies in the past six years indicate another radiative forcing mechanism may be responsible for modulating convection each day - Large Scale Radiative Destabilization (LRD), which is discussed next.

3.4 Large Scale Radiative Destabilization (LRD).

Dudhia (1989), Miller and Frank (1993), Fu et al. (1995), Tao et al. (1996) and Donner et al. (1997) all concluded that the dominant radiative influence on tropical convection is LRD (Fig. 3.5). Continuous long wave cooling destabilizes the tropical environment. Destabilization is related to an increase in the vertically integrated buoyancy of a parcel that rises from the sub-cloud layer. Destabilization can occur by warming or moistening the sub-cloud layer where the parcel originates and by warming or moistening the atmosphere above cloud base. In the studies listed above, greater net loss of radiation at night leads to a relative cooling and moistening of the atmosphere above the boundary layer (i.e.; above cloud base). The troposphere is not destabilized through an increase in convective available potential energy (CAPE), but through an increase in relative humidity. Increasing the relative humidity facilitates condensation, allows for less evaporation, and reduces entrainment drying of growing cumulus.

Sui et al. (1996) and Sui et al. (1997) extend this line of thought to a theorized driving mechanism of diurnal convective variability. They suggest that the nocturnal rainfall maximum is related to the destabilization by radiative heating/cooling cycle and the resultant change of available precipitable water (APW) that can be expressed as RH (W_{avg} - W*), that is, the difference between the vertically integrated saturation water vapor amount W_{avg} and a reference value of W*, with respect to a reference columnal relative humidity (RH). Assuming the diurnal variation of RH is small, the diurnal variations of rain rate due to radiative destabilization is approximated by -RH $\delta W_{avg}/\delta t$. $\delta W_{avg}/\delta t$ is considered the theoretical limit of the nocturnal rain-rate distribution. Given this consideration, observations from TOGA COARE show that the nocturnal rain-rate maximum appears to be related to the diurnal temperature cycle.

The six studies above found DNS to be of minor importance. The effect of RCF in the models was mixed as to whether it increased or inhibited precipitation. Relatively few modelling or observational studies have specifically considered LRD in relation to the diurnal cycle of tropical convection, so much more work is necessary.

3.5 Boundary Layer-MCS Lifecycle (BLML)

There are two broad categories that can be loosely classified under the heading of BLML theories:

(1) Local regime effects

(2) SST variation effects

Near-land oceanic diurnal cycles of convection can have a character very different from those over the open ocean. For example, the rainfall maximum over the GATE ship array occurred in the early afternoon (Dewart 1978). McGarry and Reed (1978) suggest that local dynamics dominated during GATE. McBride and Gray (1980) list two possible regional effects that may have influenced convection in the GATE region. First, the afternoon maximum occurs due to a combination of regime specific thermal stability, wind shear characteristics and mesoscale squall line dynamics. The end result is formation of convection in the morning followed by squall line convection which overrides the unfavorable large-scale dynamics leading to an afternoon rainfall maximum. The second possibility is that the GATE region is influenced by downwind effects from Africa and by radiative effects involving Saharan dust.

Houze et al. (1981) studied mesoscale convective systems in the vicinity of North Borneo. In this region, cloud clusters are generated diurnally by the convergence of the land breeze from Borneo with the low-level northeasterly monsoon flow just off the northern coast of the island. The evolution of resulting clusters leads to a 0800 LST precipitation maximum just off the coast. The west Pacific warm pool region

of the present study is sufficiently far from land to avoid near-land effects. However, the region is not immune to the potential influence of boundary layer change linked to diurnal variation of SSTs.

Lukas (1991) and Webster et al. (1996) discuss in detail the potential significance of diurnal changes in the bulk SST over the WP. The bulk SST is defined to be the temperature within the upper few centimeters of the ocean surface. Radiative, latent and sensible heat exchanges between the atmospheric and oceanic boundary layers depends on the state of the sea surface, and hence the bulk SST is critical for air-sea interactions.

The bulk SST and state of the PBL set the surface saturation vapor pressure and hence determine the latent heat flux. Because of the Clausius-Clapeyron relationship (Fig. 2.2), surface temperature variations of even $1^{o}C$ can have a substantial impact on air-sea interactions when the surface temperature is high. The diurnal variation of SST in the tropical west Pacific can be as high as $3.8^{o}C$ under clear, calm conditions (Webster et al. 1996). Based on these ideas about SST variability and extensive analysis of satellite data from TOGA COARE, Mapes and Houze (1993), Chen et al. (1996) and Chen and Houze (1997) hypothesize a BLML theory for the diurnal cycle of tropical deep convection. Chen and Houze summarize this theory:

> "The observed diurnal variation of tropical cloud systems suggests that diurnal heating of the tropical atmosphere and ocean surfaces provides favored conditions in the afternoon for the formation of cloud systems....and the diurnal cycle of cloudiness reflects the lifecycle of (these) cloud systems."

Chen and Houze observed two distinct diurnal cycles of convection; One during the active phase and another during the inactive phase of the ISO. During convectively suppressed phases of the ISO, the cloud field as viewed in IR satellite imagery was dominated by spatially small cloud systems. These small systems were observed to form in the afternoon, presumably sparked by the daytime heating of the sea surface. These small systems reached their maximum in about three hours and then decayed, resulting in a modest late afternoon maximum of cold cloud cover. During active phases of the ISO, spatially large convective systems dominated the diurnal cycle. Like the small systems, these larger MCSs tended to form in the afternoon, when the surface conditions were "most favorable." Since these large systems lasted about one day, they evolved throughout the night attaining their maximum areal extent of very cold cloud tops in the early morning. They decayed after sunrise.

In concert with their observations of the diurnal cycle of the large MCSs, Chen et al. and Chen and Houze documented a day-to-day local spatial behavior of convective systems which they termed *diurnal dancing*. Because large convective systems persist up to one day, low-θ_e downdrafts fill the boundary layer with air of lower moist-static energy. The systems also produce a cloud canopy that shades the ocean surface from the sun. These two effects prevent development of surface conditions favorable for a large

convective outbreak in the same location two days in a row. Instead, convection occurs in neighboring regions unaffected by the previous day's convection. This theorized diurnal dancing introduces a tendency for a bi-diurnal cycle of large convective systems occurring every other day at a given location. The bi-diurnal cycle is thought to phase-lock with westward-propagating equatorial inertio-gravity waves of similar frequency (Takayabu et al. 1996).

Rickenbach and Rutledge (1996) question the results of Chen and Houze (1997) in light of results of their own study using 90 days of TOGA COARE radar data. They conclude that the diurnal variation may be linked to differences in the size, intensity, and duration of daytime versus nighttime convective events, but is not linked to the evolution of individual events throughout the day. Later in this thesis I specifically address various facets of the Chen and Houze BLML theory including the size dependence of the diurnal cycle, afternoon initiation of convection and *diurnal dancing*.

3.6 Remote Continental Effect (RC)

Wallace and Hartranft (1969) make an early reference to a possible remote continental influence on the diurnal cycle. They indicated that continental-ocean scale circulations can produce diurnal divergence changes of 10^{-6} s^{-1} or more over North America. Foltz and Gray (1979) state that circulation variations on a continental-ocean scale might substantially contribute to the morning maximum of tropospheric subsidence over the oceans. This is the Remote Continental Effect (RC).

Most of the recent focus on RC as a possible mechanism for the diurnal cycle can be attributed to a study by Silva Dias et al. (1987). Silva Dias et al. used a linearized shallow-water model to analyze possible influences that localized diurnal convective forcing, such as the forcing over the Amazon region, could have on the large scale. Their results suggest that the observed large amplitude diurnal cycle of convection over the Amazon region is correlated to large diurnal changes of vertical motion over equatorial regions up to 5000 km away. This dynamical response, mostly related to the eastward dispersion of Kelvin waves in the model, is offered as an alternate explanation for the observed diurnal cycle of precipitation in the equatorial Atlantic. The RC hypothesis has met with both support (eg; Xu and Randall 1995) and criticism (Janowiak et al. 1994).

Janowiak et al. (1994) point out that whereas RC is plausible in the general proximity of continents, it is not so plausible over the midoceans since the mechanism to convey the dynamic forcing over several thousand kilometers is not clear. At least one other factor makes the mechanism not generally applicable to the entire tropics. As stated, the primary forcing of RC modeled by Silva Dias et al. was Kelvin waves which are equatorially trapped. This equatorial mode occurs due to the change in sign of the Coriolis parameter at the equator (Holton 1992). Much of the world's oceans lie outside the near-equatorial region

(5^{o}S-5^{o} N), and yet the same phase and amplitude diurnal cycle still occurs (Hendon and Woodberry 1993; Jacobson 1976). In addition, the diurnal character of the vertical motion fields are very similar in the Atlantic and west Pacific (McBride and Gray 1980) despite the fact that in the west Pacific, there are no equatorial continental scale land masses to create the Silva Dias et al. dynamic response. For these reasons, RC is not considered further in this thesis.

Conclusion

Quantifying and understanding the diurnal cycle of intense tropical convection is essential to defining it's role in the global climate. Over the years, many atmospheric scientists have assumed a small diurnal cycle in oceanic precipitation. The popular thinking on this subject changed in the late 1970s. To date, there are no less than six theories about the driving mechanism that might lead to a diurnal nocturnal or early morning precipitation maximum: (1) Atmospheric Tides; (2) Day vs Night Radiation-Subsidence; (3) Direct Radiative Cloud Forcing; (4) Large Scale Radiative Destabilization; (5) Boundary Layer-MCS Lifecycle; (6) Remote Continental Effect. None of the effects invoked in these hypotheses are totally mutually exclusive. Atmospheric scientists must determine which are important for various geographic regions of the planet. To what extent does one dominate or several act in concert?

Modelling and observational studies based on field projects such as GATE and TOGA COARE yield valuable information on the morphology and temporal variability of tropical weather systems. Transportability of results from these projects, however, is always questionable since they focus on relatively small portions of the globe. More studies utilizing satellite data and better numerical models offer our best hope to understand the diurnal cycle over the entire tropics. Models have greatly improved over the past 25 years. Some of the present challenges which must be overcome by modelers include the following:

(1) Particle size distributions play a significant role on interactions among radiative heating, cloud microphysics, and dynamics processes in a cloud model and need to be simulated simultaneously (Fu et al. 1995).

(2) Radiative transfer models need to accommodate the spatial variability of cirrus clouds inherent in the data. Most radiative transfer calculations cannot accommodate the important elements of cloud structure. Slight inhomogeneity can produce a significant departure in the reflected radiance and absorption as compared to plane-parallel or independent pixel computations which affects the local heating and cooling rate profiles. Local heating/cooling can generate significant horizontal thermal gradients. (Tsay et al. 1996).

(3) Cloud side cooling (not represented in modelling studies) is thought to be dynamically very important to low level convergence (Guan et al. 1995).

(4) Data used to initialize models can be a problem. For example, initializing models with conditions of the GATE III mean atmosphere are unrealistic. On a temporary basis, the atmosphere will provide a much more favorable background environment for convergence and deep convection (Gray 1995).

(5) Domain sizes in CEMs may be too small to model synoptic scale influences on convection (Miller and Frank 1993). For example, the domain size for Xu and Randall (1995) was 500 x 500 km with the largest clusters ~ 100 km in diameter. This domain size is too small to model the large scale processes included in DNS (Sheaffer 1997, personal communication), and the clusters are much smaller than the MCSs found to dominate the diurnal cycle (Machado et al. 1993; Chen et al. 1996).

(6) Accurate representation of upper level moisture as well as proper modelling of the relationship between convective cloudiness and water vapor are important challenges for GCMs (Roca et al. 1997). The loss of IR to space increases non-linearly with decreases in relative humidity. This gives substantial uncertainty to humidity in models used to simulate LW radiative processes in the tropics (Spencer and Braswell 1996).

(7) Radiative effects on clouds are quite sensitive to imposed background ascent. The larger the imposed vertical velocity, the less the impact of LW cooling on surface precipitation processes (Miller and Frank 1993; Tao et al. 1996).

(8) Cyclic lateral boundary conditions used in CEMs can usually contribute to a very large stratiform-anvil cloud coverage. This may provide favorable conditions for the cloud-top cooling and cloud-base warming mechanism (Tao et al. 1996).

(9) Two-dimensionality.

As models have improved over the past twenty-five years, so has satellite data. In the present study, satellite data from the Japanese Geostationary Meteorological Satellite (GMS-4) was used to analyze the daily variation of convective cloudiness and its relation to cloud cluster morphology over the west Pacific warm pool in the northern hemisphere. Results presented later in this thesis further advance our understanding of a puzzle which will not be fully solved for many years to come.

Chapter 4

Data and Infrared Thresholds

The primary source of data for this study was the Climatological and Historical ANalysis of clouds for Environmental Simulations (CHANCES) database (Reinke et al. 1995; Vonder Haar et al. 1995). A secondary source of data was twice daily synoptic surface charts. Winter 1994/1995 charts were provided by the Joint Typhoon Warning Center (JTWC) and summer 1994 charts were provided by the University of Guam. This chapter discusses the CHANCES database and sources of satellite related error. In the final part of the chapter I summarize various temperature thresholds used to identify features in IR imagery and discuss thresholds chosen for the present study.

4.1 CHANCES

CHANCES is a unique 1-yr (Feb. 1, 1994 - Jan. 31, 1995) global satellite imagery database with 1-hr temporal and 5-km spatial resolution. Each CHANCES image is a "seamless" global image created from a combination of geostationary and polar orbiting satellites. The data used in this study was from a west Pacific sub-sector of these global images in the domain of GMS-4. GMS-4's VIS channel (0.50-0.75 μm) and IR atmospheric window channel (10.5-12.5 μm) (Rao et al. 1990) were included in CHANCES. The nominal subpoint (0^{o}N, 140^{o}E) resolution of raw GMS-4 imagery processed for CHANCES was 5-km.

Development of CHANCES was sponsored by a Small Business Innovative Research (SBIR) Phase II, U.S. Air Force to STC-METSAT, Fort Collins, Colorado. Production of CHANCES involved a significant amount of pre-processing. This pre-processing included navigation and alignment, the creation of radiance background information, and the construction of binary cloud/no cloud (CNC) images.

Navigation and Alignment

Navigation is the process of geolocating satellite image pixels. Navigation information is part of a navigation header which is provided with each image. This internal documentation contains orbit and attitude parameters necessary to convert the satellite's location in space and its viewing angle toward to a geographic location for that point. For CHANCES, special algorithms were constructed to automatically

decode GMS-4 navigation parameters and assign a latitude and longitude to each pixel. The final output files were created by remapping the pixels into a Mollweide projection.

The proper navigation of an image does not guarantee that two images taken at different times will be aligned geographically (Kidder and Vonder Haar 1995). Often the standard navigation information is incorrect due to perturbations in the satellite's orbit and attitude parameters. Hence, imagery must also be aligned. Automated alignment can be accomplished by "warping" algorithms that stretch or shrink images to fit a predefined grid. Vonder Haar et al. 1995 describe the polynomial warp used for CHANCES.

Construction of Radiance Backgrounds and CNC Images

A useful CHANCES product is the binary CNC data. For this data, each pixel of every image was classified as cloudy or clear. The process capitalizes on the fact that clouds are generally brighter (in the VIS wavelengths) or colder (in the IR wavelengths) than the underlying background. So, the first step was to compile VIS and IR background radiance information.

The background radiance represents the cloud-free brightness count detected by the satellite at each pixel. Due to changes in background brightness or temperature with variations in sun angle and surface composition (Minnis and Harrison 1984), a different background was constructed for each observing time and only used for a fraction of a year. For the CHANCES VIS CNC, an initial background for each hour of the day was built by storing the darkest detected radiance value of each pixel over the first thirty days of data. These background images were then dynamically updated throughout the remaining eleven months of processing. A filter eliminated false background values created by cloud shadows. A different IR background was constructed for each hour based on input from the USAF surface temperature database.

To construct VIS CNC images, each pixel was individually classified as either clear or cloudy by comparing the brightness of each raw VIS image pixel to the background brightness image for the same time. Pixels more than nine counts brighter than the background were classified as cloudy (at least 50% filled with cloud). To construct IR CNC images, a pixel in a raw IR image was classified as cloudy if the pixel was 9-14 K (depending of geographic location) colder than the background.

4.2 Satellite Related Error

Various factors degrade satellite data. Kidder and Vonder Haar (1995) and Vonder Haar et al. (1995) discuss potential satellite related sources of error including calibration, attenuation, background contrast, signal contamination, displacement, foreshortening, sensor lag, and sensor interference. Below, I summarize these factors and discuss if and how they were dealt with during CHANCES pre-processing.

Calibration

GMS-4 measures upwelling radiative flux from the Earth. To make the IR data meteorologically meaningful, radiance measured at the satellite is converted to an equivalent blackbody temperature (T_{BB}). The T_{BB} is the temperature a theoretical blackbody must be to register the same amount of energy at the sensor. Converting radiance to T_{BB} requires an accurate calibration. Individual sensors are calibrated on geostationary satellites by viewing a light source of known intensity or by viewing space (which is assumed to have a radiative temperature of ~ 2 K).

Attenuation

Attenuation is a decrease in the amount of radiation reaching a satellite caused by absorption or scattering along its path from source to sensor. Attenuation causes clouds to appear cooler and thus higher in the atmosphere. This type of error is pronounced for IR sensors due to absorption by water vapor, carbon dioxide and ozone. Error can be on the order of 10 K at extreme distances from the satellite subpoint.

Background Contrast and Contamination

The GMS-4 IR sensor measures all LW radiation between 10.5-12.5 μm upwelling from the scene below. When clouds or other phenomena have a radiative temperature close to that of the underlying surface (low contrast), they can be indistinguishable from the background. A closely related source of error is contamination.

IR radiation reaching the sensor from beneath a cloud leads to contamination. Contamination is most pronounced with thin clouds such as cirrus. Additional radiation in the path from below the cloud makes clouds appear too warm. The primary technique to account for contrast or contamination problems is sampling of scenes in multiple spectral intervals. No direct corrections for contrast or contamination were applied during CHANCES production.

Displacement and Foreshortening

Displacement results from viewing angle geometry and the projection of image data onto a 2-D plane for display as an image. It causes the top of a cloud to be projected onto a pixel farther away from the satellite subpoint. Displacement increases with the distance from satellite subpoint and height of the cloud. No attempt was made to correct for this error in the CHANCES analysis. However, the effect will be largely negligible in the WP sector used for this study.

Another source of error related to viewing angle geometry is foreshortening. Foreshortening is due to the effect of the Earth's curvature on the resolution of an image. As an instrument samples at increasingly large zenith angles, each pixel receives emmited radiation from a larger geographic area. For example, GMS-4 resolution degrades to approximately 12-km at 55° from the satellite subpoint. When clouds are in the scene, the apparent fraction of the sky covered by cloud increases with distance from the subpoint because the satellite senses the sides as well as the top. Foreshortening is difficult to account for and was not addressed during CHANCES pre-processing.

Signal Interference

For geostationary satellites, raw data is transmitted to the ground, processed, then sent back to the satellite for retransmission to user ground stations. During this process, the transmitted signal often experiences interference, which appears as missing lines or garbled data. Garbled data points (noise) are very difficult to detect. However, missing lines are easily detected and can be corrected using various averaging schemes.

Missing CHANCES data were filled by applying a spatial or temporal interpolation of available pixels, or if necessary, persistence (either forward or backward in time). Small holes of one or two missing pixels were filled by a spatial interpolation of surrounding points or scan lines. Larger areas were filled by doing a temporal interpolation if data was available from within one hour. If not, images were persisted backward or forward in time from the closest available image having a good data point. In processing for this thesis, I excluded any filled or persisted data from analysis.

4.3 IR Temperature Thresholds

IR sensors respond to LW radiation impinging upon some collecting surface. The IR sensor on GMS-4 responds to radiation in the atmospheric window region. The raw output is a filtered radiance that depends on the spectral response of the instrument. This radiance is converted to a T_{BB} (or brightness temperature) between 180 K and 330 K by inverting the Planck function (Kidder and Vonder Haar 1995). The brightness temperature is then stored in an image array as a digital count between 0 and 255. The uncertainty for high cloud-top temperatures for optically thick clouds is ~ 3 K, associated primarily with the radiance measurements (Machado and Rossow 1993; Liu et al. 1995). An image is displayed by assigning a color or shade or gray to each count value. When using the data, digital counts can be converted back to brightness temperature using a simple formula or look-up table.

In general, clouds can be identified in IR imagery because pixels containing clouds usually have lower radiance and hence a lower T_{BB} than the warmer background. The temperature is an estimate of the

actual temperature of the top of the cloud. Accuracy of the temperature estimation is highest for the coldest clouds (Liu et al. 1995). Fluctuations in cloud top height can be inferred from changes in T_{BB}. In the tropics this provides important insight into the structural, radiative and diabatic properties of convective systems.

Clouds of various types can be differentiated in IR pictures using the knowledge of characteristic altitudes, hence the approximate temperatures, at which they occur (Kidder and Vonder Haar). Tropical deep convective clouds are easily identified on IR satellite pictures because convective clouds extend to very high, cold altitudes. The simplest, most frequently used technique for objectively extracting cloud information from digital images is the IR threshold technique. For example, Liu et al. (1995) classify mid-level clouds as those between 0°C and -40°C. Using this principle, researchers have developed criteria to separate precipitating from non-precipitating cloud (eg; Richards and Arkin 1981). Also, various IR thresholds have been used to identify cloud associated with tropical convection.

There are several drawbacks to the use of T_{BB} to understand convective variation. Actual rainfall rates and hence latent heating are not measured; they are only inferred. Also, diurnal variations of important microphysical properties of organized convection are not resolved (Houze et al. 1981). These microphysical variations play a key role in the diurnal variation of the radiative properties of the convection, such as its albedo (Hartmann et al. 1991). Similarly, T_{BB} alone does not always accurately identify cloud type. Below, I summarize IR thresholds used in previous projects and discuss the thresholds chosen for the present study.

Table 1 lists IR temperature thresholds used in various tropical studies. At the cold end of the range are the -75°C and -65°C thresholds used by Lajoie and Butterworth (1984) and Mapes and Houze (1993). Lajoie and Butterworth used these thresholds to identify the cirrus canopy of Australian region tropical cyclones. Mapes and Houze empirically determined these thresholds from their subjective impression of an approximate correspondence to radar echo patterns observed in mature nocturnal oceanic MCSs during the Equatorial Mesoscale Experiment (EMEX, Mapes and Houze 1992). Chen et al. (1996) and Chen and Houze (1997) used -65°C for similar reasons. Muramatsu (1983) used -70°C as a threshold to isolate active deep convection in mature typhoons with GMS IR data. The correlation of -70°C to deep convection in typhoons was supported by Steranka et al. (1984). Machado et al. (1993) used -66°C to identify high level cloud. Gray and Sheaffer (1995) used -65°C based on a theoretical approach.

The -65°C level is approximately the maximum height to which convective clouds receive buoyancy from latent heat release. Analysis by Reid et al. (1989) suggests that the mixing ratios associated with maximum SST values observed in the west Pacific warm pool correspond to latent heat release which will contribute significantly to the buoyancy of undiluted parcels up to a level of approximately 150 mb.

TABLE 1: Infrared temperature thresholds used in previous studies of tropical convection.

T_{BB} (K)	T_{BB} (°C)	Reason/Cloud Type	Justification or comments	Author(s)
198	-75	Deep Convection	Conservative estimate of EMEX radar echo area	Mapes and Houze 1993; Lajoie and Butterworth 1984
203	-70	Deep Convection	Corresponds to tropopause penetrating convection	Muramatsu 1983; Steranka 1984
207	-66	High Level Cloud		Machado et al. 1993
208	-65	Deep Convection	Moderate estimate of EMEX radar echo area	Mapes and Houze 1993
208	-65	Deep Convection	Likely maximum height to which convective clouds receive buoyancy from latent heat release	Gray and Sheaffer 1995; Zehr 1987,1992
208	-65	Deep Convection	Threshold is close approx. to boundary of precipitating core of west Pacific tropical deep convective systems	Chen et al. 1996; Chen and Houze
208	-65	High Level Cloud		Lajoie and Butterworth 1984
213	-60	Deep Convection	Estimate of MONEX radar echo area	Williams and Houze 1987
215	-58	Deep Convection	Isolates convective cells embedded with cloud clusters. Comparable to combined IR-VIS technique.	Fu et al. 1990; Zhang 1993; Janowiak et al. 1994
215	-58	Convective Rain	Improvement to the GPI method to better estimate convective rain from IR imagery	Nelkin et al. 1996
217	-56	ID MCCs	Conservative definition of west Pacific MCCs	Miller and Fritsch 1991
218	-55	High Level Cloud	Characterize behavior of deepest cold clouds	Albright et al. 1985
218	-55	High Level Cloud		Machado et al. 1993; Lajoie and Butterworth 1984
219	-54	ID MCCs	Defines MCC	Maddox 1980
219	-54	Deep Convection	Separate deep convective from warmer cloud	Evans and Shemo 1996
220	-53	Deep Convection	Good first approximation for cutoff to isolate deep convective cloud	Fu et al. 1990; Meisner and Arkin 1987
223	-50	Convective Cloud	Cutoff between cloud regimes with different diurnal characteristics	Browner et al. 1977; Muramatsu 1983
225	-48	Convective Cloud	Cold Cloud Index: $I = (225 - T_{BB})/5$	Nakazawa 1988; Lau et al. 1991
225	-48	Deep Convection	Intermediate convective threshold	Janowiak et al. 1994
228	-45	Thin Cirrus/Stratus	Coldest observed IR T_{BB} for residual thin stratiform cirrus clouds	Hendon and Woodberry 1993; Gray and Sheaffer 1995
220-235	-40 to -53	Cirrus Anvil Cloud		Gray and Sheaffer 1995
230	-43	Convection	Optimuum linear regression with GATE rainfall	Richards and Arkin 1981
230	-43	Deep Convection	Deep Convection Index: $DCA = (-43^{\circ}C - T_{BB})$	Hendon and Woodberry 1993
233	-40	Mid/High Cloud	Cloud level threshold based on physical considerations	Liu et al. 1995
235	-38	Tropical Convective Cloud and Rainfall	Threshold has a high linear regression with area averaged GATE rainfall	Arkin 1979; Meisner and Arkin 1987; Janowiak and Arkin 1991
235	-38	Rainfall	GOES Precipitation Index Method	Arkin 1983; Shin et al. 1990
235	-38	Precipitation	Negri-Adler-Wetzel IR rain-rate algorithm criteria	Evans and Shemo 1996
235	-38	High Cloudiness	General estimate of high cloudiness associated with deep convection based on many previous studies	Mapes and Houze 1993; Chen et al. 1996
235	-38	Cold Cloud	Warm threshold	Janowiak et al. 1994
237	-36	Rainfall	Optimuum linear regression with GATE rainfall	Albright et al. 1985
245	-28	High-Level Clouds	Buoyant parcels reaching this level are convective	Machado and Rossow 1993
253	-20	Rainfall	Griffith and Woodley IR precipitation algorithm	Augustine 1984
253	-20	High Level Cloud/	Determined using the histogram evolution technique	Duvel 1989
253	-20	Mid-Level Cloud		Machado et al. 1993
~253	-20	Deep Convection	Intensity index of cloud top temp. minus 400 mb temp.	Murakami 1983
257	-15/-16	Tropical Cloud Shield		Gray and Sheaffer 1994/95; Steranka 1984
~258	-15	High-Cloud Fraction	ISCCP-C2 Data Archive (High Cloud ~ 440 mb)	Bergman and Salby 1996
258-228	-15 to -45	Thin Cirrus/Warm Cld.	Cirrus are cold but look warm due to contamination	Zehr 1987,1992
~262	-10	High-Level Cloud	Cloud colder than 39 K or more below sfc. temp.	Minnis and Harrison 1984
~267	-6	High/Low-Level Cloud	Trop. oceans have bimodal dist. of cld. w/ 500 mb min.	Fu et al. 1990
270	-2	Tropical Cloud Shield	Should identify all cloud except low stratus	Meisner and Arkin 1987
282	+9	Cloud/No Cloud	Temperatures warmer than 282 K are cloud free	Gray and Sheaffer 1995

The observed mean temperature at 150 mb is about -65°C. Therefore, this is the beginning level for overshooting (and hence rapidly decelerating) convective plumes in intense tropical Pacific convection. Results of Zehr (1987,1992) support this idea. He found that areas of cloud colder than -75°C and -85°C had a diurnal variation of the same phase as cloud colder than -65°C. The diurnal phase shifted, however, for cloud area between -45°C and -65°C. Results from Gray and Sheaffer were also consistent with Reid et al..

Slightly warmer thresholds have also been used to identify deep convection. Williams and Houze (1987) found that fractional cloud cover at -60°C and colder closely corresponded to radar echo patterns observed during the Winter Monsoon Experiment (WMONEX). Janowiak et al. (1994) used -58°C based on work by Fu et al. (1990). Fu et al. chose -58°C as a threshold for tropical *deep convective cloud* based on an empirical study. Pixel comparisons showed that -58°C identified convective areas comparably to a more rigorous IR-VIS bi-spectral technique. Nelkin et al. (1996) used -58°C as an improvement to the GOES (Geostationary Operational Environmental Satellite) Precipitation Index (GPI) to more accurately estimate convective rain from IR imagery. The standard GPI uses -38°C.

Several other cold thresholds have been used to analyze tropical deep convective cloudiness. Miller and Fritsch (1991) used -56°C as a conservative definition of a mesoscale convective complex (MCC) over the west Pacific. Lajoie and Butterworth (1984), Albright et al. (1985) and Machado et al. (1993) chose -55°C to identify high-level cloud. Evans and Shemo (1996) used -54°C to separate deep convective cloud from warmer, non-precipitating cloud. Fu et al. (1990) and Meisner and Arkin (1987) chose -53°C as a good first approximation to isolate deep convection. The high cloudiness index used by Nakazawa (1988) and Lau et al. (1991) contains the threshold -48°C. Finally, Janowiak et al. (1994) used -48°C as an intermediate value to identify deep convective cloud.

At warmer thresholds, Richards and Arkin (1981) found a high correlation between the fractional coverage of cloud colder than -43°C and observed convective GATE rainfall. An index based on this threshold was recently used by Hendon and Woodberry (1993) in light of results presented by Richards and Arkin (1981) and Fu et al. (1990). Liu et al. (1995) used -40°C to distinguish between middle and high-level cloud. Arkin (1979) found that -38°C gave the best linear regression with GATE rainfall; this threshold has since been retained by Meisner and Arkin (1987) and Janowiak and Arkin (1991). Arkin (1983) defined -38°C as criteria for the GPI. This was recently used by Shin et al. (1990). Negri et al. (1984) defined -38°C as criteria for their Negri-Adler-Wetzel IR rain-rate algorithm. This algorithm was recently used by Evans and Shemo (1996). Mapes and Houze (1993) chose -38°C based on various previous studies as an estimate of integrated rainfall amount. Janowiak et al. (1994) and Chen et al. (1996) similarly used -38°C as a general estimate of high cloudiness associated with deep convection. Murakami

(1983) defined an intensity index based on the amount of cloud top colder than 400 mb, which corresponds to a temperature of about -20°C (McClatchey et al. 1972). Augustine (1984) used -20°C in the Griffith-Woodley IR rainfall algorithm. This has been the warmest threshold used to analyze tropical convection. Other thresholds warmer than -38°C listed in Table 1 have been used to generically delineate between middle and high-level cloud (Bergman and Salby 1996; Duvel 1989; Fu et al. 1990; Machado et al. 1993; Machado and Rossow 1993; Minnis and Harrison 1984) and cloudy vs clear (Gray and Sheaffer 1995). Various authors have also used warm temperature thresholds to identify all cloud in the tropical cloud shield. Meisner and Arkin (1987) used -2°C while Gray and Sheaffer suggested a more conservative -16°C. Steranka et al. (1984) found -16°C to define the edge of the central dense overcast of tropical cyclones.

The area covered by cold cloud as a function of temperature threshold for the present study is shown in Fig. 4.1. The area has been normalized by -15°C cloud cover. The solid line is the mean for all times of day during JJA. The dashed line shows cloud cover for NDJ. In general, cloud tops colder than -53°C and -65°C cover about 20% and 10% of the area of cloud top colder than -15°C, respectively. The cumulative fractional cloud cover in Fig. 4.1 decreases in nearly linear fashion as the temperature decreases to about 220 K (-53°C). Below -53°C, the area covered at each threshold decreases at a greater rate. Therefore, in general agreement with Fu et al. (1990), Machado et al. (1993), Janowiak et al. (1994) and Evans and Shemo (1996), I have chosen -53°C as a first guess cutoff to isolate deep convection from warmer, possibly non-precipitating cloud. Based on those studies and also Steranka et al. (1984), Albright et al. (1985), Hartmann and Recker (1986), Zehr (1987), Hendon and Woodberry (1993), Gray and Sheaffer (1995) and Liu et al. (1995), I consider cloud-top T_{BB} between -53°C and -38°C to be associated with stratiform cirrus anvils and not active deep convection.

Figures 4.2 and 4.3 show the area covered by cold cloud as a function of temperature threshold in the present study, normalized by -53°C cloud cover. Cloud tops colder than -65°C cover about 40% of the cloud area colder than -53°C. A noticeable change in the slope of these curves is evident in these figures at around -65°C. This is consistent with sharp drop in pixel counts for temperatures colder than -65°C observed by Gray and Sheaffer (1995) that prompted them to use -65°C to identify deep convection. As mentioned above, studies by Muramatsu (1983), Lajoie and Butterworth (1984), Mapes and Houze (1993), Machado et al. (1993), Chen et al. (1996), Chen and Houze (1997) and Zehr (1987,1992) also used thresholds near -65°C.

While Chen and Houze (1997) indicate that the choice of a -65°C threshold is "rather arbitrary," the results described above, as well as additional analysis presented in chapters 5 and 6 indicate that -65°C provides the best T_{BB} threshold for observing active, intense tropical convection in the diurnal cycle.

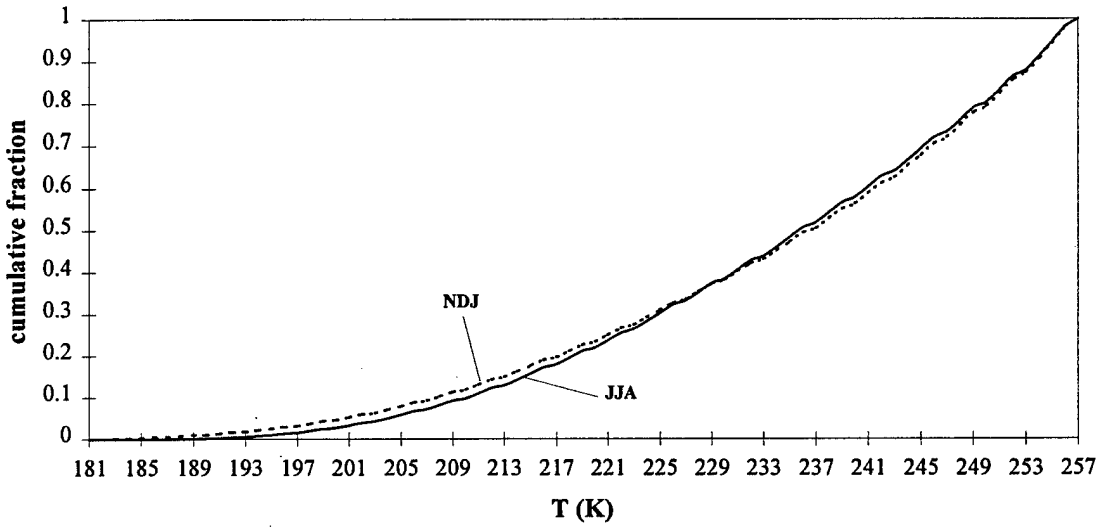

Figure 4.1: Area covered by deep convective cloud as a function of temperature normalized by -15°C cloud cover for JJA (solid) and NDJ (dashed).

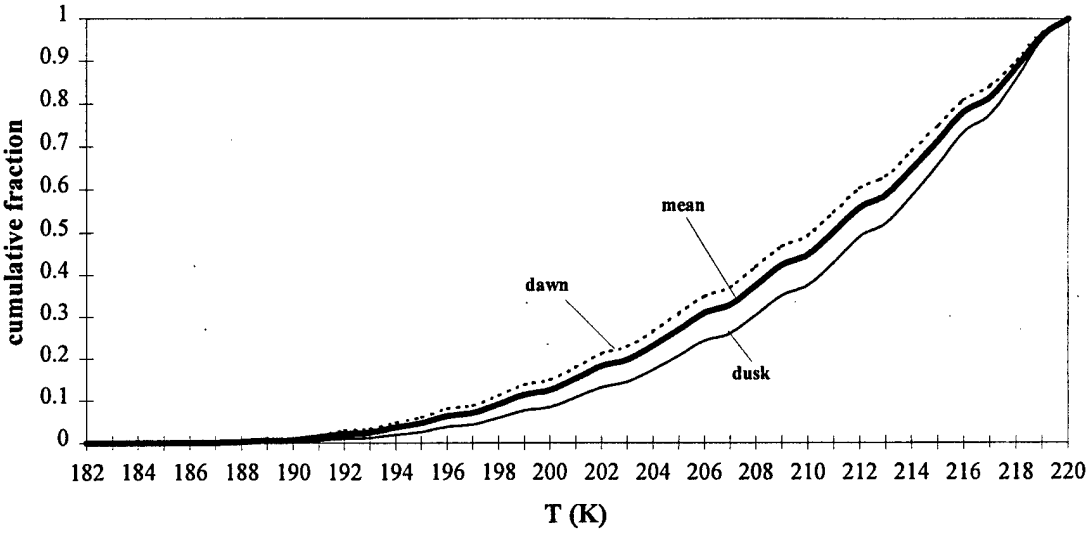

Figure 4.2: JJA area covered by deep convection as a function of temperature threshold normalized by -53°C cloud cover for sunrise (dashed), sunset (thin, solid) and grand mean (thick, solid).

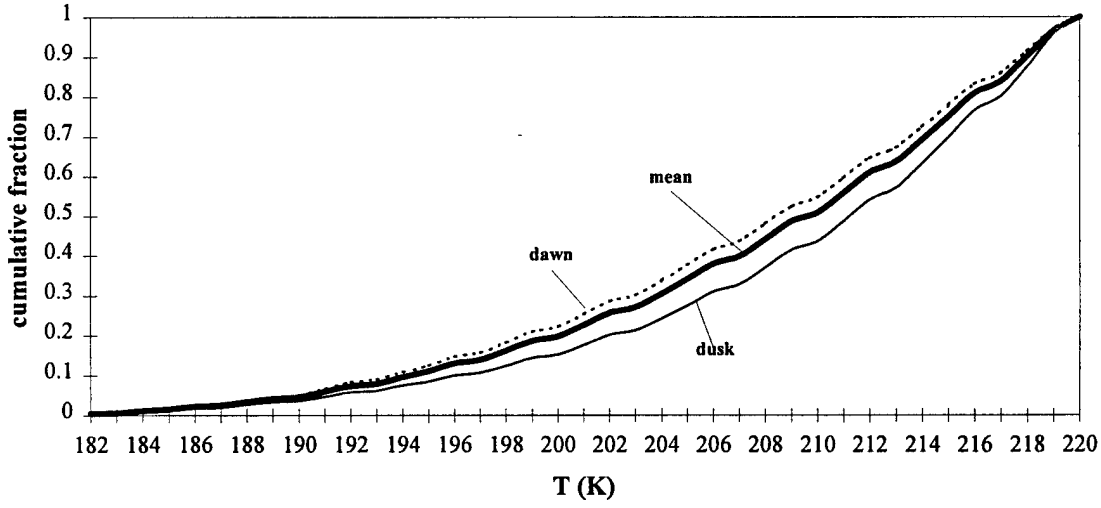

Figure 4.3: NDJ area covered by deep convection as a function of temperature threshold normalized by -53°C cloud cover for sunrise (dashed), sunset (thin, solid) and grand mean (thick, solid)

Several papers indicate a physical basis for this choice. As stated earlier, Reid et al. (1989) show that convection breaching -65°C is comprised of overshooting tops. Muramatsu (1983), Lajoie and Butterworth (1984), Gray and Sheaffer (1995) and Zehr (1987, 1992) show that cloud cover varies with similar phase and amplitude for all thresholds colder than -65°C.

An underlying assumption in using a very cold threshold is that colder cloud-top temperatures (averaged over sufficiently long periods) imply more intense precipitation than cloud tops with warmer temperatures in the tropics. Janowiak et al. (1994) , Liu et al. (1995) and Nelkin et al. (1996) present evidence of this. Janowiak et al. verify from TOGA COARE SSM/I data, optical rain gauge data and ship reports that the heaviest rain events occur within satellite cloud areas colder than -58°C. These intense rain events were found to contribute disproportionately to total rainfall over tropical oceans. Results from Nelkin et al. comparing radar, SSM/I and satellite derived rainfall rates agree with this finding. In a more recent study combining microwave data and IR imagery, Liu et al. found that the maximum contribution to precipitation totals comes from regions of cloud clusters with a cloud top brightness temperature less than -60°C. They also showed that 90-95% of cloud regions with tops colder than -65°C overlie SSM/I derived precipitation within that SSM/I pixel.

Fu et al. (1990) suggest that a sufficiently cold IR threshold will allow an analyst to distinguish deep convective clouds from their associated mesoscale anvils. Comparing VIS and IR imagery, they found a distinct break in the cloud distribution whereby very little bright, cold cloud appears warmer and very little dull-cold cloud appears colder than -43°C. Various other studies support this finding. Steranka et al. (1984) investigated 23 tropical cyclones over the Atlantic Ocean and found that the cloud canopy of tropical cyclones occurs between 10-11 km (~ 40°C) whereas, the mean top altitude of the deep convection was near 12 km (~ 50°C). Hendon and Woodberry (1993), Gray and Sheaffer (1995) and Zehr (1987, 1992) found the coldest T_{BB} normally observed for residual thin stratiform cirrus in the tropics is -45°C. Gray and Sheaffer further state that bright, thick cirrus anvil cloud appears between approximately -40°C and -53°C. Browner et al. (1977), Muramatsu (1983) and Albright et al. (1985) found -50°C to be a cutoff between colder convective cloud and warmer stratiform cloud with very different diurnal cycles. Gray and Sheaffer, Janowiak et al. (1994) and Zehr found a distinct phase shift in the diurnal cycle of cloud colder than about -65°C and cloud between -65°C and -45°C. This indicates that -65°C delineates two different cloud regimes. The balance of recent evidence points to ~ -65°C as the most reliable T_{BB} threshold to identify tropical deep convection in IR imagery. So, based on the theories and observations of many previous studies, I used -65°C as the primary threshold to study the diurnal cycle of WP deep convection and inferred rainfall in the present study.

Chapter 5

Qualitative Overview of Summer 1994 and Winter 1994/95 TWP Convection

The unique high-resolution CHANCES database provides the opportunity to gain new insights into the structural and temporal variation of deep convection in the tropics. In this chapter, I discuss the synoptic settings for JJA and NDJ. I then summarize the qualitative characteristics of the temporal and structural variation of convection in the WP during JJA and NDJ from animated loops of digital IR imagery. As mentioned previously, JJA spans 22 June 1994 - 5 August 1994. NDJ includes 30 November 1994 - 31 January 1995. The WP sector for this study focuses on an area spanning from approximately 0^{o}-20^{o}N, 140^{o}-180^{o}E (Fig. 1.1).

5.1 Synoptic Setting

1994 was a weak El-Nino year (see *Climate Diagnostics Bulletin.* CAC/NMC/NOAA, July 1994). Figure 5.1 shows the synoptic situation for JJA derived from JTWC surface synoptic charts. Convergence was concentrated along the monsoon trough which was oriented northwest to southeast through the WP sector. Low-level easterly trade winds of 10-25 kt characterized the eastern and northern portions of the region while southwesterly to westerly monsoon flow dominated the southwest quadrant. High pressure was centered just north of the region at about 25^{o}-30^{o}N, creating a subsidence regime in the northwest quadrant throughout the summer. Isotherms of SST in Fig. 5.1 were derived from NOAA Reynolds SST data (Reynolds and Marsico 1993) downloaded over the internet from http://ferret.wrc.noaa.gov/fbin/climate_server_debug. SSTs over most of the region were greater than 28^{o}C.

Figure 5.2 is a 2000 UTC composite cold cloud climatology for JJA. The monsoon trough Fig. 5.1 has been overlain on the composite. In this composite, the percentage frequency occurrence of cold cloud at each pixel was calculated as the fraction of total pixels classified as colder than -65^{o}C in IR pictures during the 45 days of JJA. This threshold isolates deep convection as discussed in chapter 4. Therefore, Fig. 5.2 represents the percentage frequency of intense convection. During JJA, deep convection was focused along the monsoon trough region within the 29^{o}C isotherm. Subsidence suppressed convection in the northeast quadrant of the sector.

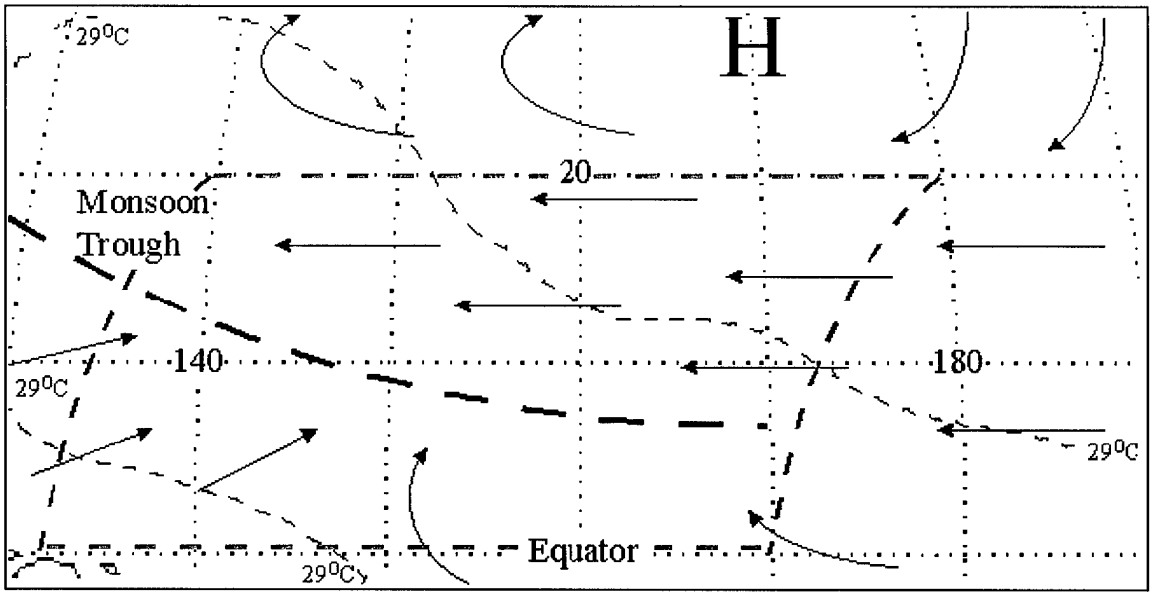

Figure 5.1: Synoptic setting for region of study during JJA derived from JTWC surface charts. The actual WP sector of the present study is outlined by the blue, dashed line.

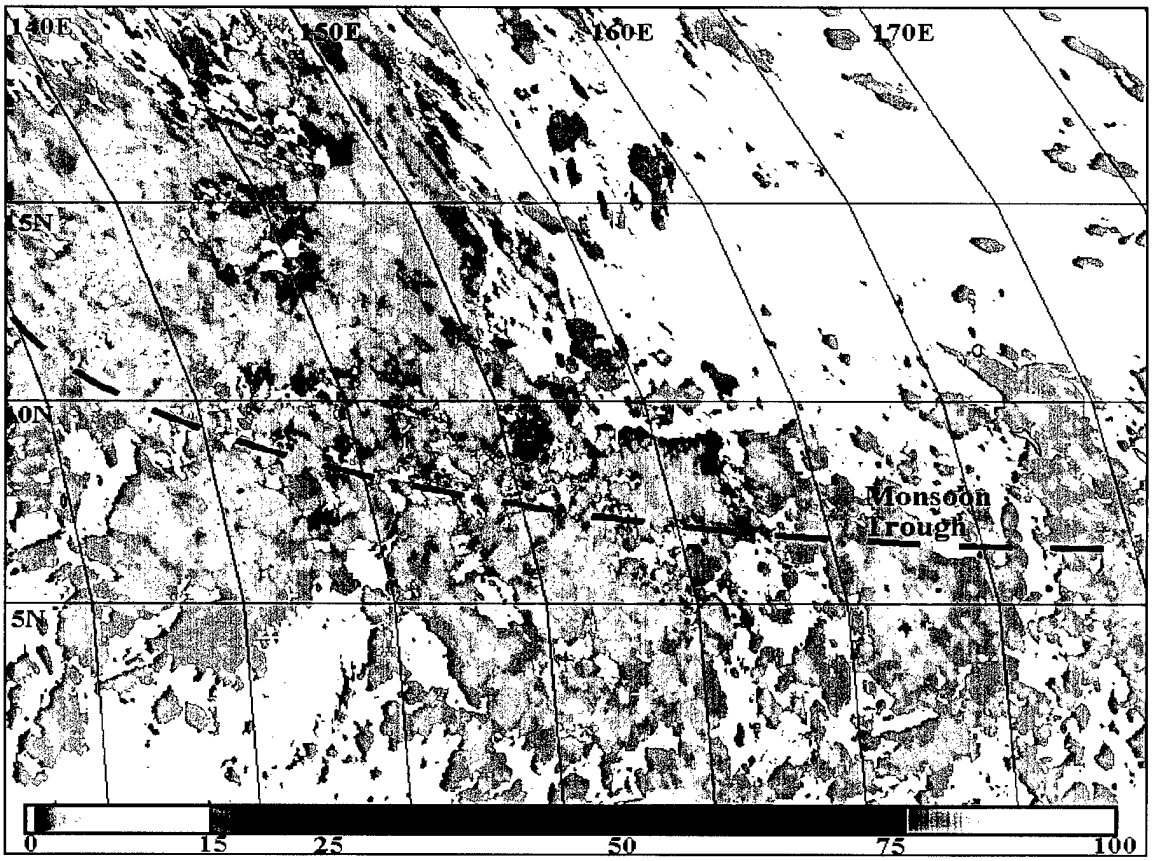

Figure 5.2: Deep convective cloud composite climatology at 2000 UTC for JJA. The percentage frequency occurrence of cold cloud at each pixel was calculated as the fraction of total pixels with $T_{BB} \leq -65^{o}C$ for the period. 0% is colored white. The highest percentages for JJA ranged between 15-20%.

Figure 5.3a is a daytime composite of all cloud created from the CHANCES hourly VIS CNC product described in chapter 4. Each pixel represents the daily average percentage frequency of occurrence of cloud for JJA. Comparison of Fig. 5.3a with Fig. 5.2 reveals that most of the cloud detected at any location was associated with deep convection, occurring at many locations up to ~ 50% of the time. Figure 5.3b is an analogous daytime cloud composite derived from the CHANCES IR CNC product. Comparison with Fig. 5.3a shows a much higher frequency of cloud detected by the IR sensor with many pixels cloudy more than 95% of the time. The presence of a veil of thin, sub-visual cirrus accounts for this difference. A strength of using IR data is the ability to detect thin, cold cloud that is not reflective enough to be detected by VIS sensors (Kidder and Vonder Haar 1995). The thin cirrus reflects the moistening effect of deep convection on the upper levels of the troposphere.

Figure 5.4 depicts the typical synoptic setting for NDJ derived from JTWC synoptic charts. Tropical easterly trades of 10-30 kt dominated the low-level winds with a near-equatorial ITCZ. The convergence was centered between 0^{o}-5^{o}N in December and slid south to between 2^{o}S-2^{o}N during most of January. Convection was largely confined to 0^{o}-10^{o}N (Figs. 5.5a,b) within the 28^{o}C SST isotherm. Synoptic conditions during NDJ were characterized by one complete cycle of the ISO (see *Climate Diagnostics Bulletin*, CAC/NMC/NOAA, January 1995). A convectively active phase occurred during December followed by an inactive phase in January. Figure 5.5 shows composites of deep convection for December (5.5a) and January (5.5b). Comparing the composites, one can quickly identify the reduction in convection during January. During December some areas were covered by deep convection ~ 25% of the time while through January the highest frequency of occurrence was ~ 10%. Two tropical storms developed in the WP sector during December.

5.2 Analysis of Time Sequenced IR Imagery

Animated "movie" loops of IR imagery provided the first qualitative look at cloud in the WP sector. To focus on deep convection, each individual picture was enhanced as in Fig. 2.3. With this enhancement three IR thresholds are highlighted. Active convective cores with cloud tops colder than -65^{o}C appear bright white. These cores are surrounded by a ring of cloud between -65^{o}C and -53^{o}C colored dark black. Cloud top temperatures from -15^{o}C to -53^{o}C representing the rest of the convective tropical cloud shield (Gray and Sheaffer 1995) are white. Colors then fade gradually from white to black as temperatures increase from -15^{o}C to 30^{o}C. As described in chapter 4, results from many previous studies indicate that a -65^{o}C threshold allows the analyst to distinguish deep convective clouds from their associated mesoscale stratiform cirrus cloud canopy. From the enhanced imagery analyzed for the present study, it appeared that

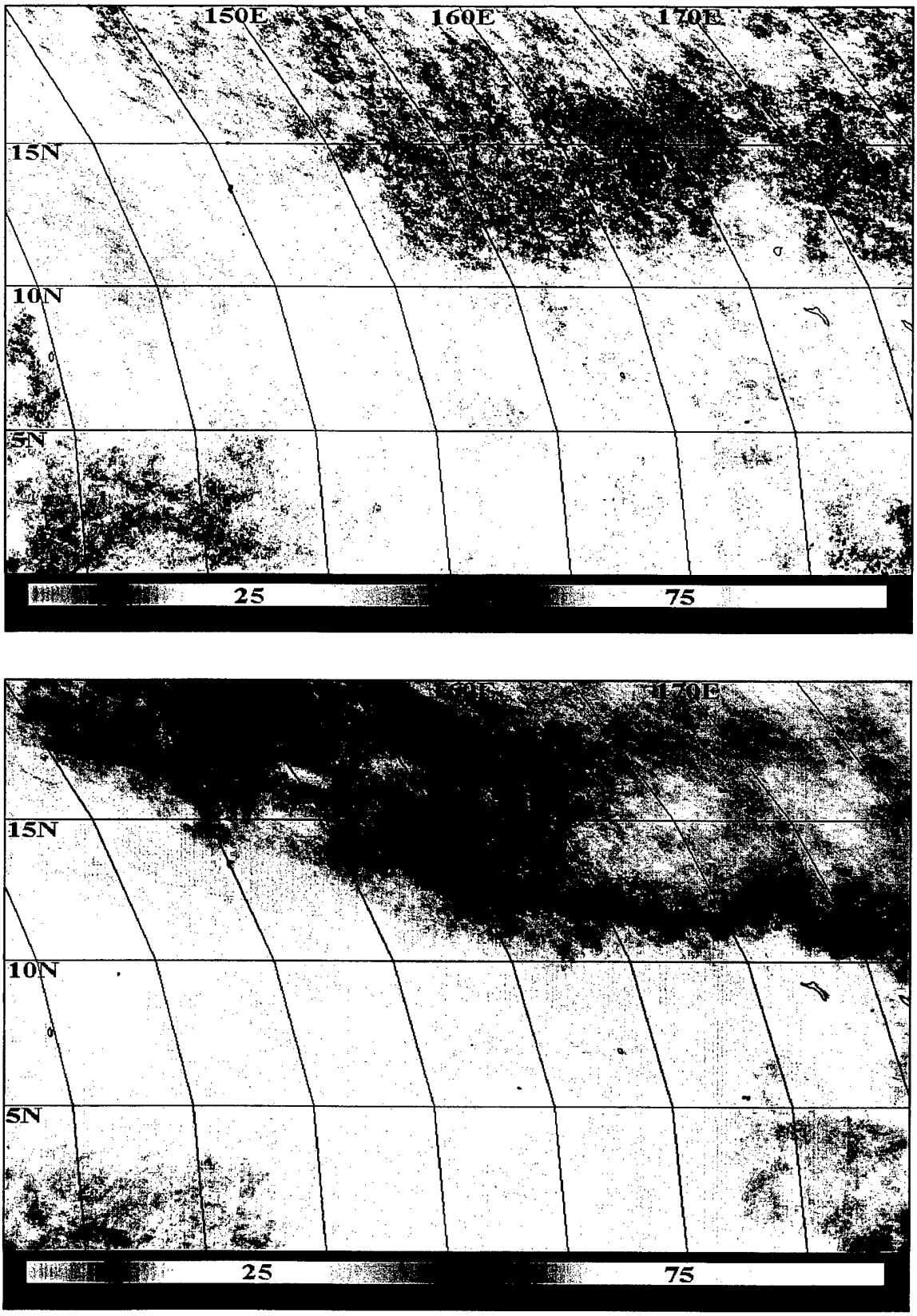

Figure 5.3: (a) Daytime VIS composite of all cloud. (b) Daytime IR composite of all cloud.

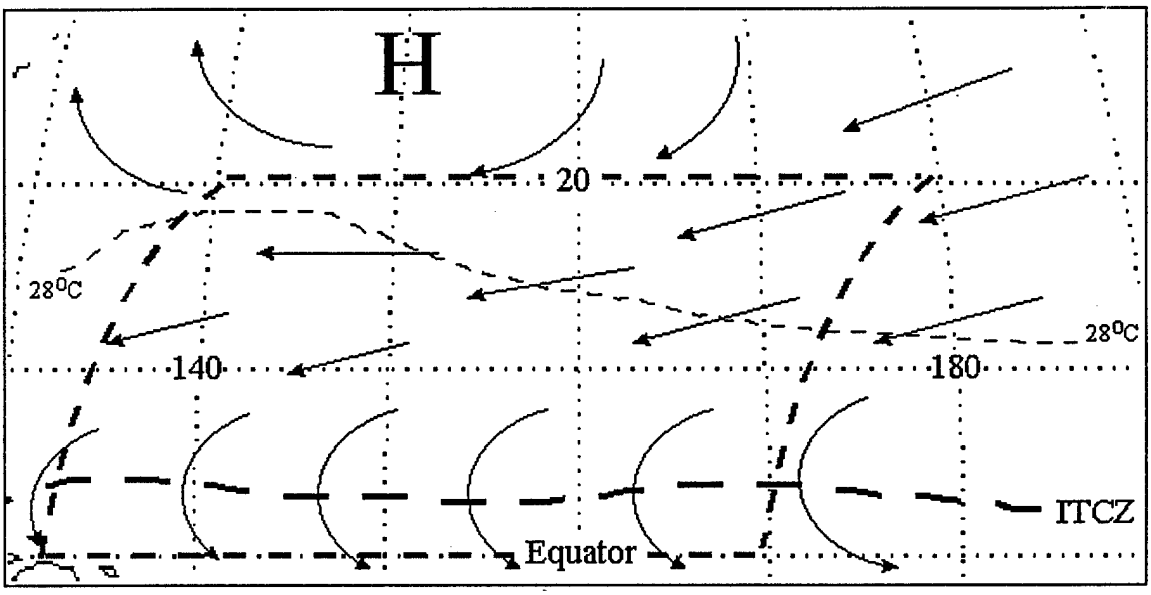

Figure 5.4: Average synopitic setting for region of study during NDJ derived from JTWC surface charts. The WP sector of the present study is outlined by the thick, dashed line.

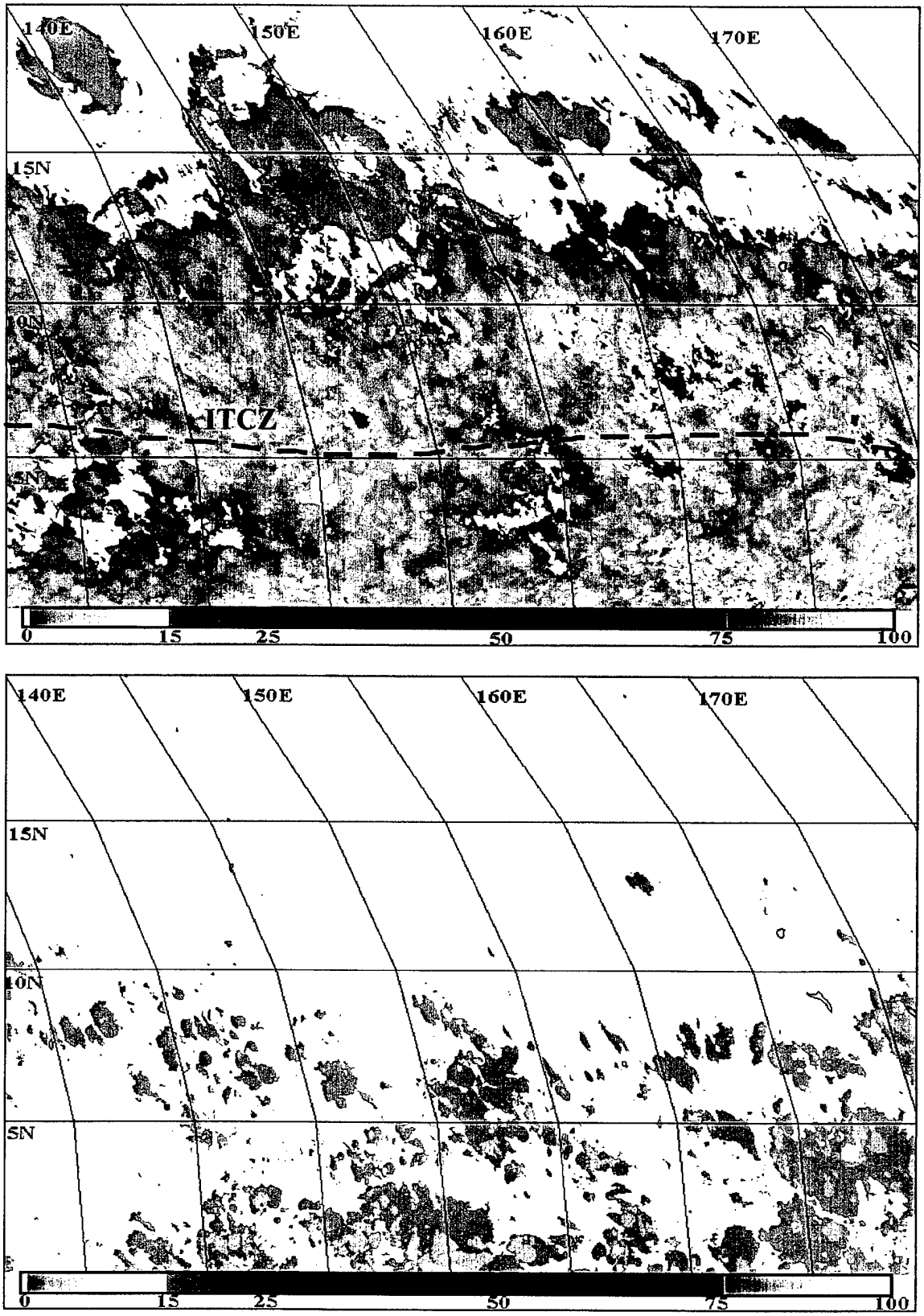

Figure 5.5: (a) As in Fig. 5.2, except for December 1994 (active ISO); (b) January 1995 (inactive ISO).

using a -65°C threshold effectively isolated deep convective cores from their associated stratiform cirrus shields.

Enhanced IR imagery viewed as animated loops revealed that convection on all spatial scales existed at all times of day and night in the WP. Individual organized weather systems grew, reached maturity and dissipated seemingly at random. However, growing clusters persisting into or forming during the night tended to grow spatially larger with more intense convective cores than similar systems during the day. Also, there seemed a greater tendency for downdrafts and colliding cold pools to spark new rapidly growing convection at night than during the day. This observation agrees with the results of Weickmann et al. (1977) of rapidly growing cumulonimbus clouds during GATE. No preference was observed for formation of new convection in clear zones. Based on the imagery, I classified the convective activity into three loosely defined regimes: (1) Undisturbed (persistent, relatively clear conditions); (2) Disturbed (intense convection in the same location for at least two consecutive days); (3) Neutral (spatially and temporally random small or large scale convection).

Several regions of the WP sector were largely undisturbed for each season. For example, in Fig. 5.2 vast areas in the northeast quadrant of the sector show a 0% occurrence of cloud colder than -65°C, indicating that deep convection never occurred there during JJA. Similarly, large undisturbed regions are evident north of 10°N during December (Fig. 5.5a) and throughout the entire sector during January (Fig. 5.5b).

Disturbed regimes are not defined in the opposite sense to undisturbed regimes. In a very general sense, for example, the monsoon trough region was the focus of convection throughout JJA. I have not, however, labeled the trough region as a disturbed regime. Disturbed is a shorter term characterization. On any particular day, the trough region was characterized by convectively active and suppressed zones. However, several times large convective disturbances occurred in one geographic region two or three days in a row. These are the temporary disturbed regimes.

The observations are consistent with the DNS, RCF and LRD hypotheses of the diurnal cycle of tropical convection. They are not consistent with BLML mechanism due to lack of formation in cloud free regions. However, the observations are only qualitative. A quantitative discussion of these data is presented in chapters 6 and 7.

Chapter 6

Short Time Scale Variability of Deep Convection and Associated Cloud

Detailed investigations of short time scale, primarily diurnal, variations of rainfall over tropical oceans date to the late 1950s. From a small data set of six hourly shipboard rainfall measurements, Garstang (1958) found that 50% more rain was measured at night (1800-0600 LST) than during the day (0600-1800 LST). Kraus (1963) used a more extensive data set of three-hourly reports from nine weather ships for the period 1950-61. He found that 50% more rain reports came at night (2100-0600 LST) than during the day (0900-1800 LST) with precipitation most likely during the second half of the night (0200-0600 LST). Lavoie (1963) and Finkelstein (1964) studied the daily cycle of rainfall from measurements taken on various Pacific island stations. Both documented early morning and mid-afternoon precipitation maximums while Finkelstein further found the afternoon maximum to be dominant on larger islands.

Holle (1968) studied the diurnal cycle from 3 cm shipboard radar measurements. The highest cloud tops occurred near sunrise. Radar echoes occurred twice as often between 0200-0500 LST than from 1300-1800 LST. Brier and Simpson (1969) analyzed precipitation from 12 years of hourly Wake Island surface observations and found the rainfall frequency was twice as high at 0500 LST as at 1500 LST. Inchauspe' (1970) found similar results with over 5 years of hourly data from French Polynesian atolls. Maximum rainfall was observed between 0400-0800 LST with an evening minimum between 1200 and 2300 LST. A secondary maximum of precipitation was identified near 1500 LST. Takeuchi and Nagatani (1974) measured lightning activity in the western Pacific using a field mill and a sferics counter tuned to 3 kHz. They observed peak lightning activity to occur between midnight and early morning. Ruprecht and Gray (1974, 1976) reported a significant diurnal variation for cloud clusters with morning (0700-1200 LST) heavy rainfall amounts (> 1.0 cm/hr) more than two and a half times greater than early evening amounts (1900-2400 LST) in the west Pacific.

Despite these early studies, the notion of a significant diurnal oceanic cycle of rainfall was not largely accepted until a paper by Gray and Jacobson (1977). Observational evidence cited in that paper comes from Jacobson (1976) which was undertaken to further study the diurnal variations documented by Ruprecht and Gray. Jacobson analyzed rainfall data from eight west Pacific atolls (from March through October) for the period 1961-1973. His results showed that in all cases an early morning maximum occurs between 0300 and 0600 LST. Larger islands also had a significant afternoon maximum attributed to

daytime surface heating. In agreement with Ruprecht and Gray, heavy rain events (> 25 mm/hr) were responsible for the morning rainfall maxima. Subsequent to Jacobson (1976), atmospheric scientists began to rely primarily on satellite and radar remote sensing techniques to study the diurnal problem (eg; Kidder and Vonder Haar 1977; McGarry and Reed 1978; Riehl and Miller 1978). Various studies have focused on tropical regions around the world. Below, I summarize diurnal studies that have focused on or included the west Pacific in their analysis.

Kidder and Vonder Haar (1977) studied oceanic precipitation frequencies from Nimbus 5, 19.35 GHz microwave data. Their results showed an increasing tendency for heavier tropical precipitation events to occur near local noon. Dorman and Bourke (1979) documented an evening or very early morning rainfall maximum from ship observations. A study of outgoing IR values in the water vapor window measured by scanning radiometers aboard a polar orbiting NOAA satellite was made by Short and Wallace (1980). Their analysis of clouds over the tropical oceans revealed a three-tier structure with a pronounced morning bias in the frequency of dense cirroform clouds of possible convective origin.

Murakami (1983) studied western Pacific deep convection using GMS-1 IR data. Murakami developed an index to quantify convection defined by the difference between the satellite observed T_{BB} and 400 mb GMS standard atmospheric temperature. The results showed a positive anomaly (indicating more intense convection) over a large portion of the western Pacific in the early morning. Muramatsu (1983) used GMS-1 IR data and found four regimes of cloud variability associated with mature typhoons. Areal coverage of cloud top colder than -70°C maximized at 0600-0730 LST and minimized between 1500-2100 LST. Cloud in the ranges -70°C to -50°C, -50°C to -30°C and -30°C to 0°C peaked at 0900-1200 LST, 1500-1800 LST and near 2100 LST, respectively. Lajoie and Butterworth (1984) found that cloud top area of tropical cyclones with T_{BB} less than -65°C peaks around 0300 LST. The minimum occurs near 1800 LST. A slight secondary maximum occurs at local noon. Augustine (1984) also used geostationary IR imagery in a Pacific Ocean diurnal rainfall study. Augustine applied the Griffith and Woodley Technique (Griffith et al. 1976; Woodley et al. 1980) to generate satellite-derived rain estimates from archived SMS-2 IR digital data. Then he used a harmonic analysis technique (Panofsky and Brier 1968) to determine which component frequencies accounted for the variance. His results showed most of the variance was accounted for by frequencies at 12 and 24 hours. Semi-diurnal maxima occurred in mid-afternoon and near dawn, local time. Minima occurred approximately two hours before local noon and between 2200 and midnight.

Albright et al. (1985) used GOES-West IR satellite data (~ 1.5° latitude/longitude and 3 hourly resolution) from January-February 1979 to study the diurnal variation in the central tropical Pacific. They analyzed the variation of cold cloud at 1°C intervals from +30 to -90°C. They found the deepest clouds, with tops cooler than -65°C, to exhibit maximum areal coverage near sunrise and minimum coverage near

sunset in all geographic locations. The time of the maximum is delayed with decreasing cloud-top altitude. Clouds with tops between -30 and -50°C in the ITCZ show a large diurnal variation but with maximum coverage between 0900 and 1300 LST and a minimum near midnight. Zehr (1987, 1992) documented similar findings for tropical cyclones. Zehr reported a single-cycle, large amplitude diurnal variation with a morning peak of cold cloud area (T_{BB} < -65°C). The minimum follows by 8 to 12 hours. The maximum extent of thin stratiform cirrus (-15°C < T_{BB} < -45°C) occurs near 1800 LST. Intermediate cloud temperatures (-45 to -65°C) show a preference for maximum area around local noon.

Meisner and Arkin (1987) and Shin et al. (1990) used GOES IR data from the Visible Infrared Spin Scan Radiometer (VISSR). The three-hourly data was retrieved from the NOAA/Climate Analysis Center where it is archived by classifying the brightness temperature into a histogram of 16 temperature classes for every 2.5° x 2.5° grid box. Using a -53°C threshold, Meisner and Arkin found that the maximum at most points occurred near 0900 LST. At much warmer thresholds, they used -2°C to identify all cloud in the tropical shield. At this threshold, maxima between 15°N and 15°S generally occur near 1800 LST. Shin et al. (1990) quantified the diurnal variability of area averaged satellite GPI derived rainfall through spectral analysis. The region in their study partially overlaps the eastern edge of the WP sector of the present study. In this region he found a mid-afternoon diurnal maximum. Shin et al. also discussed a possible weak semi-diurnal cycle.

Fu et al. (1990) partitioned rainfall in the tropics into deep convective cloud and cirrus anvil cloud components using an IR threshold that closely approximated daytime cloud classification from a bispectral (combined IR and VIS data) technique. They found that the frequency of the cirrus anvil component exhibits a peak in the afternoon, while the deep convective cloud portion peaks 9-12 hours earlier. Fu et al. also found the diurnal amplitude is greater the more intense the convection. About one year later, Sharma et al. (1991) estimated the diurnal cycle of oceanic precipitation from 12 months of Special Sensor Microwave Imager (SSM/I) data. Their results showed strong evidence in favor of the existence of a modest diurnal cycle of oceanic rainfall. In a similar study, Chang et al. (1995) documented a nocturnal or early morning rain maximum in most oceanic areas where the total precipitation is high.

Mapes and Houze (1993) took a different approach to the west Pacific diurnal problem. Mapes and Houze applied a technique developed by Williams and Houze (1987) to objectively identify and track areas or cloudiness with T_{BB} less than a specified threshold. This allowed them to study the diurnal cycle in relation to the structure of cloud clusters. Defining cloud clusters by closed -65°C isotherms they found that the overall diurnal cycle of cold cloud area is dominated by the variation of the largest quartile of detected clusters (> 65000 km^2). The greatest total number of large clusters occurs during the early morning. Fewer large clusters occur during the evening. These findings are supported by Chen et al.

(1996) and Chen and Houze (1997) who also report that the characteristic occurrence and lifecycle of clusters varies during active versus inactive phases of the ISO. Active phases of the ISO contain large clusters with a predominant morning maximum as described above. Inactive phases of the ISO, however, are characterized by relatively small scale convection which tends to maximize in the late afternoon (Chen and Houze 1997).

Hendon and Woodberry (1993) examined the diurnal cycle of convection over the global tropics through spectral analysis of time series constructed from ISCCP IR cloud data. They found the diurnal cycle of oceanic convection at a singular geographic point difficult to distinguish from background convective variance. This led them to question the occurrence of a significant peak at the diurnal frequency for all oceanic regions including the WP sector in the present study. The part of the signal they could discern showed a weak morning convective maximum over the west Pacific ITCZ with a peak in warmer stratiform cloud about 6 hours later. A latitudinal structure of deep convective activity was identified over the western Pacific ITCZ. Deep convection forms near dawn just off the equator and propagates poleward toward the center of the ITCZ over the course of several hours. Zonally averaged, the diurnal cycle of deep convection showed significant spectral power with minimal latitudinal phase variation.

Janowiak et al. (1994) performed a harmonic analysis on the seasonal means of fractional coverage of cloud at three T_{BB} thresholds (-38°C, -48°C and -58°C). In the WP, they found the daily peak in deep convection to occur at about 0600 LST. The minimum occurs around 1800 LST. Precipitation totals computed from SSM/I, optical rain gauge data, and ship reports showed that 50% of the total rainfall is provided by the heaviest 10-15% of the observations, with 30% contributed to the total by the heaviest 5% of all observations. These heavy rain events tend to occur in the predawn hours, spatially and temporally concurrent with the maximum fractional coverage of cloud colder than -58°C.

Gray and Sheaffer (1995) conducted an observational study of the diurnal cycle of intense tropical convection using 7 years of ISCCP stage B-1 satellite cloud data. They examined the entire range of T_{BB} for the WP in 5°C increments, from -100°C to +30°C. Very warm pixels (> +10°C) were considered to represent "relatively cloud free" areas. A strong expansion of these warm areas occurs at night. Sharp drop offs in total pixel counts were documented at ~ -45°C and ~ -65°C. These were interpreted to be cut-offs between various convective regimes. the -45°C level is where active convection becomes separated from mixed convection and residual stratiform cloud while -65°C is the approximate beginning level for overshooting convective plumes. Fractional coverage of clouds colder than -65°C peaks around 0300 to 0600 LST. Warmer stratiform cirrus clouds initially increase in phase with the very coldest clouds but go on to achieve their maxima near 1200-1500 LST. A distinct phase propagation of increased pixel

incidence occurs from the coldest cloud in the early morning through to the -30°Cto -20°C domain by late afternoon. Gray and Sheaffer identify four distinct component diurnal cycle modes; < -60°C, -60°C to -20°C, -20 to 0°C and warmer than 0°C.

In another recent project, Bergman and Salby (1996) studied diurnal variations in cloud cover using 2.5° spatial resolution ISCCP-C2 cloud statistics. High cloud for these data is defined in terms of fractional cover of cloud with cloud-top pressure less than 440 mb (~ -15°C). Similar thresholds have been used by other authors (Table 1) to represent the total stratiform cirrus tropical cloud shield. Over the WP, maximum high cloud fraction occurs between 1630 and 1930 LST. A slight secondary maximum occurs near 0500 LST associated with deep convection.

Rickenbach and Rutledge (1996) studied the dependence of diurnal convective variation on convective organization from 90 days of TOGA COARE radar data. They found a weak diurnal rainfall variation hypothesized to result from the superposition of stronger individual rainfall variations associated with separate organizational modes. The most significant diurnal rainfall variation occurs with nonlinear MCS scale events which maximize near 0230 LST. Linear MCS scale events showed evening maxima. Sub-MCS scale non-linear events displayed significant diurnal and semi-diurnal variation. Nelkin et al. (1996) also document a possible semi-diurnal cycle during TOGA COARE.

Most of the foregoing literature delineates distinct diurnal maxima and minima associated with deep convection and/or its associated stratiform cirrus cloud shield. Brier and Simpson (1969), Augustine (1984), Steranka et al. (1984), Shin et al. (1990), Nelkin et al. (1996) and Rickenbach and Rutledge (1996) suggest that some of the observed diurnal variability of rainfall could be based in a semi-diurnal variation. Other authors suggest that the diurnal variation might also be related to a bi-diurnal (two day) cycle. Chen et al. (1996) conclude that deep convective activity in the equatorial warm pool region is modulated strongly by wavelike disturbances. In their study, convection was frequently concentrated into westward-propagating disturbances with a local periodicity of ~ 2 days. Chen and Houze (1997) suggest this local bi-diurnal oscillation is driven by large convective systems. They call this oscillation *diurnal dancing* (as described in chapter 3) and hypothesize that it works in concert with westward-propagating near equatorial interio-gravity waves of quasi-2-day periodicity as described by Takayabu et al. (1996). The existence of a quasi-2-day mode is also mentioned in Lau et al. (1991) and Hendon and Liebmann (1994). Gray and Sheaffer (1996) consider a two-to-three day cycle. They suggest that convective debris following an outbreak of intense convection could hinder the DNS mechanism at a particular location by filling the upper levels with stratiform debris and water vapor. This upper level moisture could temporarily reduce clear region radiative cooling and hence reduce nocturnal subsidence.

In this chapter, I document the phase and day-to-day variability of deep convection and its associated cloud in the WP for JJA and NDJ. I examine time scales of variability through Fourier decomposition of cold cloud pixel time series using the lag correlation method. Diurnal histograms of hourly cold cloud areal coverage define the phase and amplitude of variation at various T_{BB} thresholds. These IR thresholds were defined from analysis of IR data at $1^{o}C$ T_{BB} intervals.

6.1 Spectral Analysis of Deep Convection Time Series

With 5-km spatial and 1-hr temporal resolution, CHANCES is well suited for time series analysis. I have constructed time series of hourly cold pixel counts for JJA and NDJ. In this section I describe the method, results and implications of a spectral analysis of these time series.

Method/Results

Figures 6.1 and 6.2 are hourly time series of cold cloud pixel counts. Each hourly count is simply the arithmetic sum of all pixels in the entire sector with T_{BB} less than $-65^{o}C$. As such, each count represents the presence of that amount of deep convection. Figure 6.1 is a time series of deep convection for 30 June 1994/0600 UTC through 19 July 1994/2300 UTC. Figure 6.2 is a similar time series for 29 November 1994/0000 UTC through 31 January 1995/2300 UTC.

During JJA, deep convection was active throughout the time series with a local maximum during the first few days of July. Through the 45 days of JJA, deep convection did not detectably vary on time scales longer than 7-10 days. However, during the winter two distinct phases of the 30-45 day ISO occurred. The ISO strengthens in winter (Falvey 1992). In Fig. 6.2, the blow up of cold pixel counts in December implies an active phase of the ISO while the relative paucity of very cold pixels during January reflects the inactive phase.

Power spectra for these time series were computed using the standard lag-correlation method. All power spectra were computed using a 10 day lag. Figure 6.3 shows the power spectrum for the time series in Fig. 6.1. The thin dashed lines represent the background red noise spectrum and its 95% confidence limit (a priori). All spectra in this study were normalized by the total variance. The 95% confidence limit in Fig. 6.3 was computed assuming two individual spectra were independent. Spectral peaks occurred at one day and two days consistent with my visual impression of the time series. The diurnal peak is statistically significant at the 95% level above the red noise background. There was no detectable semi-diurnal variation of cold cloud (0.5 days).

The NDJ power spectrum is shown in Fig. 6.4. As with JJA, a dominant spectral peak occurs at one day significant at the 95% level. The 95% confidence level was computed assuming six degrees of

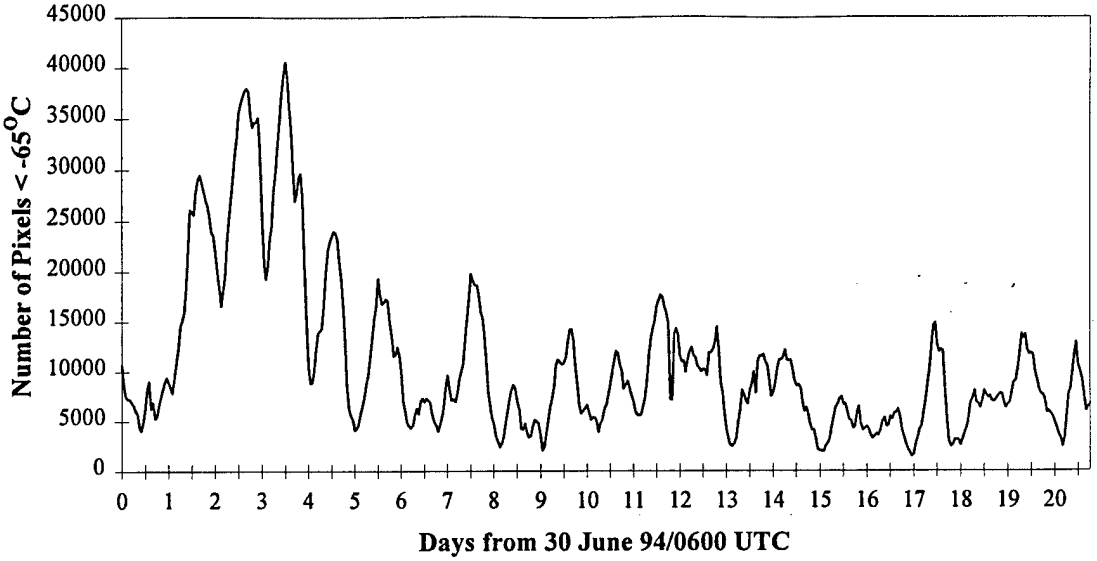

Figure 6.1: Hourly time series of deep convection pixel counts for 20 days of JJA. Each hourly count is simply the arithmetic sum of all pixels in the entire sector with cloud-top $T_{BB} \leq -65^{o}C$.

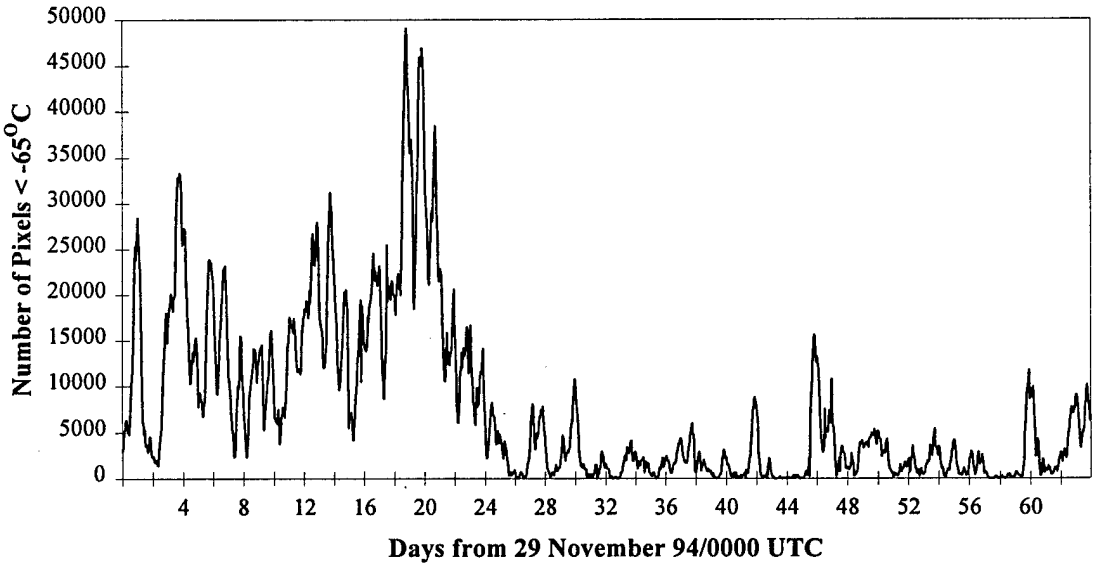

Figure 6.2: As in Fig. 6.1, except for the time period NDJ.

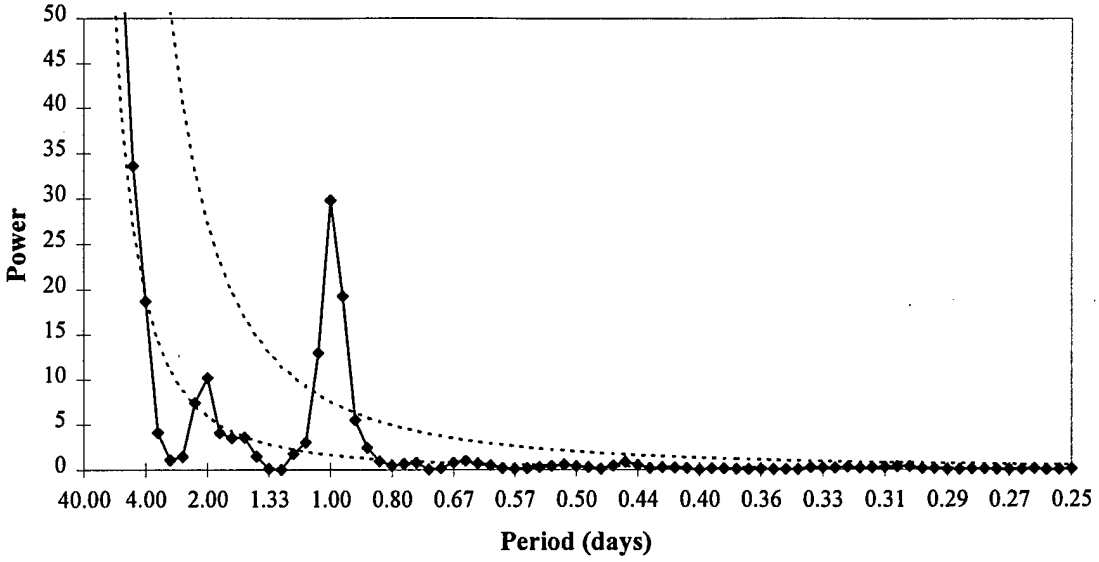

Figure 6.3: Power spectrum for JJA time series in Fig. 6.1. Dashed lines represent the background red noise spectrum and its 95% confidence limit (a priori). The 95% confidence limit was computed assuming two degrees of freedom in 20 days of data.

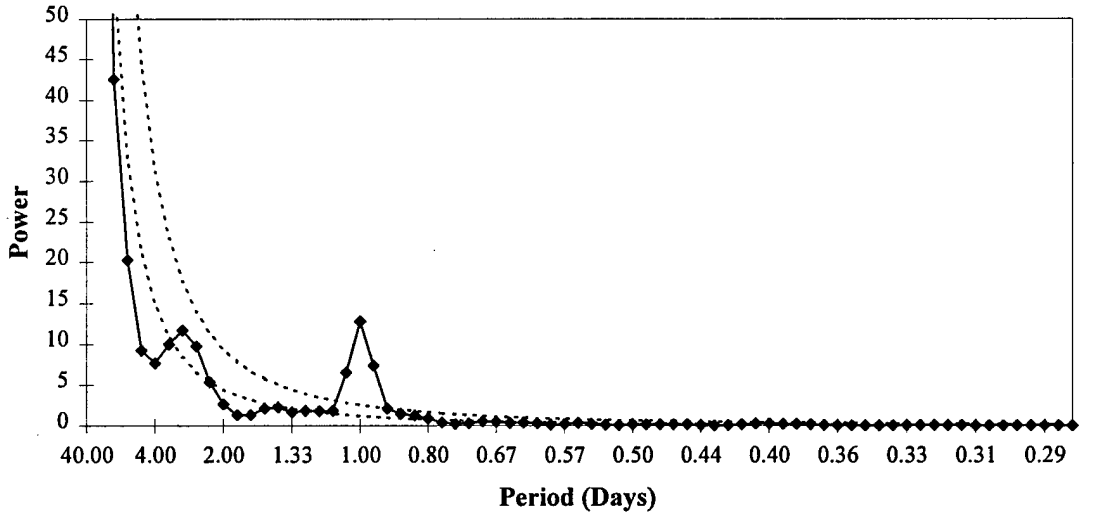

Figure 6.4: Power spectrum as in Fig. 6.3, except for NDJ time series (Fig. 6.2). The 95% confidence limit was computed assuming six degrees of freedom in 64 days of data.

freedom. There is a suggestion of a peak at three days, although it is well below the 95% confidence level (a posteriori, not shown). As in JJA, there is no semi-diurnal peak. To further analyze the NDJ data, the time series were separated into active and inactive phases of the ISO. Fig. 6.5 is the power spectrum for 29 November 1994 through 28 December 1994 (active phase). A significant spectral peak occurs at one day. As in Fig. 6.4, the peak at three days is not significant to the 95% level. The power spectrum for the inactive phase (January 1995) is shown in Fig. 6.6. Spectral peaks significant at the 95% confidence level occur at one day and two days. Peaks at ~ 30 hours and about four days are not significant at the 95% confidence level (a posteriori).

As mentioned above, Takayabu et al. (1996) and others document a quasi-2-day convective variation hypothesized to be driven by near-equatorial waves. Since the power spectrum for JJA identified a significant two day spectral peak, I divided the larger WP sector into two sub-sectors. One sector encompassed an off-equatorial region spanning 5^{o}-20^{o}N. The other sector was a near-equatorial region limited to 0^{o}-5^{o}N.

Figure 6.7 is the time series of near-equatorial deep convection for JJA and Fig. 6.8 depicts the corresponding power spectrum. As in Fig. 6.3, the diurnal cycle dominates with a secondary spectral peak at two days significant near the 95% confidence level consistent with a visual inspection of the time series. Figure 6.9 shows the 24-72 hr band pass filtered (48 hr) cycle of deep convection for the near-equatorial time series. Each value in Fig. 6.9 is the difference between the 24 hr and 72 hr running means. As indicated, a faily regular bi-diurnal cycle occurs through much of the time series. The maximum-minimum pair from hours 132-156 is an artifact created by convection which advected northward out of the near-equatorial sector. During the first 24 hours, a tropical depression (TD 08W, the beginnings of Tropical Storm Tim) formed south of 5^{o}N in the western part of the WP sector creating a convective maximum around hour 132. The following day, it moved north of 5^{o}N creating an artificial convective minimum near hour 156 in Fig. 6.9. The regular two day cycle from hours 36-84 and 156-468 is not disrupted by these type of effects. From IR imagery it appears that disturbances randomly located throughout the near-equatorial region, grew relatively more intense every other day. Also, there was a tendency for disturbances to advect into the region from the east every 48 hours. *Diurnal dancing* associated with convection forming every other day in any particular location, was not observed.

Figure 6.10 shows the power spectrum for the off-equatorial region. As in Fig. 6.3, spectral peaks occur at one day and two days. There is less power at both peaks for the off-equatorial than for the near-equatorial region. The peak at two days is prominent above the red noise background but not significant at the 95% confidence level. Figure 6.11 depicts the band pass filtered 48 hr cycle of deep convection for the off-equatorial time series (not shown), analogous to Fig. 6.9. In Fig. 6.11, a clear quasi-2-day oscillation of

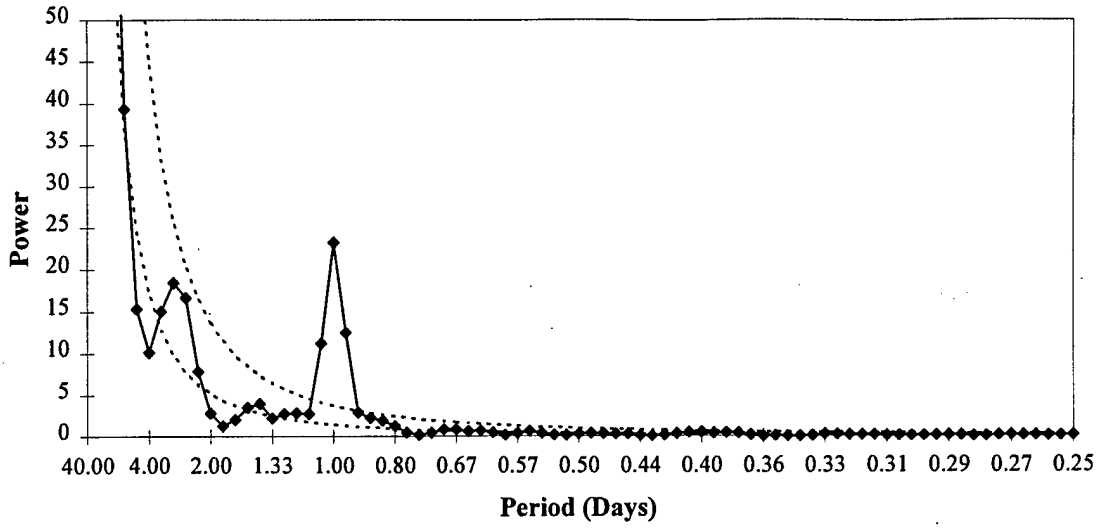

Figure 6.5: Power spectrum as in Fig. 6.3, for time period 29 November-28 December 1994 (active ISO). The 95% confidence limit was computed assuming three degrees of freedom in 30 days of data.

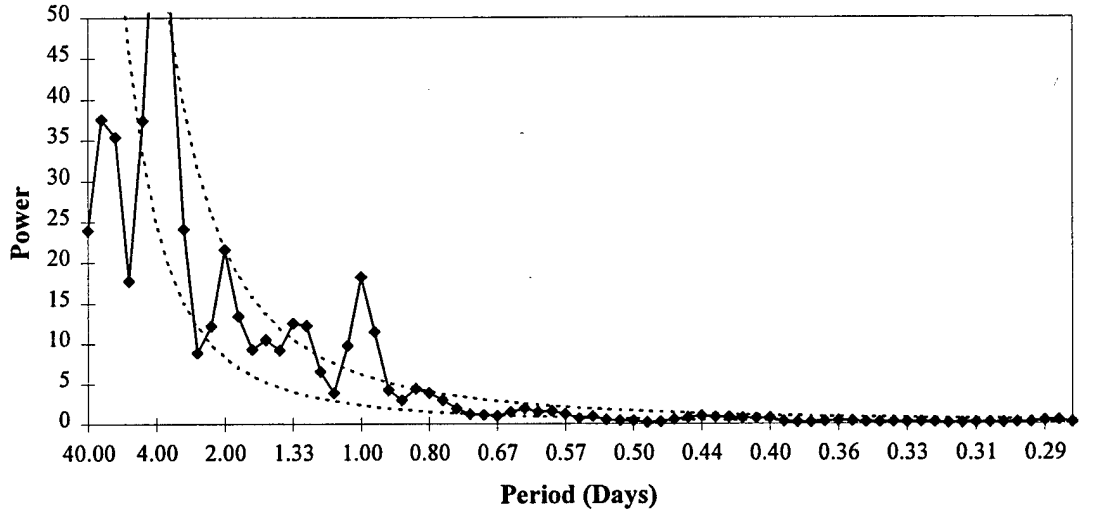

Figure 6.6: Power Spectrum as in Fig. 6.3, for the period 1-31 January 1995 (inactive ISO). The 95% confidence limit was computed assuming three degrees of freedom in 31 days of data. Peaks at ~ 1.3 days and ~ 4 days are not significant at the 95% level (a posteriori).

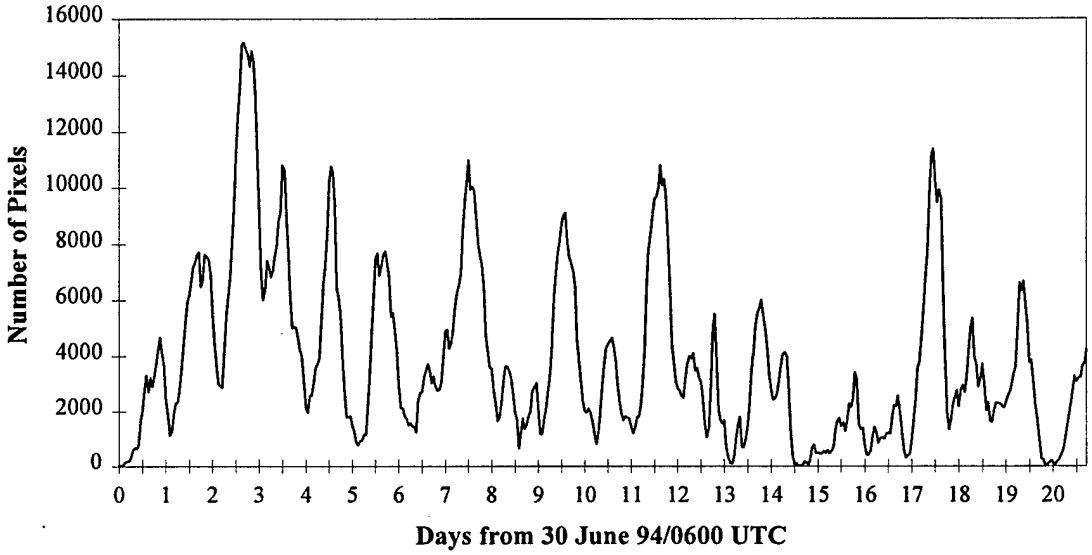

Figure 6.7: Hourly time series of cold cloud pixel counts for JJA as in Fig. 6.1, except limited to the near-equatorial region (0^{o}-5^{o}N).

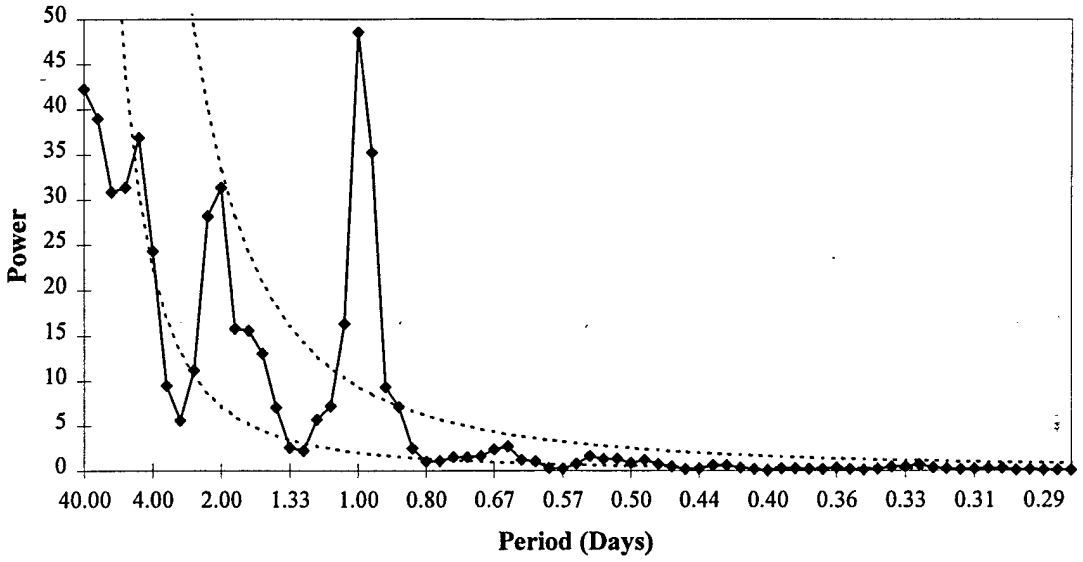

Figure 6.8: Power spectrum as in Fig. 6.3, except for the near-equatorial (0^{o}-5^{o}N) time series in Fig. 6.7.

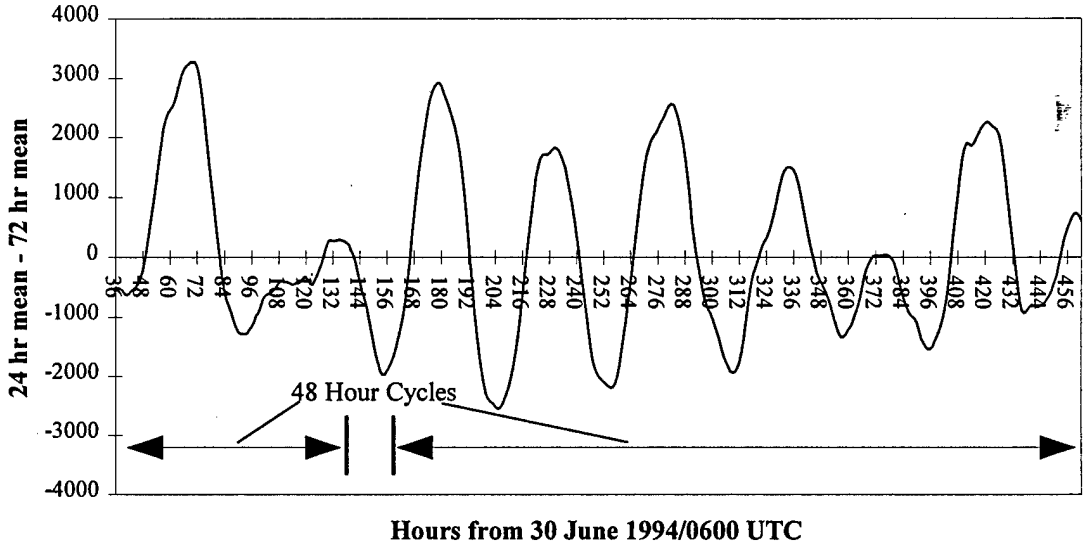

Figure 6.9: Band pass filtered 48 hr (bi-diurnal) cycle of deep convection computed from near-equatorial time series in Fig. 6.7. At each hour, the value is the difference between the 24 hr and 72 hr running means.

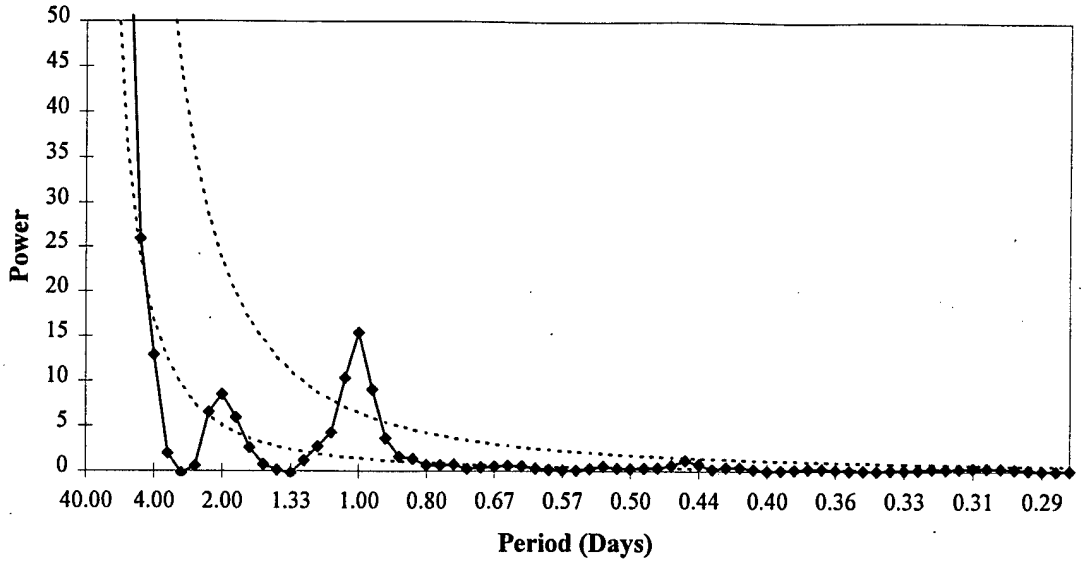

Figure 6.10: Power spectrum as in Fig. 6.3, but for off-equatorial region (5°-20°N) during JJA.

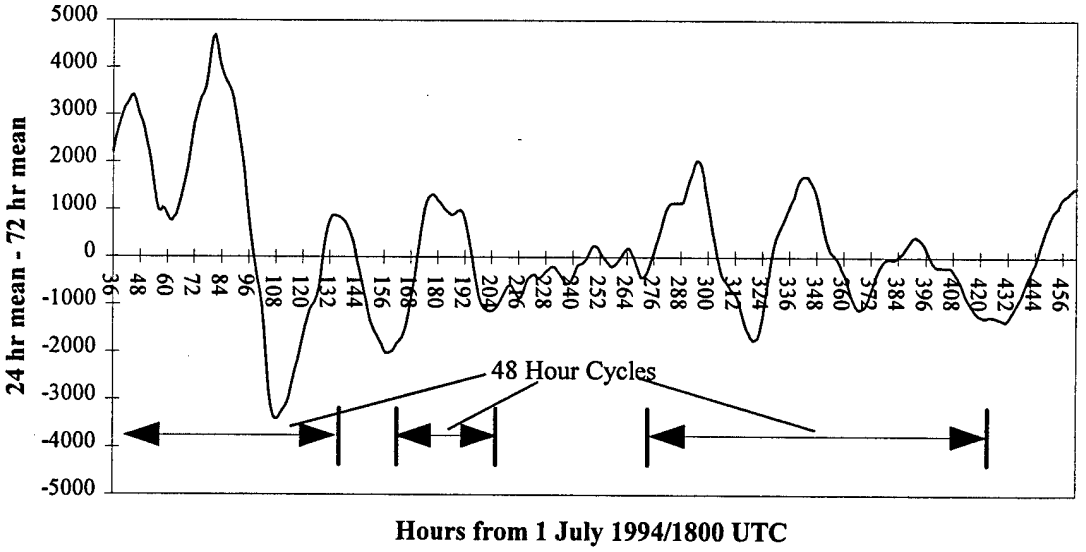

Figure 6.11: As in Fig. 6.9, except for off-equatorial region (5°-20°N) during JJA.

convection occurred from about hours 36-132, 156-204 and 276-420. From analysis of IR imagery, I have excluded the maximum-minimum pair from hours 132-156. During the preceding 24 hr period, TD 08W (as mentioned above) formed in JJA while a large area of intense convection dissipated in the off-equatorial sector. By hour 132, TD 08W moved northwest into the off-equatorial sector creating a maximum. The following morning, TD 08W moved off the western edge of the image creating a minimum. The bi-diurnal cycle from hours 36-120 occurred during a blow up of convection evident between hours 24 and 120 in Fig. 6.1. The convection from hours 24-72 in Fig. 6.11 was associated with a spatially large region of cloud clusters that formed in the about the same place both days. The active region expanded to the east on the second day, creating a relative maximum from hours 48-72. The bi-diurnal cycle evident from hours 156-204 is not completely independent from the cycle shown for the same period of time for the near-equatorial sector shown in Fig. 6.9. A single large cluster caused the maximum in both regions. The bi-diurnal cycle occurring from hours 276-396 occurred during a relatively suppressed period. Although the signal is real, an inspection of imagery reveals no apparent direct spatial relation between day-to-day outbreaks of convection (i.e.; d*iurnal dancing* was not observed).

Discussion

Of all the satellite studies cited in the beginning of this chapter, only Augustine (1984), Hendon and Woodberry (1993) and Janowiak et al. (1994) quantified deep convection in the same WP sector considered in the present study. Augustine found a significant semi-diurnal cycle. However, the very warm threshold he used best represents area averaged stratiform rain, rather than intense, deep convection. The results of the present study agree most closely with the harmonic analysis performed by Janowiak et al. (1994) and spectral analysis of zonally averaged deep convection by Hendon and Woodberry (1993). Findings show significant power in the diurnal cycle of deep convection during summer and winter both near and far from the equator. On a slightly longer time scale, the present study found a statistically significant large scale near-equatorial bi-diurnal cycle from satellite data and demonstrated that a two day cycle may occur at all tropical latitudes of the tropics up to 20^{o}N. Longer records are needed to confirm the existence of a bi-diurnal variation that exceeds the 95% confidence limit. Contrary to the conclusions of Brier and Simpson (1969), Augustine (1984), Shin et al. (1990) and Nelkin et al. (1996), this study shows no semi-diurnal variation of deep convection. This latter result supports the contentions of Gray and Jacobson (1977), Lindzen (1978) and McBride and Gray (1980) that the magnitude of pressure variations caused by the S_2 tides are too small to influence deep convection.

Several authors have recently considered a bi-diurnal cycle. Takayabu et al. (1996) documented a quasi-2-day cycle in TOGA COARE data which they related to near-equatorial inertio-gravity waves.

Chen et al. (1996) and Chen and Houze (1997) hypothesized that such near-equatorial waves are part of a more significant local, bi-diurnal, BLML driven spatial variation of convection which they term "diurnal dancing" (chapter 3). However, Chen and Houze also note that the occurrence of *diurnal dancing* would not necessarily lead to an apparent two day oscillation of cold pixel counts in a time series with values derived from a large area. Convection every other day in some local geographic region (eg.; TOGA COARE intensive flux array) does not disallow active, deep convection area averaged over a larger geographic region to have only a diurnal peak. Gray and Sheaffer et al. (1996) suggest that upper level moisture from convective outbreaks could impede the DNS diurnal mechanism giving the possibility of a bi-diurnal cycle in near and far equatorial regions. To test these ideas I divided the WP sector into the near equatorial region (0^{o}-5^{o}N) and the off-equatorial tropics (5^{o}-20^{o}N).

For both near and off-equatorial regimes (Figs. 6.8 and 6.10) the power at two days is secondary only to the diurnal cycle. The two day oscillation for the near-equatorial sector occurred through most of the time series (Fig. 6.9). A weak bi-diurnal cycle occurred in the off-equatorial region about one third of the time (Fig. 6.11). This cycle occurred on such a large scale that a two-day periodicity of cloudiness did not necessarily occur at a fixed longitude. As stated previously, the presence of a strong, regular two day cycle in the near-equatorial region supports Takayabu et al. (1996). However, the presence of a possible two day cycle in the off-equatorial region implies other mechanisms could be at work.

Results presented in chapter 5 (Figs. 5.3a,b) suggest that convection adds moisture to the upper troposphere. Average conditions over the tropical oceans consist of a very moist boundary layer (~ 85% relative humidity) and very dry middle and upper levels (Webster 1994). Due to the concentration of moisture in the low-levels, the top of the marine boundary layer acts as the effective radiating surface. Building on Gray and Sheaffer (1996), I propose that the following effects are associated with added upper level tropospheric moisture. The presence of cloud and moisture in the upper levels effectively raises the radiative surface and hence reduces net LW radiative cooling. Reduced clear region LW cooling locally impedes both the DNS and LRD diurnal mechanisms thereby reducing convection the night following an intense outbreak. After a day to recover, the DNS and LRD mechanisms act in full force again facilitating a more vigorous diurnal cycle. When conditions are right, the overall effect is a two day cycle superimposed on the diurnal cycle. In the near equatorial region, the effect may enhance or reduce convection in concert with near equatorial waves of quasi-2-day periodicity.

6.2 Diurnal Variation

A significant diurnal cycle of intense convection dominates variation on all other time scales resolved in this study. In this section I focus on the diurnal cycle of deep convection and associated cloud

for both JJA and NDJ data. As outlined in the beginning of this chapter, much evidence of a significant diurnal cycle of tropical deep convection has accumulated over the past 25 years. Ongoing studies utilizing data from field projects such as GATE and TOGA COARE have greatly enhanced our understanding of the diurnal cycle. However, these studies are geographically limited in scope.

Satellite observations allow us to define the diurnal cycle for the great expanses of the tropical oceans. By nature, however, satellite studies are limited by computer storage and processing capabilities. These computational restrictions have limited many recent global and regional satellite cloud studies to databases with greatly reduced spatial and temporal resolution (eg; ISCCP). Recent exceptions are Chen et al. (1996) and Chen and Houze (1997) who used hourly GMS data with about 10-km resolution (re-sampled from the original 5-km pixel size). To date, no published studies have used full resolution GMS data (1-hr temporal, 5-km spatial) to specifically study the diurnal cycle for the west Pacific warm pool sector delineated in the present study. Below, I focus on the diurnal cycle of deep convection and associated cloud observed in this region during JJA and NDJ.

Method/Results

Histograms in Figs. 6.12 and 6.13 show the diurnal cycle of deep convection expressed as T_{BB} colder than -65°C during JJA and NDJ. The value for each hour represents the percentage of the total area (for the season) covered by cloud colder than -65°C. The total possible area each hour equals 14,274,700 km^2, minus the area occupied by missing or filled pixels. Cold cloud area is then simply the arithmetic sum of pixels colder than -65°C at each hour multiplied by 25 km^2. Since the actual resolved dimensions of each pixel varies slightly across the domain from ~ 4-km at satellite subpoint (0°, 140°E) to ~ 6-km near the dateline, 25 km^2 is an acceptable approximation of the area of each individual pixel.

To compute accurate local standard time, the large WP sector was subdivided into 8 longitudinal sub-sectors of ~ 5° width. The local time assigned to pixel counts within each sub-sector was estimated for the median longitude of each sector, making it accurate to within 10 minutes. Due to a satellite problem during July, IR data was consistently missing around 1400 or 1500 LST. As a result, some of the data at these hours for individual sub-sectors is a linear temporal interpolation from the adjacent hours. This did not greatly impact the results. Figure 6.12 shows that JJA deep convection had a single cycle oscillation with a maximum at 0600 LST and a minimum at 1900 LST. Similarly, NDJ (Fig. 6.13) peaked at 0600 LST with a minimum at 1800 LST. These histograms represent the spatially averaged diurnal cycle for the entire WP sector of the study. This spatial averaging masks small regional variations in the diurnal cycle. Local deep convective maximums in 10° x 5° latitude/longitude sub-sectors ranged between 0400-0800 LST.

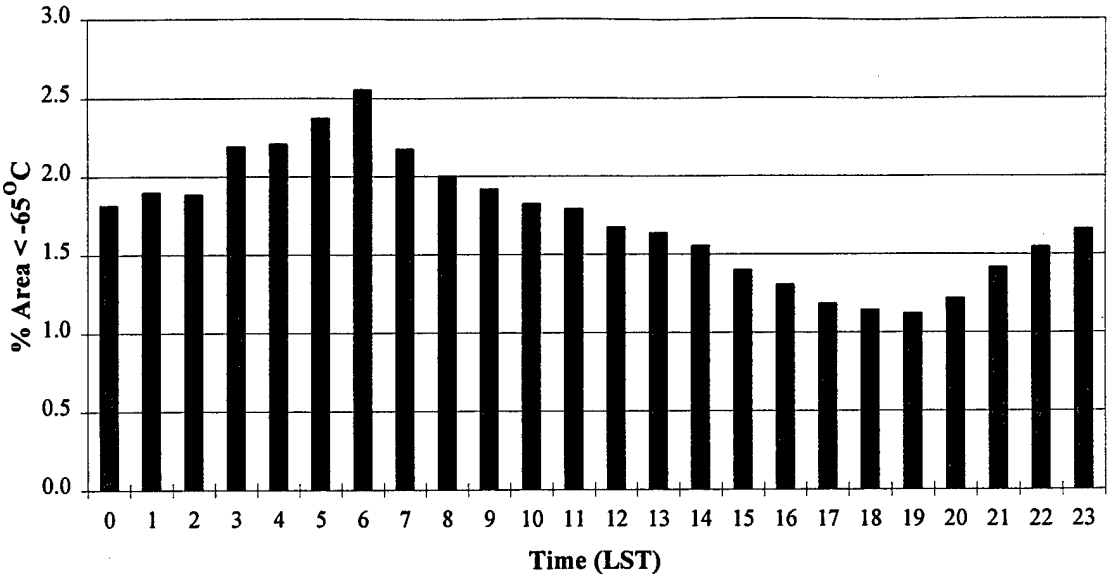

Figure 6.12: Diurnal cycle of total regional deep convection in WP sector (cloud-top with $T_{BB} \leq -65^{o}C$) for JJA.

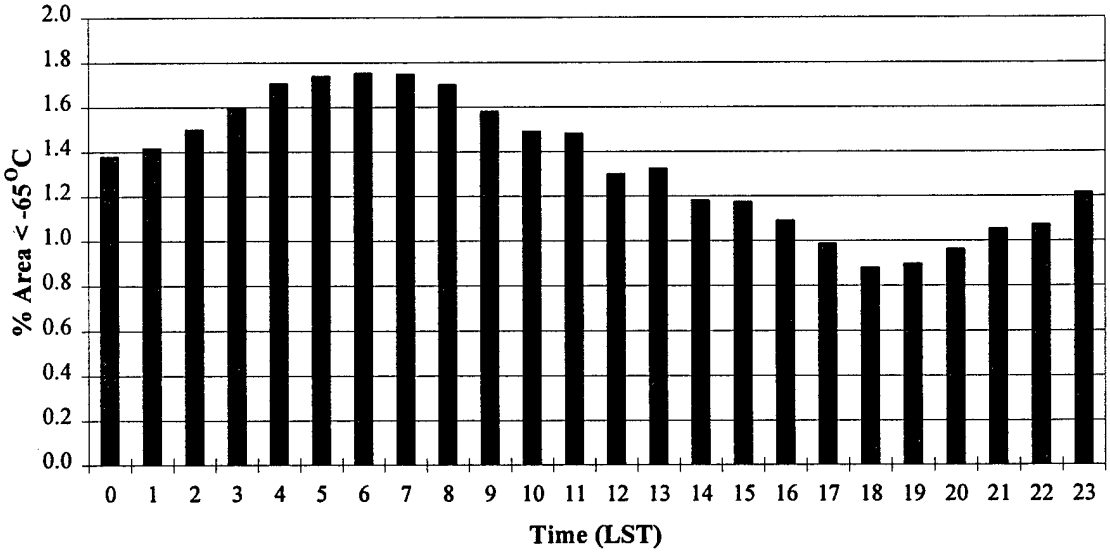

Figure 6.13: As in Fig. 6.12, for time period NDJ.

Figure 6.14 shows results similar to Figs. 6.12 and 6.13 using several IR thresholds to define the number of pixels detected at each hour in 5^{o} T_{BB} intervals from -83°C to -28°C for JJA. Three diurnal cloud regimes reflecting two distinct modes of variability are identified by the vertical lines drawn on the figure. From a similar analysis at 1^{o}C intervals (not shown), these regimes are more precisely defined as follows: (1) $-83^{o}C \leq T_{BB} \leq -60^{o}C$; (2) $-59^{o}C \leq T_{BB} \leq -53^{o}C$; (3) $-52^{o}C \leq T_{BB} \leq -23^{o}C$. These same cloud regimes also prevailed during NDJ.

Figure 6.15 depicts the relative diurnal variation of cloud in each of these regimes for JJA. The thick, solid line represents the diurnal cycle of clouds in the coldest regime (deep convection). The diurnal variation is expressed in terms of the percent relative deviation of cloud areal coverage at each local time from the grand mean of all times. Consistent with Fig. 6.12, the morning to evening ratio of deep convection (regime (1)) was greater than 2:1 with a maximum at 0600 LST and minimum at 1900-2000 LST. Clouds in regime (2) (dotted line) reached local maximums at 0600 LST and 1400 LST, with minimums at 0800-1000 LST and in the evening at 2000 LST. In regime (3) (dashed line), clouds show a single cycle diurnal oscillation with a minimum at 0200 LST and a peak in the late afternoon near 1700 LST. Clouds in regime (3) dominated the diurnal cycle of the tropical cloud shield ($T_{BB} < -15^{o}C$; not shown) which also had a minimum at 0200 LST and a maximum at 1700 LST.

As described in chapter 4, one of the products in the CHANCES database is a binary global cloud/no-cloud image for each hour. The thin, solid line in Fig. 6.15 shows the relative variation of clear pixels for JJA composited in a manner similar to the cloud data. At each local time, the value represents the relative variation in percentage of total area covered by pixels indicated to be clear in the IR CNC image. For JJA the percentage of clear pixels increased from an overnight minimum to a maximum in late morning.

Figure 6.16 shows the diurnal cycle of clouds associated with deep convection and clear for NDJ. As in JJA, deep convection peaked at 0600 LST and reached a minimum at 1900 LST. Clouds in regime (2) peaked in the morning at 0700-0800 LST and again at 1500 LST. The fractional coverage of warm clouds in regime (3) increased from a minimum at 0900 LST to a peak at 1600-1700 LST. The areal coverage of clear increased from a 0400 LST minimum to a late morning maximum.

As discussed previously, December 1994 coincided with an active phase of the ISO while a suppressed phase occurred during January 1995. During the active phase (Fig 6.17), the diurnal cycles of clouds associated with deep convection closely mimicked those for the all of NDJ (Fig. 6.16). In fact, the pixel counts for the NDJ were dominated by deep convection that occurred during December. Figure 6.18 illustrates the data for the inactive phase. As in the active phase, deep convection peaked in the early morning (0500 LST) and minimized in the evening (1800 LST). In addition, a secondary peak occurred at

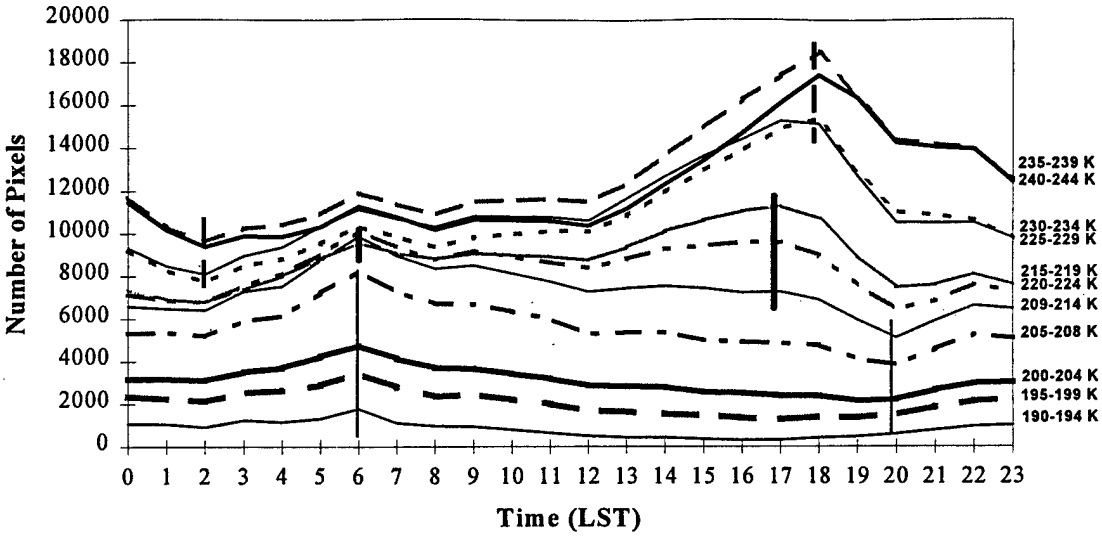

Figure 6.14: Hourly pixel counts for JJA cloud-top T_{BB} presented in 5°C increments. The maxima and minima of three diurnal cloud regimes are delineated by vertical lines. Thin, solid vertical lines indicate the deep convection regime; thick, solid lines are a mixed deep convection and cirrus anvil regime; dashed lines are a stratiform cirrus regime.

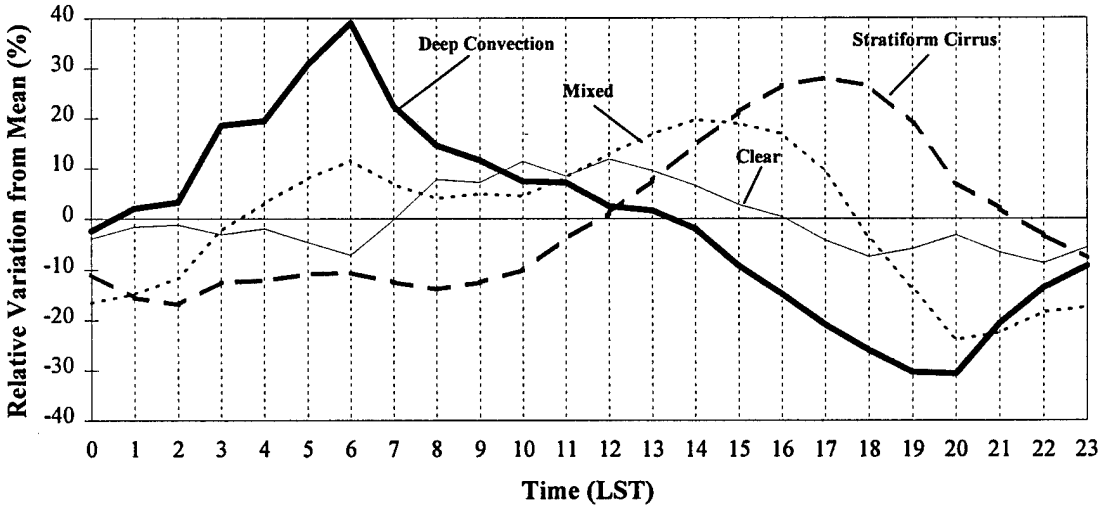

Figure 6.15: JJA relative percent variation of area from mean covered by cloud in three regimes: (1) -83°C ≤ T_{BB} ≤ -60°C (thick, solid line); (2) -59°C ≤ T_{BB} ≤ -53°C (thin, dashed line); (3) -52°C ≤ T_{BB} ≤ -23°C (dashed line). Relative variation of cloud-free area is indicated by thin, solid line.

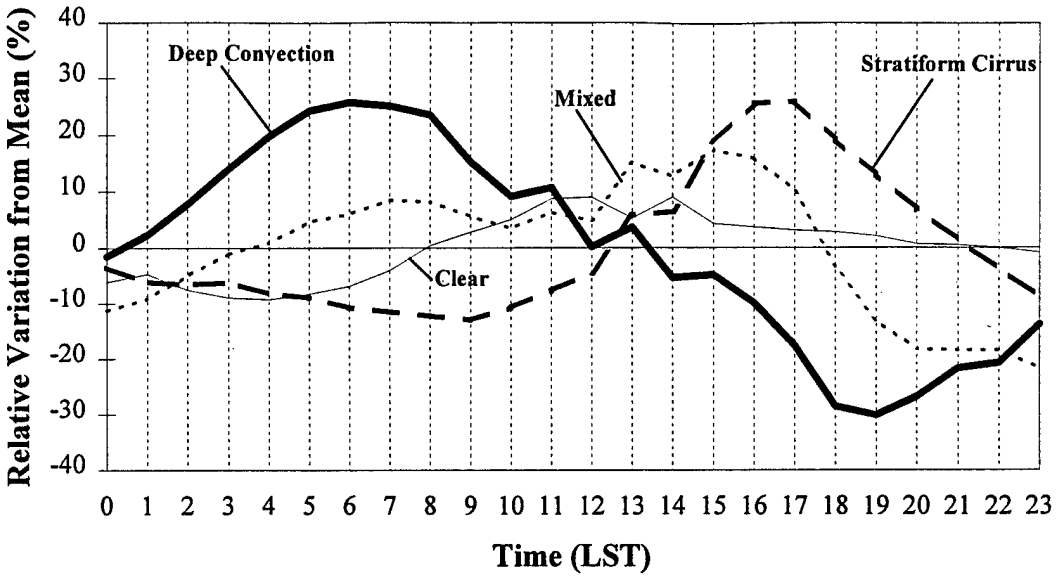

Figure 6.16: As in Fig. 6.15, for NDJ.

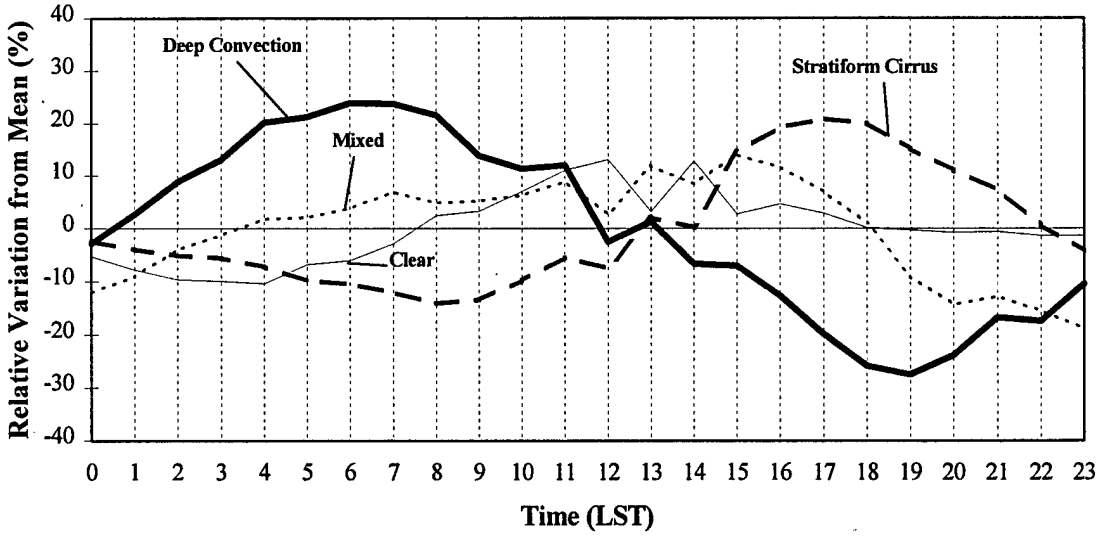

Figure 6.17: As in Fig. 6.15, for the active phase of the ISO (December 1994).

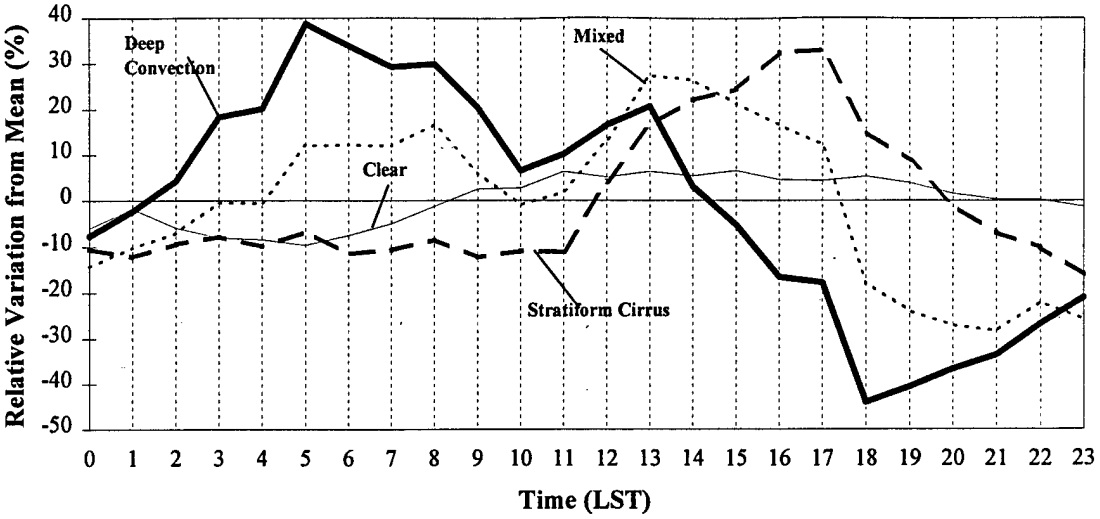

Figure 6.18: As in Fig. 6.15, for the inactive phase of the ISO (January 1995).

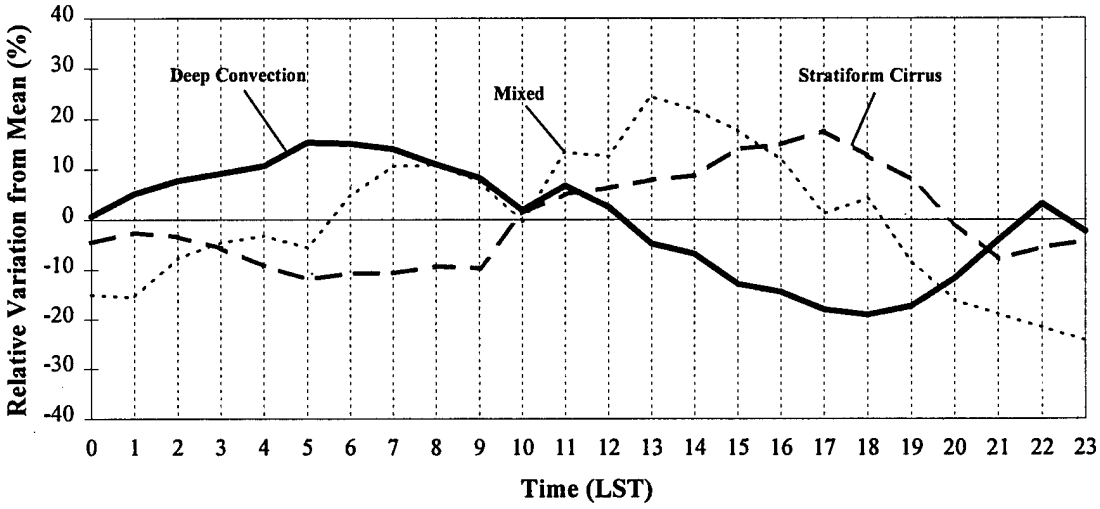

Figure 6.19: As in Fig. 6.15, for tropical storms Axel and Bobbie.

1300 LST. Clouds in regime (2) also had a significant secondary peak at 1300 LST. As in JJA and December 1994, the amount of clear area increased rapidly from early morning to just before local noon. However, instead of a sharp peak, the fractional amount of clear exhibits a broad maximum throughout the afternoon.

During December 1994, tropical storms Axel and Bobbie formed in the WP sector which dominated WP convection during 10 days of the month. To analyze the diurnal cycle of cloud associated with these storms, pixels within a 10^{o} x 10^{o} latitude/longitude box centered on each storm were analyzed. Based on storm movement, the box was repositioned every 6 hours. Though smaller than the relative variation indicated in the active phase composite (Fig. 6.17), the diurnal cycle of convective cloud associated with these storms (Fig. 6.19) had a similar phase. Deep convection peaked at 0500 LST and reached a minimum at 1800 LST, whereas cloud in regime (2) peaked a 0700-0800 LST and again at 1300 LST. Cloud in regime (3) increased from a minimum at 0500 LST to a maximum at 1700 LST.

Discussion

Albright et al. (1985), Duvel (1989), Fu et al. (1990) and Zehr (1987,1992) noted that the amplitude and phase of the diurnal cycle strongly depends on T_{BB} threshold used to specify convective regimes. My analysis of the diurnal cycle at $1^{o}C$ increments shows that the relative and absolute amplitudes were largest for the threshold representing deep convection. In a general sense, the maximum of the diurnal cycle propagated from the early morning for the clouds with the coldest tops to the late afternoon and evening for warmer clouds as previously found by Albright et al., Chen and Houze (1997), Fu et al., Gray and Sheaffer (1995), Machado et al. (1993) and Zehr. However, this phase shift in the diurnal maximum with increasing temperature is not continuous.

For brightness temperatures colder than about $-23^{o}C$, the phase shift occurred in two distinct modes, a deep convection mode and a stratiform cirrus mode. The coldest regime ($\leq -60^{o}C$) comprises a deep convection mode whereas the warmest regime ($-52^{o}C \leq T_{BB} \leq -23^{o}C$) corresponded to the stratiform cirrus cloud shield associated with tropical convection. The middle range of cloud-top T_{BB} ($-59^{o}C \leq T_{BB} \leq -53^{o}C$) represents a mixed regime with diurnal maxima coincident with deep convection in the morning and the stratiform cirrus cloud canopy in the late afternoon. Similar diurnal maxima and minima for analogous threshold regimes have previously been documented by Short and Wallace (1980), Muramatsu (1983), Albright et al. (1985), Hartmann and Recker (1986), Fu et al. (1990) and Gray and Sheaffer (1995). So, as stated in Kidder and Vonder Haar (1995), various cloud types can be analyzed by choosing appropriate IR thresholds. In the WP, a $-60^{o}C$ threshold isolates deep convection. Given +/- $3^{o}C$

uncertainty in IR T_{BB} at these very cold temperatures, -65°C serves as the most effective threshold to study the diurnal cycle from IR satellite imagery.

Results of the present study show that intense convection had a near 0600 LST maximum with an 1800-1900 LST minimum during both winter and summer. Similar findings for the west Pacific have been published in more than a dozen papers reviewed above. During winter, tropical storms had similar diurnal variability in all three cloud regimes as the other morphologies of NDJ convection. This is consistent with previous studies by Muramatsu (1983), Steranka et al. (1984) and Zehr (1987, 1992). A new result of this study is the finding that nearly the same diurnal cycle of deep convection occurred in both the active (Fig. 6.17) and inactive (Fig. 6.18) phases of the ISO. Chen and Houze (1997) found an afternoon convective maximum during inactive periods occurred during TOGA COARE. Inactive periods during TOGA COARE were characterized by calm winds and clear skies. Under these conditions, SSTs can rise by up to ~ 4°C during the day (Webster et al. 1996) leading to afternoon initiation of small scale convection. These truly undisturbed conditions did not occur in convectively active regions during JJA and NDJ.

Three notable papers are broadly in conflict with the conclusions of the present study including Augustine (1984), Shin et al. (1990) and Bergman and Salby (1996). Augustine and Bergman and Salby found only a weak morning peak of satellite derived rainfall with a strong afternoon maximum. Shin et al. found only an afternoon maximum. Conclusions related to diurnal convective variability from these studies were biased by the mixture of cloud regimes included in their analysis.

Figure 6.20 shows results obtained for JJA CHANCES data using the T_{BB} thresholds from various papers. The precipitation algorithm of Shin et al. which uses -38°C (Table 1) is represented by the thin, solid line in Fig. 6.20. This threshold yields an apparent semi-diurnal cycle with a weak maximum in the morning and a primary maximum around 1500-1600 LST. The ISCCP high-cloud statistics used by Berman and Salby are equivalent to assuming a T_{BB} threshold of ~ -15°C (thick, dashed line). A similar threshold of -20°C defines cloud analyzed by Augustine. These thresholds encompass nearly all cloud in the tropical shield (Steranka 1984; Gray and Sheaffer 1995; Meisner and Arkin 1987) and essentially indicate a diurnal cycle with a single prominent 1600-1700 LST maximum.

Two other IR curves used in previous studies are illustrated in Fig. 6.20. Hendon and Woodberry utilized a deep convective index in place of fractional cold cloud cover defined as -43°C minus T_{BB} of the pixel. This weights the index toward the coldest cloud. The dark, solid line shows that their index produces a significant single oscillation diurnal cycle of nearly identical phase and amplitude to that produced by using a -65°C threshold as in Fig. 6.15. The ISCCP data used in their study has 3 hourly temporal resolution. Spatially, the data consisted of full resolution pixels sampled at 25 km intervals. Power spectra computed by reducing the spatial (from 5km to sampled at 30 km intervals) and temporal

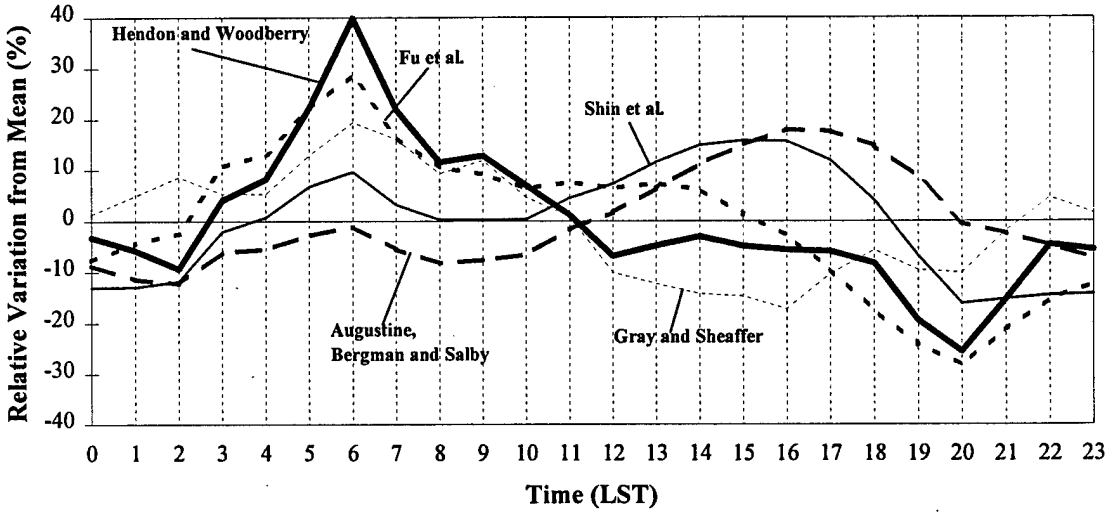

Figure 6.20: Illustration of results that would have been obtained from the CHANCES database using IR analysis techniques and T_{BB} thresholds of other studies. The thin, solid line is a -38°C threshold diurnal curve and simulates results of Shin et al. (1990). The thick, dashed line represents results using a -20°C threshold analogous to Augustine (1984) and Bergman and Salby (1996). The medium, dashed line is the diurnal cycle of cloud using the -53°C threshold suggested by Fu et al. (1990) as a first approximation to isolate deep convection. The thick, solid line is the index developed by Hendon and Woodberry (1993). The very thin, dashed line is the +10°C threshold used by Gray and Sheaffer (1995) to identify clear pixels.

resolution (from 1 to 3 hourly) of JJA time series (not shown) revealed that the reducing the spatial resolution has the greatest impact on the spectral power at the diurnal frequency. However, the diurnal cycle was still significant well above the 95% level for both tests. The other threshold tested was the -53°C (thin, dashed line) suggested by Fu et al. (1990). This threshold produces a significant diurnal cycle, but represents a mixed regime slightly contaminated by stratiform cirrus cloud as evidenced by the local maximum near 1300 LST.

A new result of this study is the diurnal variation of clear shown by the thin, solid line in Figs. 6.15-6.18. During the summer the fractional amount of clear area began to increase near the time of peak convection and reached a maximum near local noon. I interpret this strong expansion of clear areas to reflect the cumulative effects of cloud dissipating subsidence in large clear zones immediately surrounding active clusters. Compensating subsidence is forced near active, deep convection and could be enhanced by clear-cloud radiative effects discussed by Gray and Jacobson (1977). This expansion of clear area also likely reflects increased sinking motion in large subsidence zones far removed from the active convection. Gray and Sheaffer (1995) made similar inferences about clear air by assuming pixels warmer than +10°C to be cloud free. I have tested this idea for JJA. In Fig. 6.20 the thin, dotted line represents the diurnal cycle of pixels warmer than +10°C. Comparing this curve to the curve I obtained from the CHANCES CNC product plotted in Fig. 6.15, it appears that pixels near +10°C are contaminated by low cloud with a separate diurnal cycle not representative of clear air.

In general, my results imply that the strongest diurnal cycle occurred with the most intense convection. In the tropics, intense convection occurs primarily in organized weather systems (Gray and Jacobson 1977; Williams and Houze 1987; Evans and Shemo 1996). An early morning peak in deep convection means either more of these systems formed throughout the night than during the day, or the ones that happened to exist into the morning were spatially larger and/or more intense. These findings are consistent with the DNS, RCF, LRD and BLML theories of the diurnal cycle.

Other evidence, however, does not support RCF. The ratio of morning to evening deep convection was more than 2:1. Janowiak et al. (1994) and Liu et al. (1995) indicate that the rainfall associated with the relatively rare very deep convection contributes disproportionately to total rainfall. Jacobson (1976) found that 75% of all heavy precipitation events (> 1.0 cm/hr) occurred between 0700-1200 LST. In recent modelling efforts (Xu and Randall 1995), RCF primarily impacted expansive stratiform cloud decks (Xu 1997, personal communication). Rickenbach and Rutledge (1996) suggest RCF only affects rain rates in stratiform regions with no discernible effect on deep convective cloud. Given that understanding, it is not suprising that models do not produce rainfall reflecting 2:1 morning to evening differences in the amount of deep convection. Only DNS and BLML theories are consistent with this finding.

The BLML mechanism, however, was not at work in the WP sector during this study. First of all, low level wind conditions during JJA and Dec 1994 were disturbed (chapter 5). BLML requires clear, calm conditions to allow sea surface heating (Webster et al. 1996; Chen and Houze 1997). In addition, a major component of BLML, *diurnal dancing*, was not observed at any time during JJA and NDJ. Finally, though January 1995 coincided with an inactive phase of the ISO giving the opportunity for significant boundary layer and surface heating, early morning convection still dominated the diurnal deep convective cloud statistics.

Conclusion

Spectral analysis revealed a powerful diurnal cycle of deep convection for JJA and NDJ significant well above the 95% confidence level. Also, the analysis revealed a statistically significant bi-diurnal cycle during JJA and January 1995, most prevalent in the near-equatorial region during JJA. No semi-diurnal cycle occurred in the time series of deep convection.

Consistent with many other studies, deep convection exhibited an early morning maximum around 0500-0600 LST with an evening minimum near 1800-1900 LST during summer and winter. This same cycle also occurred in both active and inactive phases of the ISO and for two tropical storms. On average, there was a greater than 2:1 ratio of morning to evening intense convection.

Clouds associated with deep convection showed two distinct diurnal modes representing deep convection and stratiform cirrus regimes. The coldest regime included all cloud top T_{BB} colder than -60 ^{o}C and verified -65^{o}C as the best threshold to isolate deep convection. My results are consistent with the DNS, LRD and BLML diurnal theories. However, BLML was not observed to occur in the WP region of this study.

Chapter 7

Relation of Satellite Observed Morphology to Diurnal Spatial and Temporal Variation

Most tropical precipitation is associated with mesoscale convective systems (Garstang 1958; Gray 1973; Gamache and Houze 1983). More than half of the rainfall in these systems is produced by convection (Houze 1977; Gamache and Houze 1983; Houze 1989). Deep convection embedded in organized cloud clusters is the seat of most of the total heating in the tropics (Williams and Houze 1987). Given this knowledge, various studies throughout the past 25 years have sought a quantified a relationship between the mesoscale structure of deep convection and its diurnal cycle. In this chapter I present new results for the WP on the relation of the diurnal cycle to the satellite-observed structure of cloud clusters.

Ruprecht and Gray (1976) documented a striking diurnal variation of rainfall associated with west Pacific tropical weather systems from island precipitation data coincident with satellite observed cloud clusters. They found that net morning rainfall (0700-1200 LST) is two and a half times greater than early evening amounts (1900-2400 LST). Rainfall not directly associated with cloud clusters also accumulates larger morning amounts but with small percentage differences relative to the evening. Gray and Jacobson (1977) reached the same conclusion from a more extensive west Pacific data set. They found that the more intense the deep convection and the more associated it is with organized weather systems, the more evident the diurnal cycle.

Weickmann et al. (1977) identified a tendency for oceanic cumulonimbus cloud systems to form near midnight and explosively intensify to reach an early morning maximum during GATE. McGarry and Reed (1978) also studied GATE data. They found evidence that the overall diurnal cycle of deep convection results not from local showers whose mass flow is compensated in the near environment but rather from systems whose mass inflow encompasses large areas.

Williams and Houze (1987) developed an objective technique to identify and track connected areas of cloudiness in IR imagery with T_{BB} less than a specified threshold. They tested the method on data from the Winter Monsoon Experiment (WMONEX) and found that cluster sizes, like many other parameters describing atmospheric convective clouds (Lopez 1977) are nearly lognormally distributed. Their results also showed that most of the cumulative cloud, and hence total rainfall, is attributable to a few clusters which reach a maximum size. Up to 85% of cloud in their study was associated with clusters larger than 3.0×10^4 km^2. Mapes and Houze (1993) improved the objective satellite cluster tracking technique to

study cloud clusters over the oceanic warm pool. They divided clusters into size classes based on the areal coverage of -65°C cloud top within the cluster. Their results showed a pronounced diurnal variation in the total number of large -65°C clusters over the open ocean with numerous systems observed during early morning and fewer in the evening hours. The diurnal cycle in the area covered by large clusters also peaked in the early morning. The largest class of clusters (> 65000 km^2) was strongly diurnally modulated with a dawn-to-dusk ratio of 2:1 or more. This variation of large clusters dominated and largely determined the overall cycle of very cold cloudiness.

Chen et al. (1996) used the Mapes and Houze algorithm to study deep convection during the TOGA COARE Intensive Observation Period (IOP) in a region bounded by 10°N-10°S, 152°E-180°. The IOP spanned 1 November 1992 - 28 February 1993. Their results showed that the diurnal cycle of the -65°C cloud clusters in the COARE IOP is size dependent. Whereas the area covered by the smallest clusters has a very small amplitude of diurnal variation, the largest clusters show a strong diurnal variation with a peak in the early morning hours and a minimum in the afternoon. The amplitude (dawn to dusk ratio) is nearly 10:1, somewhat larger than that found by Mapes and Houze. Within the active phase of the ISO, results of Chen et al. show deep convection frequently concentrates into westward-propagating disturbances with a local periodicity of ~ 2 days. The mechanism of the diurnal cycle documented by Chen et al. and its implication to the ISO and 2-day disturbances was examined extensively by Chen and Houze 1997.

Chen and Houze analyzed the -65°C cloud top T_{BB} portion of cloud clusters in terms of four classes sizes as done previously by Mapes and Houze (1993) and Chen et al. (1996). Two full cycles of the ISO were observed in the TOGA COARE IFA during November 1992 through February 1993. During convectively suppressed ISO phases cloud systems were spatially small, preferentially forming in the afternoon and lasting one to three hours. This small scale convection also had a minor early morning maximum surmised to be triggered by outflow from a few larger systems. During convectively active phases of the ISO, fractional cloud coverage and its diurnal cycle was dominated by spatially large, long-lived cloud systems. These systems were observed to form in the afternoon and reach maximum extent in the early morning (0000-0600 LST). Large convective systems tended to occur every other day at a given location and hence were unlikely two days in a row. As mentioned previously, they term this spatial variation *diurnal dancing*.

Machado et al. (1993) used ISCCP-B2 IR satellite data (30x30 km resolution) from Meteosat to study short time-scale fluctuations of the size distribution of cloud clusters over West Africa and the Atlantic Ocean. An algorithm similar to the one developed by Williams and Houze (1987) was used to objectively identify areas covered by cold cloud. Over the ocean, the highest probability of finding large clusters (radius > 100 km) occurred during the late night and early morning, and the minimum probability

between 1900 and 2200 LST. Their results demonstrate that the diurnal variation of Atlantic Ocean convective cloudiness is due primarily to large systems.

Evans and Shemo (1996) identified various types of organized tropical convection in satellite imagery with an objective algorithm and computed rainfall rates using various automated techniques. In their study, increasingly organized systems (i.e.; tropical storm vs tropical depression) were longer lived and had higher precipitation rates. In another recent study, Rickenbach and Rutledge (1996) considered the dependence of the diurnal rainfall variation on the morphology of surface rainfall organization from TOGA COARE radar data. Morphology was classified in terms of four types of organization: linear and non-linear sub-MCS scale; linear and non-linear MCS scale. They found that convection of all morphologies in various stages of maturity occurred at all times of day and night. The highest amplitude rainfall variance was found with MCS scale non-linear events, which peaked near 0230 LST. Sui et al. (1997) found that cumulus convection in late morning and afternoon is shallower while nocturnal convective systems consist of deeper cells and larger areas of stratiform rain.

For the results presented in this chapter, objective techniques were used to study the relation of the diurnal cycle of deep convection to various size scales of convection. The results give new insight into daily temporal and spatial variation of cloud clusters in the WP. As in earlier sections of this study, I focused on JJA and NDJ divided into active and inactive phases of the ISO.

7.1 Relation of Morpholgy to Temporal Variation

As described above, various authors have documented relations between the degree of convective organization and the diurnal cycle. This section details an objective technique developed to identify cloud clusters in IR imagery and characterize them according to size for NDJ and JJA. The same method was used to analyze related cloud-free regions. A specialized application of the technique was developed to isolate deepening cloud clusters from existing or dying convection.

Method/Results

Throughout this thesis, the term cloud cluster has been used to generically describe large tropical mesoscale convective systems that are not tropical storms. At increasingly cold T_{BB} thresholds, clusters of deep convective cold cloud represent smaller organized portions of the larger mesoscale cloud clusters. In this section, *cloud cluster* is defined as a region at an instant of time within a single closed isotherm of T_{BB} less than -65°C. Chen et al. (1996) state that the region of convective cloud enclosed within the -65°C isotherm in the tropics corresponds to what is commonly called an MCS.

To characterize convection in terms of the size of cloud clusters, required an objective satellite cluster detection technique (Fig. 7.1). To identify clusters at a particular time, connected segments (adjacent pixel spans) of cloud with cloud-top $T_{BB} < -65^{o}C$ are identified within each line (latitude row) of the data array comprising one satellite image. These segments, or intervals of cloud are called *line clusters* (Mapes and Houze 1993). Because of the large variety of cluster shapes observed, one can assume the ensemble average of all shapes of clusters is approximately circular (Machado et al. 1993). A line cluster, then, represents a characteristic horizontal dimension of the larger cloud cluster. On average, line clusters measured through many images represent random line segments drawn across various sized circular clusters. Through simple geometric arguments, the average of all random line segments through a circle is ~ 84% of the diameter. In other words, in the ensemble sense the equivalent cluster diameter represented by many line clusters of any particular length is 1.19 times the length of the line. Once you know the diameter, it is trivial to compute the equivalent cluster spatial area. Another consequence of assuming a circular shape, is that the choice of detecting intervals latitudinally or longitudinally is arbitrary.

Line clusters can be described in terms of length or area. For example, a line cluster composed of 20 contiguous 5 x 5 km pixels would be 100 km in length. Given an area of 25 km^2 per pixel, this same line cluster covers 500 km^2. Around 25% of line clusters detected in any image consisted of just one or two pixels. These could be single isolated clouds or fragments of larger clouds. Because of this uncertainty, one and two pixel cloud intervals were excluded from the statistics. Their inclusion, however, would not have largely changed the results as they only accounted for ~ 3% of the total area covered by cold cloud, and their daily cycle closely followed that of other small scale cloud intervals.

Figure 7.2 displays the distribution of total sampled cold cloud area as a function of line cluster length for JJA. From the graph, no apparent breaks occur which might suggest obvious cluster size categories. The character of the distribution also typifies NDJ data. Figure 7.3 shows the JJA diurnal cycle for the continuum of $-65^{o}C$ cloud cluster sizes. The ordinate is the area of cloud clusters in 25 km^2 increments up to about 150000 km^2. To derive these statistics, line clusters were converted into an equivalent area based on the geometric arguments described above. The abscissa is the maximum morning to evening ratio of the number of clusters detected for the season. Clusters smaller than ~ 25000 km^2 were twice as likely to occur in the morning as in the late afternoon. Larger than ~ 25000 km^2, the diurnal cycle of clusters increased rapidly with size up to nearly 25:1 for clusters comprised of greater than ~ 100000 km^2 of cloud colder than $-65^{o}C$. Based on these results, I divided line clusters for JJA into two size classes comprising two apparent modes of variability. Clusters < 25000 km^2 were categorized as Class 1, while clusters ≥ 25000 km^2 were grouped into Class 2.

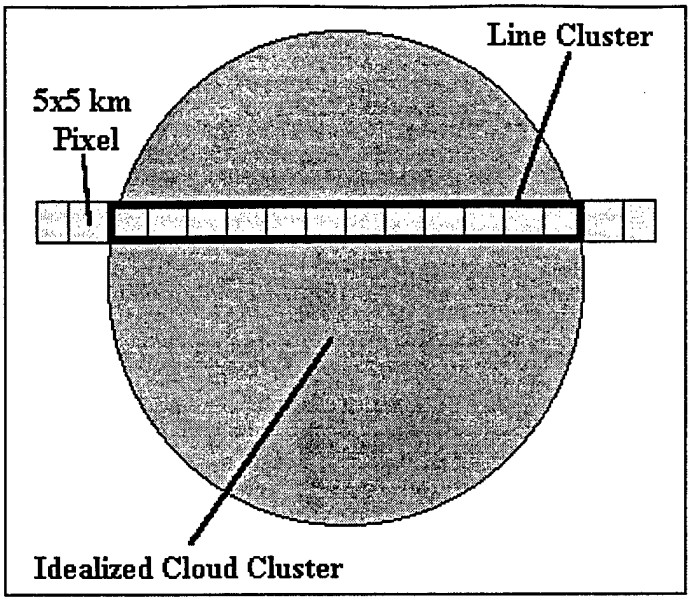

Figure 7.1: Schematic of line cluster technique to objectively identify clusters of cloud colder than -65°C in an IR image. The circle represents an idealized cluster. Assuming a random distribution of shapes, the average is circular. The bold rectangle represents an interval of cold cloud which would be identified as a line cluster by the algorithm.

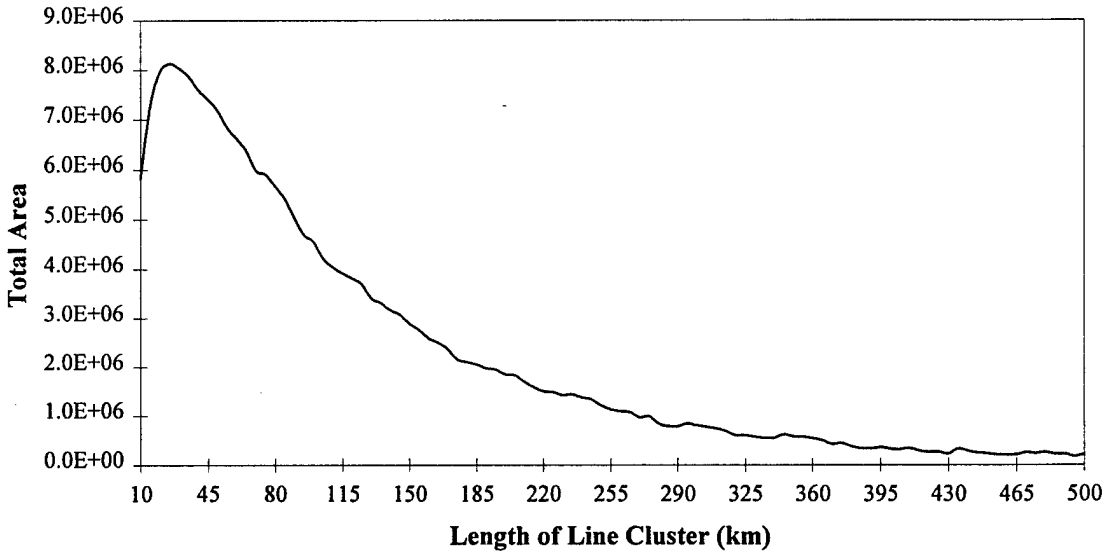

Figure 7.2: Distribution of total sampled cold cloud area as a function of line cluster length for JJA. The distribution for NDJ (not shown) was nearly identical.

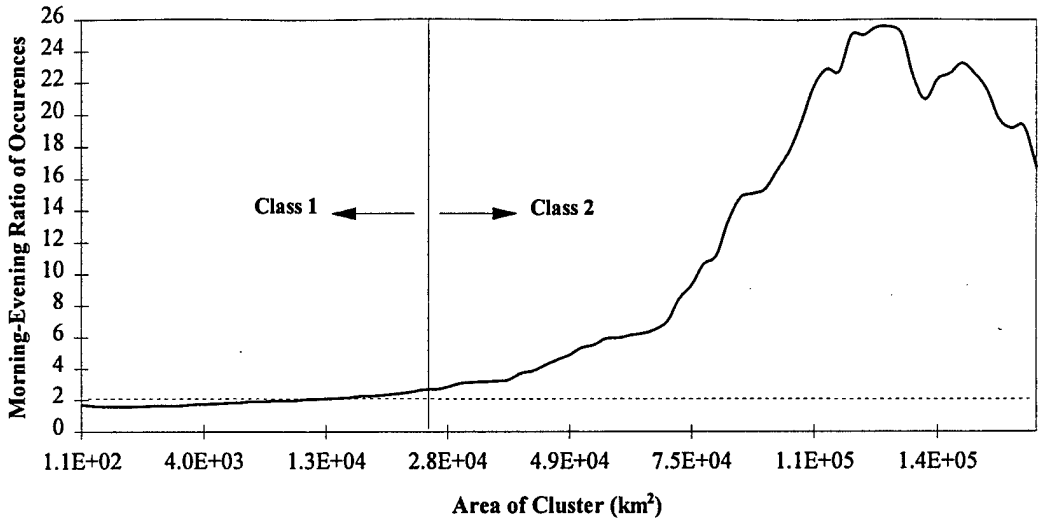

Figure 7.3: JJA diurnal cycle for the continuum of cluster sizes in 25 km^2 increments up to ~ 150000 km^2. The abscissa is the diurnal cycle expressed as the maximum morning to evening ratio of the number of detected line clusters.

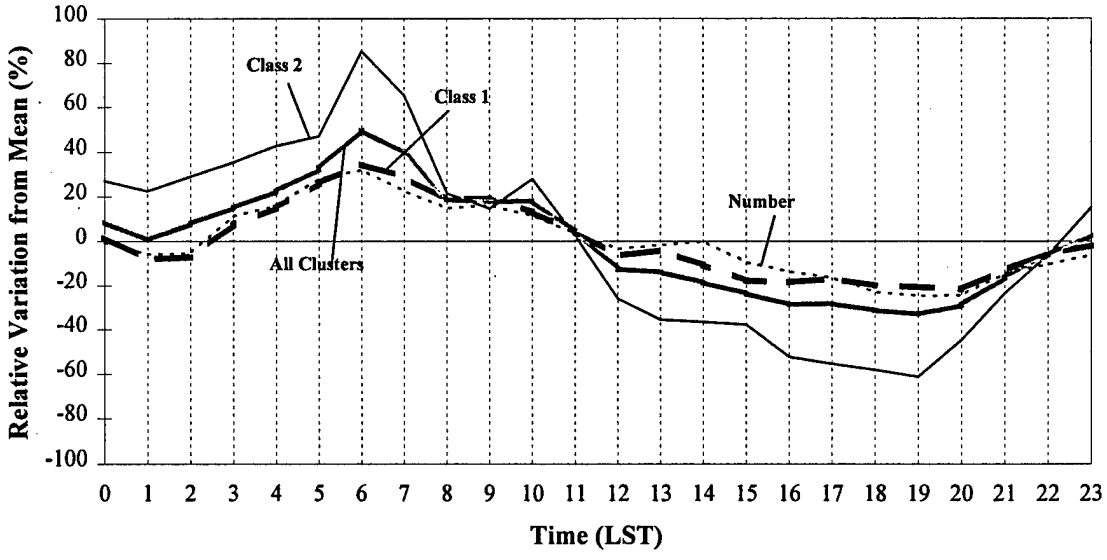

Figure 7.4: JJA relative percentage variation from the mean amount of area covered by Class 1 clusters (thick, dashed line), Class 2 clusters (thin, solid line) and all clusters (thick, solid line). Relative variation of total number of clusters at each hour is indicated by the thin, dotted line.

Figure 7.4 depicts the relative deviation from the mean amount of area covered by Class 1 clusters (thick, dashed line), Class 2 clusters (thin, solid line) and all clusters (thick, solid line). Both Classes 1 and 2 peaked at 0600 LST and decreased to a minimum at 1900 LST. After 1900 LST relative amount of cold cloud increased again throughout the night and early morning. Class 2 clusters had a much larger daily variation than Class 1. In terms of area, Class 2 clusters covered nearly five times more area on average at 0600 LST than at 1900 LST. The morning to evening ratio of area covered by Class 1 clusters was 1.7:1. The diurnal cycle of area from all clusters had a 2.3:1 morning to evening ratio consistent with the results shown in Fig. 6.12. While Class 2 clusters accounted for only 10% of clusters detected of all sizes for JJA, they accounted for 30% of the total area covered by cloud colder than -65°C and 54% of the total diurnal cycle. The relative variation of the total number of clusters at each hour from the average number of all clusters is indicated by the thin, dashed line. The maximum number of clusters occurred at 0600 LST decreasing to a minimum around 1900-2000 LST. The relative variation was similar to the variation in area accounted for by Class 1 clusters, but much less than the relative variation of area associated with Class 2 clusters.

Figure 7.5 shows the diurnal cycle for December 1994 (active ISO) as a function of cluster size, analogous to Fig. 7.3. For December, clusters smaller than ~ 70000 km^2 had an approximately 2:1 ratio of morning to afternoon deep convection. For clusters larger than ~ 70000 km^2, the diurnal cycle rose sharply with increasing size to greater than 10:1 for ~ 250000 km^2 clusters. For these data, 70000 km^2 was closen as the boundary between Class 1 and Class 2 clusters. In Fig. 7.6, I show the relative diurnal variation of deep convection for Class 1, Class 2 and all clusters as in Fig. 7.4. Deep convection for both classes peaked in the early morning and reached a minimum in mid-afternoon. Class 2 clusters comprised 9% of the total sampled number of all clusters, contributed 32% of the total area of cold cloud (< -65°C) and accounted for 36% of the 0600-1500 LST diurnal cycle. As in JJA (Fig. 7.3) the relative variation of the total number of clusters (thin, dotted line) at each hour closely mimicked the variation of area accounted for by Class 1 clusters.

As mentioned previously, January 1995 coincided with an inactive phase of the ISO. On many days, small scale convection prevailed. Figure 7.7 shows the diurnal cycle for the continuum of cluster sizes as in Figs. 7.3 and 7.5. During this period, clusters exhibited a 2:1 ratio of morning to evening deep convection for sizes up to ~ 11000 km^2. For clusters larger than 11000 km^2, the 0500-1900 LST diurnal cycle rapidly increased to 16:1 just beyond 90000 km^2. So, the cutoff between Class 1 and Class 2 was set to 11000 km^2.

Figure 7.8 shows the relative variation of deep convective cloud as in Figs. 7.4 and 7.6. Class 2 clusters had a broad morning peak between 0400-0800 LST with a minimum around 1800-1900 LST.

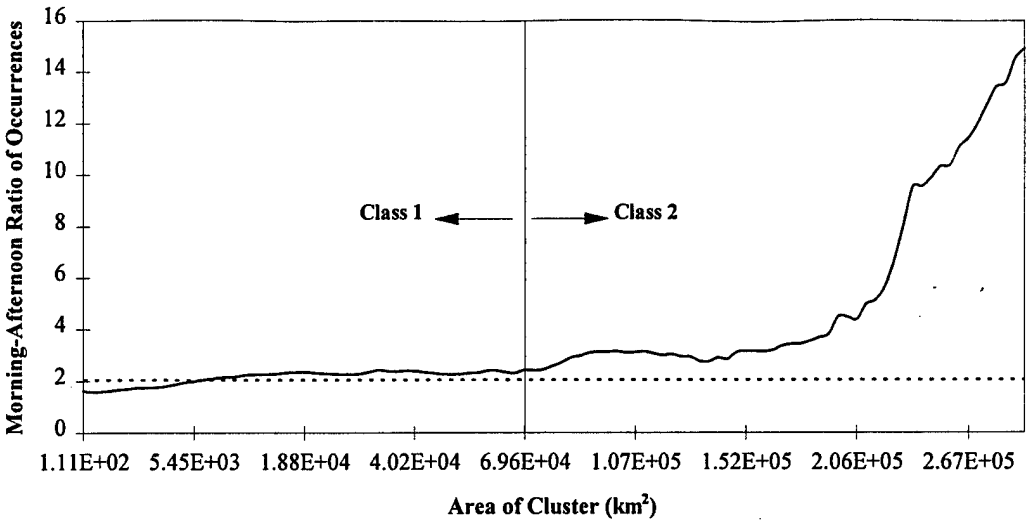

Figure 7.5: As in Fig. 7.3, for December 1994 (active ISO).

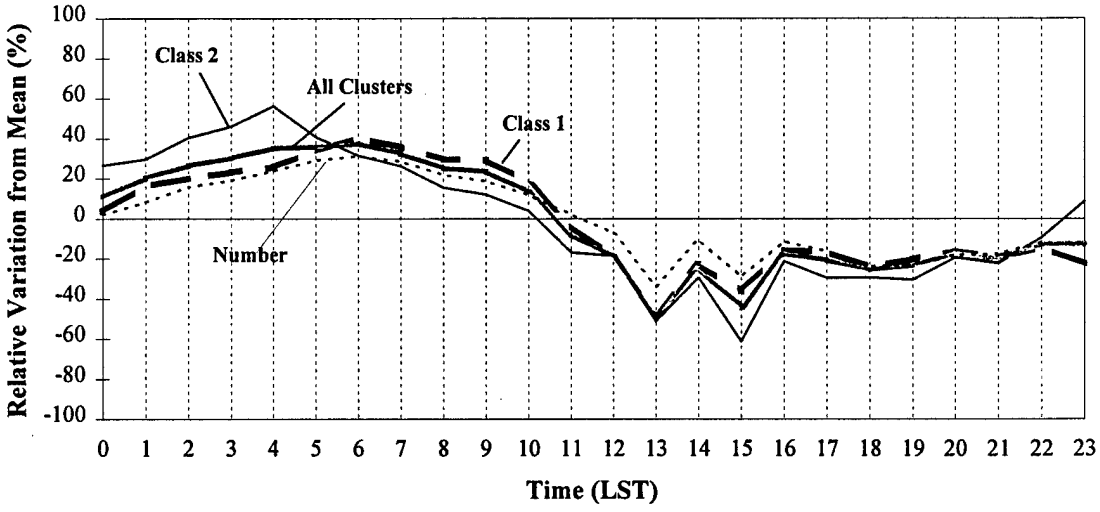

Figure 7.6: As in Fig. 7.4, for December 1994 (active ISO).

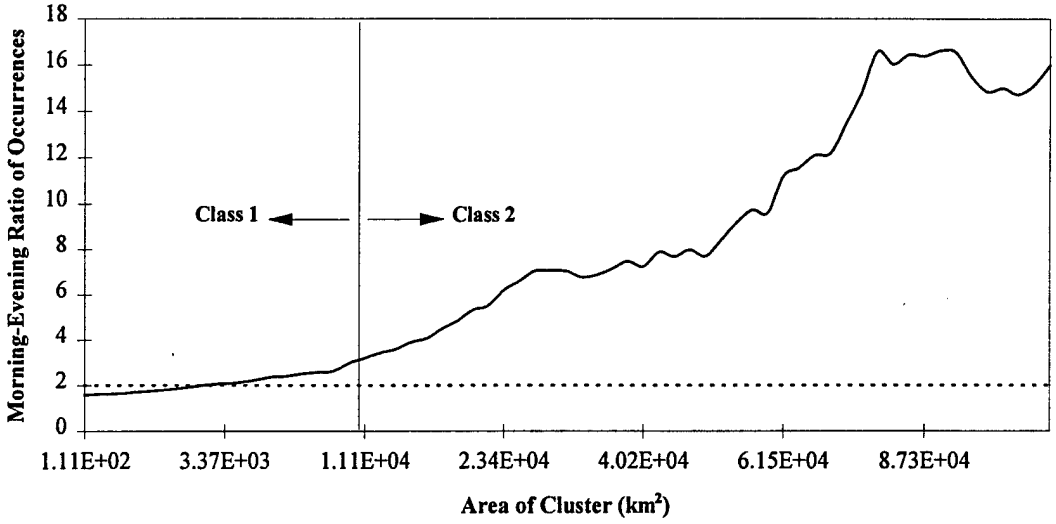

Figure 7.7: As in Fig. 7.3, for January 1995 (inactive ISO).

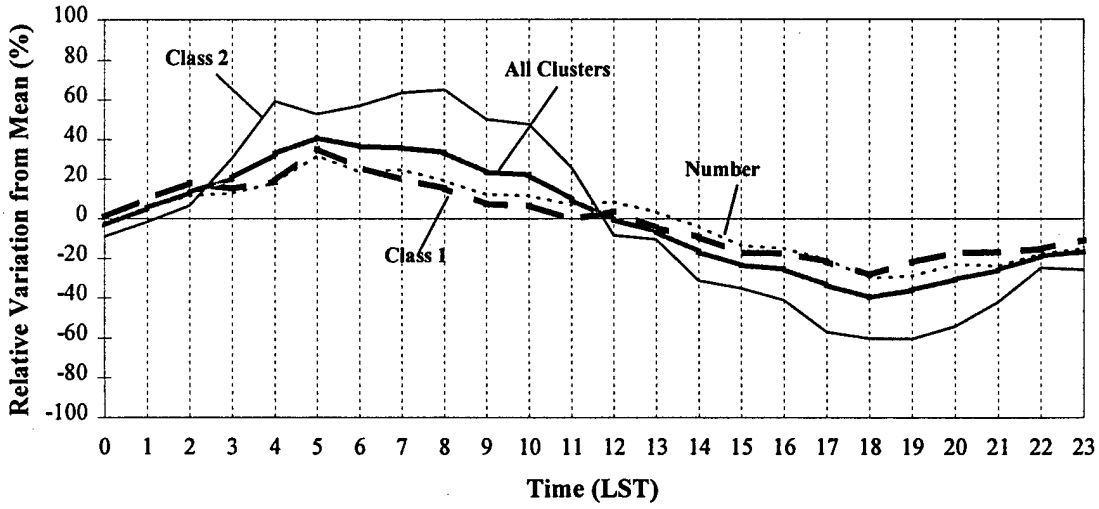

Figure 7.8: As in Fig. 7.4, for January 1995 (inactive ISO).

Class 1 convection was most likely around 0500 LST and least likely near 1800 LST. Class 2 clusters comprised 14% of all detected clusters, contributed 36% of the total area of cold cloud and created 54% of the 0500-1900 LST monthly average diurnal cycle. The relative variation of the number of clusters at each hour closely followed the variation of Class 1 clusters.

The diurnal variation of clear areas derived from the CHANCES IR CNC product was shown in Figs. 6.15-6.18. Figure 7.9 shows the relative diurnal variation of clear intervals for JJA analyzed similarly to the cold cloud intervals described above. Because of the large spatial size of cloud-free regions, clear intervals were analyzed for the entire WP sector at every UTC time. Therefore, the local time calculation could be in error by up to 1 hour. As with the cloud clusters, I divided the clear intervals into two classes. Class 1 (dashed line) is comprised of cloud-free intervals ≤ 875 km long. Class 2 (thick, solid line) clear intervals span from 875-1500 km. Class 2 intervals had the greatest relative diurnal variation. While both classes peaked at 0900 LST, Class 2 clear intervals comprised only 9% of the total cl area and yet accounted for 58% of the 0200-0900 LST diurnal cycle.

An integral part of the cluster analysis above was the assumption that -65°C separates active, deep convection from other types of cloud. To further test this idea, I developed a more advanced application of the line cluster technique called *threshold initiation.* The threshold initiation technique identifies line clusters which build from warmer levels through a T_{BB} threshold by comparing two consecutive hourly IR images.

Starting with an IR image array at any time, a line cluster is identified using the technique described in the first part of this section. Then, the line cluster is compared to nearby pixels in the previous hourly image. If no single pixel within a 25 km buffer zone surrounding the original line cluster has T_{BB} colder than -62°C, the case is counted as a threshold initiation. A 25 km zone was chosen to eliminate cold cloud that could advect into the scene assuming 6 ms^{-1} horizontal winds. However, the results were not sensitive to minor changes in the size of the buffer zone. Tests of this technique with 10 km and 40 km zones yielded qualitatively consistent results.

Figure 7.10 shows results for JJA. The thick, solid line depicts the initiation of deep convection in terms of the initiation of Class 2 line clusters through the -65°C level. Class 1 line clusters are illustrated by the dashed line. The abscissa represents the relative variation of the number of occurrences of threshold initiation from the mean number. In absolute terms, there were near 1000 occurrences in the early morning and just over 100 occurrences in the late afternoon. So, results demonstrate that mature Class 1 and 2 line clusters existed at all times of day. However, clusters were more likely to reach maximum intensity near 0400-0600 LST and least likely at 1700-1900 LST. The time of day was much more crucial for Class 2 clusters. In absolute terms, there were around 16000 occurrences of Class 1 line clusters in the early

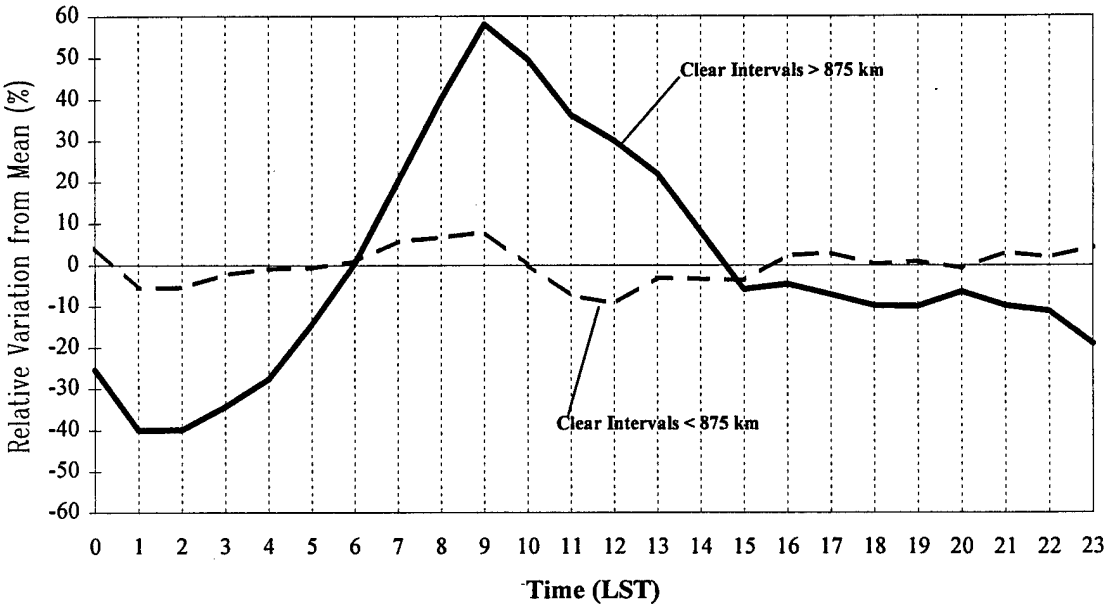

Figure 7.9: JJA relative percentage variation of area covered clear intervals divided into two class sizes. Class 1 (dashed line) is comprised of intervals < 875 km long. Class 2 (thick, solid line) clear intervals span from 875-1500 km.

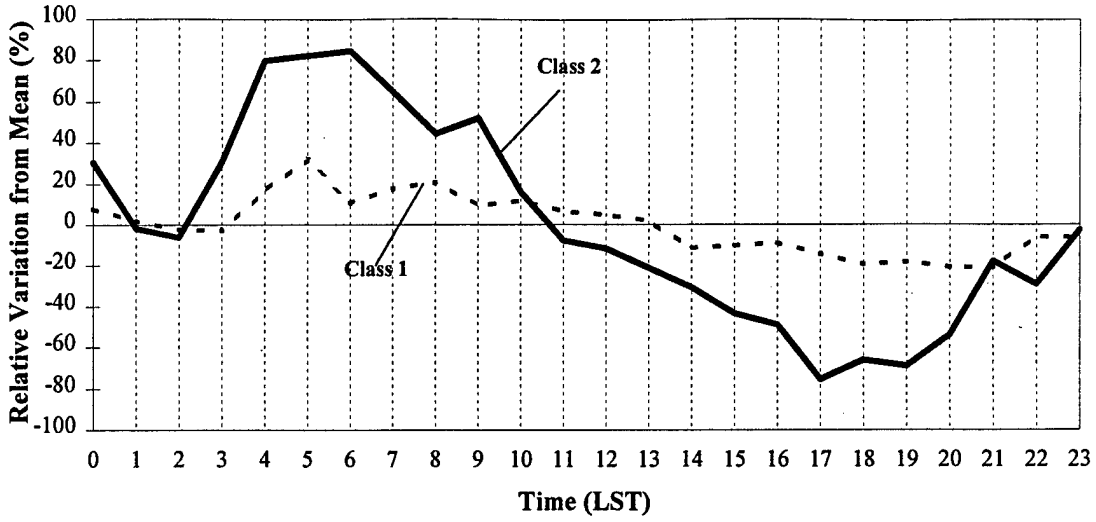

Figure 7.10: Results of threshold initiation algorithm. Thick, solid line represents hourly relative percentage variation of number of occurrences of JJA Class 2 deepening convection. The dashed line shows the analogous relative variation of number of occurrences of building JJA Class 1 line clusters. The results of NDJ (not shown) were not substantially different from the results in this figure for JJA.

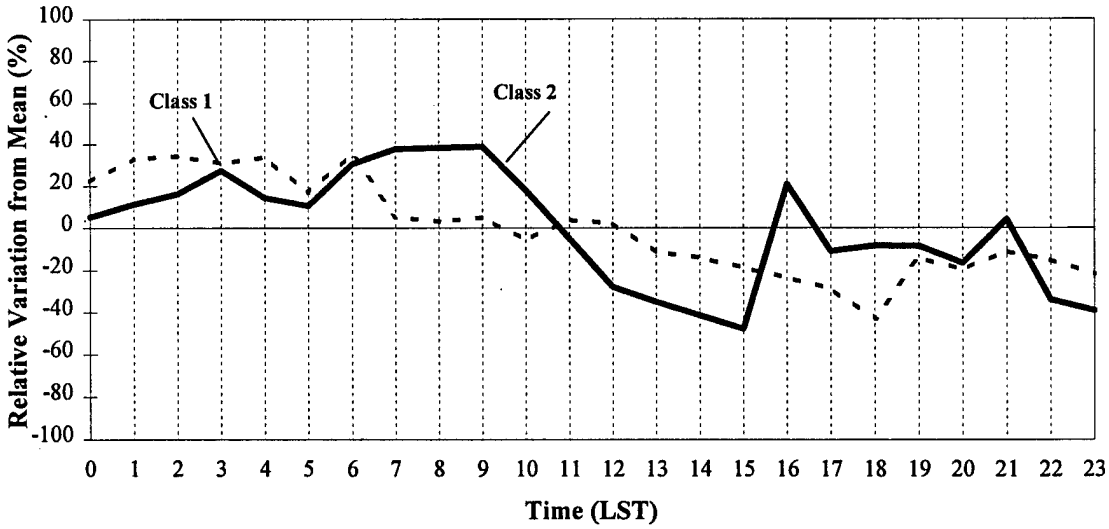

Figure 7.11: As in Fig. 7.10, for January 1995 (inactive ISO).

morning and 12000 occurrences in the late afternoon. Threshold initiation of Class 1 and Class 2 line clusters was similar for December 1994 (not shown).

Threshold initiation results for January 1995 are shown in Fig. 7.11. As with other seasons, Class 1 and 2 clusters were most likely in the morning and least likely in the evening. However, this tendency was not as dramatic as in other seasons. Part of the reason is a secondary maximum of intensifying convection in the afternoon. A population of building Class 2 clusters occurs between 1500-2100 LST. These tended to be sized at the smaller end of Class 2. A slight increase in the number of deepening Class 1 clusters occurred between 1800-2100 LST.

Discussion

Machado et al. (1993) state that the spatial structure of convective cloudiness is closely related to the mechanisms that generate and maintain the cloudiness. Analysis of the structural characteristics of tropical convection is thus a source of information for the improvement of convective parameterization schemes in GCMs. Satellite observation reveals structure at smaller and larger scales than model resolution. Hence, satellite studies are relevant for the validation of GCMs because they give a statistical view of the spatial and structural organization of convection. The present study shows that this organization varies greatly on diurnal time scales.

Figure 7.2 shows that tropical cloud systems form a single continuous size distribution over seasonal time scales. This agrees with results presented by Machado and Rossow (1993) for large portions of the tropics. Because of this distribution, previous studies have devised various techniques to subdivide the continuum of clusters into various size categories. Machado et al. (1993) defined radius intervals varying logarithmically with radius size. Mapes and Houze (1993) arbitrarily divided clusters into four quartiles (Classes 1-4), each comprising 25% of the total cold cloud area. For example, Class 4 contained the 25% of cold cloud area contributed by the largest clusters. This same technique was subsequently used by Chen et al. (1996) and Chen and Houze (1997). Neither of these techniques create cluster size groups with specific physical meaning.

In the present study, I divided the range of cluster sizes according to the characteristic diurnal cycle of each size expressed as the maximum morning to afternoon/evening ratio of cold cloud ($< -65^{o}C$). For each season, Class 1 consisted of all small scale convection with a diurnal cycle of ~ 2:1 or less. In each case, the ratio was near 2:1 from single pixel clouds up to some critical size cluster. Beyond this critical size, the diurnal ratio rose rapidly with increasing cluster size. For all three periods, Class 2 clusters comprised between 30-36% of all deep convective cloud. The class 2 definition, then, turned out to create a similar grouping to the Mapes and Houze Class 4 definition. An interesting result is the variation in the

cutoff between Class 1 and 2 size categories for JJA, December 1994 and January 1995 (Figs. 7.3, 7.5 and 7.7).

During JJA, the diurnal cycle of deep convection was dominated by Class 2 clusters of size $\geq \sim 25000$ km^2 (Fig. 7.4). By the Mapes and Houze method, the largest class would have been defined similarly by clusters $\geq \sim 30000$ km^2. While only comprising 30% of the total cloud, Class 2 clusters accounted for a disproportionate 54% of the diurnal cycle. The relative variation of cold cloud is much more significant than the diurnal increase in total number of clusters. This indicates that the diurnal cycle of deep convection was primarily due to the intensification and expansion of a relatively small number of large clusters. Results presented in Fig. 7.10 demonstrate that the early morning maximum was created by deepening, intense convection. Conversely, much less building convection at the -65°C T_{BB} level was present in the afternoon. Machado et al. (1993) studied Atlantic Ocean clusters during summer and found the diurnal cycle due primarily to already developed clusters with radius > 100 km. In the present study, the equivalent radius of JJA class 2 clusters was ~ 90 km.

For December 1994, the diurnal cycle of deep convection was dominated by Class 2 clusters of size $\geq \sim 70000$ km^2 (Fig. 7.6). Taking only the clusters sizes constituting the top 25% of cold cloud, the Mapes and Houze technique would have defined the largest class as clusters $\geq \sim 75000$ km^2. Again, while comprising only 9% of all detected clusters and 32% of the total cloud, Class 2 clusters drove nearly 40% of the total diurnal cycle. As in JJA, the diurnal variation of area covered by cold cloud was greater than the relative variation of number of clusters. Chen and Houze (1997) similarly found that the diurnal cycle during TOGA COARE (November 1992 - February 1993) was dominated by clusters larger than ~ 90000 km^2.

The natural class division for January 1995 occurred at ~ 100 km. This is equivalent to clusters of ~ 11000 km^2. As with JJA and December 1994, the diurnal cycle was dominated by Class 2 clusters which comprised 54% of the 0500-1900 LST diurnal cycle (Fig. 7.8). Chen and Houze (1997) found the diurnal cycle during suppressed ISO phases to be largely determined by smaller scale clusters ($< \sim 29000$ km^2). The cold cloud from these clusters peaked in the afternoon. Findings of the present study are somewhat different. Overall, the diurnal cycle was driven by smaller scale clusters than in either JJA or December 1994. Both Class 1 and 2 clusters from January 1995, though, exhibited the same diurnal phases as the other time periods with an early morning peak and late afternoon minimum. However, the results of the threshold initiation analysis (Fig. 7.11) suggest the existence of a minor afternoon peak which is not reflected in the mean diurnal cycle for the month (Fig. 7.8).

In support of my qualitative analysis of animated imagery loops (chapter 5), the threshold analysis verified that deep convection of all scales and stages of maturity existed at all times of day. So, convection

largely developed at random hours due to forcings discussed in section 2.5. A similar conclusion was reached by Rickenbach and Rutledge (1996). Random development does not support the BLML theory which requires clusters to preferentially form in the late afternoon and evolve to maturity throughout the night.

During both seasons, a relatively small number of large clusters comprised ~ 30% of the total area of cold cloud. These large clusters, in turn, drove a disproportionate fraction of the total diurnal variation of deep convective cloud. This bias was most pronounced in JJA and January 1995. As documented by Janowiak et al. (1994) and Liu et al. (1995), a significant portion of the total rainfall originates in convection with cloud-top $T_{BB} \leq \sim -60^{o}C$. A relatively small number of large clusters, then, dominated the diurnal cycle of WP rainfall. Also during both seasons, the cold cloud area expanded rapidly through the early morning hours while the total number of clusters increased only slightly. This suggests that the diurnal variation resulted mainly from the internal variation of large clusters during their lifetime, in agreement with Machado et al. (1993).

The results in Fig. 7.9 show that more than half of the diurnal cycle of total clear area shown in Fig. 6.15 was contributed by the variation of a relatively few large clear intervals longer than 875 km. This is interpreted to be a reflection of the dissipative effects of increased subsidence. The summation of convectively forced and naturally increased nocturnal subsidence (McBride and Gray 1980) maximizes a few hours after maximum deep convection. This reflects processes consistent with the DNS theory of the diurnal cycle.

The attribution of the diurnal cycle to primarily large clusters agrees with the observations of Gray and Ruprecht (1976) and Gray and Jacobson (1977). But even without large clusters, my results show that tropical rainfall would have an early morning maximum. For all time periods, the ratio of Class 1 morning to afternoon convection was ~ 2:1. Evidently, strong nocturnal forcings exist that affect all scales of convection. One or more mechanisms conspire to most strongly force the largest systems.

Conceptually, RCF could be at work on all scales of convective organization. However, in modeling studies (eg; Xu and Randall 1995) RCF primarily effects large stratiform regions (Xu, personal communication 1997) and so does not create an overall daily cycle of convective rainfall to the extent implied by Janowiak et al. (1994), Liu et al. (1995) and the results of the present study. Rickenbach and Rutledge (1996) reached this same conclusion from TOGA COARE radar data. For many large clusters, the daily variation of heavy rainfall inferred from the present study may be 10:1 or more. One problem with the models is likely domain size. The domain used Xu and Randall, for example, was 500x500 km. Within the domain, the largest clusters were ~ 100 km in diameter. Results of the present study show the greatest effect on WP rainfall variation comes from clusters $\geq \sim$ 180 km in diameter during JJA and $\geq \sim$

300 km in diameter during winter. Until models improve their representation of the deep convective component of the diurnal cycle, it is difficult to assign any amount of diurnal forcing to RCF.

Two other mechanisms that could be at work on all scales are LRD and DNS. LRD may conspire to enhance DNS, but would not be able to act alone. Cornejo-Garrido and Stone (1977) show that convection is usually correlated with minimum evaporation. Considering this, low-level convergence must supply most of the local moisture for convection. This conclusion was confirmed by Thompson et al. (1979).

The observation that the total number of clusters slightly increased at night may reflect more favorable middle-level environmental moisture conditions due to LRD. Given the deep west Pacific convergence profiles documented by McBride and Gray (1980), enhanced middle-level available precipitable water could enhance the nocturnal moisture convergence. However, the fact that systems existed day and night suggests that enough precipitable water was available at nearly all times for development of mature mesoscale weather systems. Regions of active cloud clusters produce local environments with abundant residual moisture such that these regions tend to get "locked in" as convective regimes (Gray 1973). During JJA, local regions of the monsoon trough were often the locked into convection several days in a row. Yet, these systems still exhibited the same diurnal variability as more isolated clusters. If LRD affected WP convection during the periods of this study, it must have acted in concert with other mechanisms such as DNS.

The results of this study do support DNS as a driving mechanism of the diurnal cycle. The existence of organized convection at all times of day and night supports the requirement of Gray and Jacobson (1977) for pre-existing weather systems. On the ITCZ scale, increased nocturnal subsidence would enhance nocturnal low and middle-level moisture convergence. Enhanced convergence would enhance deep convection on all scales creating a nocturnal intensification of clusters persisting into or forming during the night. For larger clusters, the ITCZ scale DNS could be enhanced by local cluster scale clear-cloudy differential radiative cooling effects.

7.2 Diurnal Spatial Variation of Large Cloud Clusters

It was stated several times in chapter 6 that *diurnal dancing* of deep convection was not observed. That is to say I did not observe the preferential formation of cloud clusters in relatively cloud-free regions. Also, I did not observe the return of deep convection to a local region every other day. In fact, my analysis of IR loops suggested deep convection in the WP was more likely to form in the same place two days in a row. In this section, I document the one to three day spatial variability of cloud clusters.

Method/Results

To analyze daily spatial variability, I first created daytime composites of cloud from the JJA CHANCES CNC database to look for formation in clear zones as observed by Chen and Houze 1997. For each day, I compared enhanced IR imagery at various hours to the cloud composites. During all of JJA, no convective events formed in relatively cloud free regions of the WP sector of this study. On the contrary, MCSs consistently formed within the cloud shields of pre-existing larger scale disturbances moving across the WP sector.

To quantify the daily spatial variation for both JJA and NDJ, I developed another application of the line cluster identification technique. First, a line cluster was identified in an IR image. If the line cluster was Class 2, an observations counter for the UTC hour was stepped by one. Then, the same pixels were examined 24 hours into the future. If convection covered at least 50% of the pixels in the line at the 24 hour point, the 24 hour counter was stepped by one. After compiling statistics for each hour for the entire period, the conditional probability of convection given convection 24 hours prior was simply the quotient of the observations counter and the 24 hour counter. For the present study, I computed three types of conditional probabilities using the same technique:

(1) Conditional probability of convection in 24 hours given Class 2 convection at initial time

(2) Conditional probability of convection in 48 hours given Class 2 convection at initial time

(3) Conditional probability of convection in 24 and 48 hours given Class 2 convection at initial time

Results are shown in Table 2 for early morning (0500-0700 LST) and for the grand mean of all times. When a Class 2 cluster occurred in the early morning during JJA, deep convection occurred in basically the same location 49% of the time. Similarly, deep convection occurred every other day in the morning 44% of the time. Of those occurrences with convection at the initial time and 48 hours for JJA, convection also occurred at 24 hours ~ 85% of the time. The results are similar for December 1994. During the convectively suppressed January 1995, deep convection occurred in the same location two days in a row 30% of the time.

TABLE 2: Conditional Recurrence Probabilities of Convection

Given a line cluster detected in the early morning, these probabilities indicate the percentage of the time deep convection recurred in the same geographic location at the indicated time intervals.

	Early Morning			All Times
Time Interval	24 Hours	48 Hours	24 and 48 Hours	24 Hours
JJA	49%	44%	36%	36%
Dec. 1994	44%	33%	21%	39%
Jan. 1995	30%	21%	8%	22%

Discussion

Figures 6.12 and 6.13 show that convection only covered about 2% of the total possible area in the WP sector for JJA and NDJ. Of course, on some days the percentage was somewhat higher and on other days close to zero. On very active days, perhaps as much as 5% of the area was covered by cloud colder than -65°C. Given such small areal coverage, one would not necessarily expect convection to ever occur in the same place two days in a row. However, my results show just the opposite is the case.

Nearly half the time during JJA and December 1994, convection occurred two mornings in a row in precisely the same location. During JJA, deep convection occurred in the same location three mornings in a row nearly 36% of the time. There are several implications of these observations.

First, in agreement with my visual inspection of IR loops and daily visible composites, *diurnal dancing* did not occur in the WP sector during JJA or NDJ. This effect is thought to be driven primarily by cloud shading of the sea surface which prevents daytime heating (Chen and Houze 1997). The second implication relates to the notion of boundary layer recovery time. Chen et al. (1996) hypothesize that low-θ_e downdrafts produced by these large convective systems may prevent new convection from developing the day after an outbreak by reducing the moist static energy. Parsons et al. (1994) observed what they interpreted as a boundary layer recovery time of up to ~ 18 hours in the wake of convective systems during TOGA COARE. Results of this study indicating deep convection every 24 hours in the same location nearly half the time during JJA and NDJ dispute the effect of low-θ_e downdraft air. Apparently, other effects take precedence. For example, (Gray 1973) suggests that convective regimes get "*locked in*" due to moisture availability. Deep convection tends to add moisture to the middle and upper levels of the tropical troposphere. Increased middle-level moisture means less entrainment of dry air and hence stronger updrafts as convection develops. Subsident regimes become locked in due to the continuous sinking and drying.

Conclusion

Various processes in the tropics lead to the formation of mesoscale systems (chapter 2). Once created, they evolve in accord with general observations of MCSs throughout the tropics (eg; Houze 1982). They typically evolve from a few initial deep hot towers, which subsequently merge and form extensive stratiform cirrus cloud shields. If they form in the late afternoon or night, additional external forcings (RCF, LRD or DNS) enhance the natural internal variation of active convective clusters allowing them to achieve a maximum potential intensity and size. All scales of convection exhibited an early morning maximum during JJA and NDJ, however the diurnal cycle was dominated by the largest 10% clusters occurring during each season.

The existence of new, deepening cloud cluster convection of all scales at all times of day suggests an almost random development. In JJA and December 1994, Class 2 deep convection occurred two days in a row in the same location 49% of the time in the early morning (near 0600 LST). This fact, combined with the observation of random development, does not support BLML as a dominant driving mechanism of the diurnal cycle. The tendency for clusters to reach a maximum potential in the early morning implies that RCF, LRD and DNS diurnal mechanisms enhance nocturnal convection. My results do not refute RCF, but do suggest that domain and cluster size are critical to realistic model simulation the diurnal cycle. Previous model results have not attributed enough of the total rainfall in the diurnal cycle to heavy convective precipitation produced by MCSs embedded within large clusters. For example, modelled simulations of the diurnal cycle of deep convection in the warm pool need a domain large enough to accommodate MCSs within cloud clusters of at least 25000 km^2 during summer and 70000 km^2 in winter. A recent study by Xu and Randall 1995 contained a domain of 500 km^2 and simulated cloud clusters of only ~ 8000 km^2.

LRD could have made conditions more favorable for convection in concert with DNS. However, particularly enhanced regimes of continuous convection for several days would not have been strongly influenced by nocturnal variations in precipitable water. Yet, those regimes had the same diurnal variability. The results do support DNS as a potential driver of the diurnal cycle. Cloud clusters on all scales could be enhanced by a ITCZ scale processes. DNS could preferentially intensify the largest, organized mesoscale clusters by summation of local cluster scale and ITCZ scale subsidence-convergence forcing. Evidence of increased nocturnal subsidence was reflected in the strong diurnal variation of large clear intervals.

Chapter 8

Summary and Conclusions

Latent heat released in west Pacific warm pool convection drives planetary scale circulations and a vigorous local hydrologic cycle. Daily changes in deep convection lead to dramatic latitudinal and longitudinal variations in cloud cover, precipitation and sea surface temperature. Studies over the past 25 years document a significant diurnal cycle of convective cloud over the world's tropical oceans. Due to various local effects, results documenting the phase and amplitude of this cycle, however, are not consistent. Also, there is no consensus on the driving force(s) motivating the diurnal cycle. Collectively, ideas about the driving mechanisms of the diurnal cycle are diverging with time. Complicating the issue, the dominant mechanism(s) may vary with geographic location, season or even with the temporary background state of the atmosphere. In this thesis, I used a high resolution satellite data set to gain better understanding of the diurnal cycle in the tropical west Pacific north of the equator. Diurnal rainfall variations will reflect the large scale environment vertical motion forcing only in regions where strong, local dynamic and thermodynamic effects are not dominant (i.e.; GATE). The WP sector of the present study in such a region.

In the west Pacific, significant convection is usually organized into large (~ 700 km diameter) organized systems called cloud clusters. More intense MCSs of up to ~ 250 km in diameter are usually embedded within these clusters. Five potential driving mechanisms of the diurnal cycle were considered to apply in the region of this study including: (1) Atmospheric Tides (AT); (2) Day vs Night Radiation-Subsidence (DNS); (3) Direct Radiative Cloud Forcing (RCF); (4) The Large Scale Radiative Destabilization (LRD); (5) and Boundary Layer-MCS Lifecycle (BLML).

Due to the paucity of surface observations, satellite data provides the only way to document the diurnal cycle for large expanses of the world's oceans. Tropical convection is easily identified in IR satellite imagery. In this study, GMS-4 digital satellite imagery with 1-hr temporal and 5-km spatial resolution was extracted from the CHANCES database. Threshold techniques were used to identify deep convection in the IR imagery. Previous work suggests that T_{BB} below at least -60°C is necessary to

effectively isolate deep convection. Results of the present study verify that -65°C is an effective threshold to identify cold cloud-tops associated with intense tropical convection.

Imagery was analyzed pixel by pixel to compile fractional coverage statistics of cold cloud for each hour. Results showed an early morning maximum with a late afternoon/evening minimum in area covered by cold cloud (< -65°C) for JJA. This same cycle occurred in both active and inactive phases of the ISO during NDJ. The ratio of maximum to minimum fractional coverage of deep convective cloud was greater than 2:1 for all time periods. Clouds associated with intense convection were characterized by three distinct diurnal cloud regimes representing deep convection, mixed deep convection/cirrus anvil and stratiform cirrus regimes. The diurnal variation of convective cloud forms in these three regimes was consistent for all time periods, including for two tropical storms which occurred in the WP during December 1994.

To quantify short time scale variability of deep convection, time series of T_{BB} < -65°C pixel counts were constructed for periods during JJA and NDJ. Spectral analysis of these time series revealed a powerful diurnal cycle significant at the 95% confidence level for JJA and NDJ. The diurnal cycle was strongest near the equator. No semi-diurnal spectral peaks occurred during either season. This does not support the semi-diurnal tides as having any discernible effect on deep tropical convection.

During JJA and January 1995, there was a strong suggestion of bi-diurnal variability. For JJA this bi-diurnal cycle was significant near the 95% confidence level for the near-equatorial region (0°-5°N), but was still evident above the red noise background for the off-equatorial WP (5°-20°N). In this off-equatorial region, a bi-diurnal cycle may reflect the impact of moisture deposited in the upper levels by large scale convection. Anomalous upper level moisture would reduce LW cooling, impeding both the DNS and LRD diurnal mechanisms, hence diminishing convection the night following an intense outbreak. In the near equatorial region, this effect may complement quasi-2-day variability driven by near-equatorial inertio-gravity waves as described by Takayabu et al. (1996).

After quantifying the overall diurnal variation of WP convective cloud, I investigated its relation to the satellite observed structural characteristics of cloud clusters. Accomplishing this required the application of several objective image analysis techniques. To characterize cloud clusters in terms of size, I compiled statistics of latitudinal cold cloud (< -65°C) intervals (*line clusters*) for each hour of the day. These line clusters represent a characteristic horizontal dimension of the deep convective portion of MCSs embedded within tropical cloud clusters. The continuum of cluster sizes was subdivided into two classes for each season based on the intrinsic diurnal variation of line clusters of each size expressed as the morning to evening ratio of number of occurrences. A second technique called *threshold initiation* allowed separation of deepening from dissipating or stable clusters.

During each season, the diurnal cycle of cold cloud was dominated by the largest class of clusters. These clusters comprised around ~ 10% of the total number of all clusters, contributed ~ 30% of the total fractional area of cold cloud and accounted for around 50% of the diurnal cycle. Throughout the night, the number of large clusters increased only slightly, while the area of cold cloud from these clusters increased significantly. The results of the threshold initiation analysis showed that intensifying convection of all scales existed at all times of day and night with a slight preference for early morning. These findings imply that a disproportionate amount of the total tropical rainfall in the diurnal cycle is associated with an internal variation of a relatively few, large MCSs (embedded within larger cloud clusters) that existed going into or formed during the night. During convectively active spans of time such as occurred during JJA and December 1994, these large clusters are $\geq \sim 200$ km in diameter.

In the final section of the study, daily spatial variability was analyzed. Enhanced IR imagery viewed as loops revealed that convection on all scales in various stages of maturity existed at all times of day and night. In some cases, organized deep convection recurred in the same geographic location many days in a row. There was no observed preferential formation of MCSs in relatively clear regions as found by Chen and Houze (1997) for TOGA COARE. This was confirmed through comparison of daily visible imagery composites with cloud clusters visually identified in hourly digital IR pictures. To quantify these observations, three types of conditional recurrence probabilities were computed.

Given deep convection at an initial time, I computed the percentage of time deep convection recurred in 24 hours, 48 hours (every other day) and in 24 and 48 hours (three days in a row). When convection occurred in the early morning during JJA and December 1994, nearly half the time it recurred the following morning in the same location. The conditional probability of convection in 48 hours was 44% in JJA and 33% in December 1994. During JJA, ~ 85% of the occurrences at 48 hours were locations that also had convection the previous morning at 24 hours from the initial time. These results show that *diurnal dancing* was not a preferred mode of spatial variation during JJA and NDJ. Given deep convection in the early morning, it was more likely for convection to occur again in 24 hours in the same location than at any other time interval beyond 12 hours. Combined with the observation of the existence of all scales of building convection at all times of day and a lack of formation in relatively cloud-free zones, the results of the present project showed that the BLML mechanism did not drive the WP diurnal cycle during the period of study. Systems did not tend to form preferentially in the afternoon and evolve to maximum intensity in early morning.

Various processes in the tropics lead to formation of mesoscale weather systems. Typically, they evolve from a few initial hot towers, which subsequently merge and form extensive stratiform cirrus cloud shields. If they form in the late afternoon or night, external radiative forcing evidently acts to enhance the

natural internal variation of active clusters allowing them to achieve a maximum potential intensity and size. Five diurnal mechanisms were considered to provide potential forcing of a morning maximum of deep convection in the WP: AT, DNS, RCF, LRD and BLML. I have stated that AT and BLML were not driving diurnal variability during JJA or NDJ. However, the results are generally consistent with DNS, RCF and LRD.

Whereas previous modelling results have been mixed, they show RCF could create a diurnal cycle of precipitation with an early morning maximum and late afternoon minimum (eg; Xu and Randall 1995). However, the amplitude of morning-afternoon precipitation changes are of smaller magnitude than rainfall variation implied by results of the present study. Model simulations to date also have not accounted for the disproportionate contribution to the diurnal variation of total rainfall by the largest MCSs as inferred in this study. In addition, the primary forcing effect of RCF on the daily variation of rainfall in models and in the atmosphere is on stratiform rain associated with the extensive stratiform cirrus cloud shield of a cloud cluster (Lilly 1988; Rickenbach and Rutledge 1996; Xu, personal communication 1997). Modeled effects of direct radiative forcing on extensive stratiform cirrus cloud decks with lifetimes of greater than a half a day cannot be assumed to apply to intense convection where individual elements (Cbs) have a lifetime on the order of only a half hour.

My results do not support LRD as having been predominant during JJA and December 1994. A large percentage of the time during these periods, convection occurred two to three days in a row in the same location. Usually, the deepest convection formed within large scale regions of residual overcast middle and high level cloud left behind from previous convection. In these regions, moisture conditions are very favorable for development of convection day and night as evidenced by the results presented in section 7.2. Any diurnal variation in tropospheric precipitable water would be negligible. However, LRD may have been significant during the suppressed conditions of January 1995.

Results are consistent with DNS. If the role of tropical convection is to balance radiational cooling as discussed in chapter 2, there must be variation in convection due to day versus night net tropospheric radiative cooling. DNS predicts conditions that would lead to an early morning maximum of rainfall for all scales of deep convection due to day versus night net cooling in regimes where local dynamics or thermodynamics are not predominant. As described by Gray and Jacobson (1977), DNS is expected to have the greatest impact on large, organized weather systems, as documented in the present study. These weather systems can experience the additive effects of clear area subsidence driven by day versus night differences in net tropospheric radiative cooling, and disturbance to ITCZ scale convergence driven by cloudy-clear differential heating/cooling. Also, DNS could be expected to force an early morning peak for all scales of convection. The main difference with the results of Gray and Jacobson is the finding of no

apparent lag time between maximum convergence predicted by DNS and deep convection. For both JJA and NDJ, the maximum and minimum areal coverage of deep convection occurred basically in phase with sunrise and sunset. However, the variation in heavy rainfall may not be precisely in phase with the variation of very cold cloud.

High temporal and spatial resolution satellite data is essential to completely document the diurnal cycle. In this thesis, I have provided a comprehensive satellite-based study of the day-to-day variation of deep convection in the northern hemisphere tropical west Pacific warm pool. Satellite observations provide the best coverage of large expanses of oceanic regions, but they tell only part of the story. Larger scale field projects, better models and higher resolution information such as radar data need to be combined with satellite imagery to get a complete picture. A crucial challenge for the future is to get accurate, representative measurements of the actual amount of heavy rainfall attributable to the large, intense MCSs embedded within tropical cloud clusters. I also believe a field project focused outside of the near-equatorial region would be beneficial. The diurnal problem is a complicated 3-D puzzle that may not be fully defined for many years to come. This thesis adds another piece to the puzzle.

References

Ackerman, S. A., and S. K. Cox, 1981: GATE Phase III mean synoptic-scale radiative convergence profiles. *Mon. Wea. Rev.*, **109**, 371-383.

Ackerman, T. P., K.-N. Liou, F. P. J. Valero, and L. Pfister, 1988: Heating rates in tropical anvils. *J. Atmos. Sci.*, **45**, 1606-1623.

Albrecht, B., and S. K. Cox, 1975: The large-scale response of the tropical atmosphere to cloud-modulated infrared heating. *J. Atmos. Sci.*, **32**, 16-24.

Albright, M. D., D. R. Mock, E. E. Recker, and R. J. Reed, 1981: A diagnostic study of the diurnal rainfall variation in the GATE B-scale area. *J. Atmos. Sci.*, **38**, 1429-1445.

Albright, M. D., E. E. Recker, and R. J. Reed, 1985: The diurnal variation of deep convection and inferred precipitation in the central tropical Pacific during January-February 1979. *Mon. Wea. Rev.*, **113**, 1663-1680.

Anthes, R. A., 1982: *Tropical Cyclones - Their Evolution, Structure and Effects. Meteor. Monogr.*, No. 41, published by AMS, Boston, MA, 208 pp.

Arkin, P. A., 1979: The relationship between fractional coverage of high cloud and rainfall accumulations during GATE over the B-scale array. *Mon. Wea. Rev.*, **107**, 1382-1387.

Augustine, J. A., 1984: The diurnal variation of large-scale inferred rainfall over the tropical Pacific Ocean during August 1979. *Mon. Wea. Rev.*, **112**, 1745-1751.

Ball, J. T., S. J. Thoren, and M. A. Atwater, 1980: Cloud-coverage characteristics during Phase III of GATE as derived from satellite and ship data. *Mon. Wea. Rev.*, **108**, 1419-1429.

Bergman, J. W., and M. L. Salby, 1996: Diurnal variations of cloud cover and their relationship to climatological conditions. *J. Climate*, **9**, 2802-2820.

Bluestein, H. B., 1993: *Synoptic-Dynamic Meteorology in Midlatitudes, Volume II.* Oxford University Press, 594 pp.

Brier, G. W., and J. Simpson, 1969: Tropical cloudiness and rainfall related to pressure and tidal variations. *Quart. J. Roy. Meteor. Soc.*, **95**, 120-147.

Browner, S. P., W. L. Woodley, and C. G. Griffith, 1977: Diurnal oscillation of the area of cloudiness associated with tropical storms. *Mon. Wea. Rev.*, **105**, 856-864.

Byrd, G. P., and S. K. Cox, 1984: A case study of radiative forcing upon a tropical cloud cluster system. *Mon. Wea. Rev.*, **112**, 173-187.

Chang, A. T. C., L. S. Chiu, and G. Yang, 1995: Diurnal cycle of oceanic precipitation from SSM/I data. *Mon. Wea. Rev.*, **123**, 3371-3380.

Chen, S. S., R. A. Houze, Jr., and B. E. Mapes, 1996: Multiscale variability of deep convection in relation to large-scale circulation in TOGA COARE. *J. Atmos. Sci.*, **52**, 1380-1409.

Chen, S. S., C. Zhang, and R. A. Houze, Jr., 1995: Surface diurnal variation - A link between solar heating and diurnal cycle of tropical convection? Preprints, *21st Conference on Hurricanes and Tropical Meteorology*, Miami, AMS, 518-520.

Chen, S. S, and R. A. Houze, Jr., 1997: Diurnal variation and lifecycle of deep convective systems over the tropical Pacific warm pool. *Quart. J. Roy. Meteor. Soc.*, **123**, 357-388.

Churchill, D. D., and R. A. Houze, Jr., 1984: Development and structure of winter monsoon cloud clusters on 10 December 1978. *J. Atmos. Sci.*, **41**, 933-960.

Chruchill, D. D., and R. A. Houze, Jr., 1991: Effects of radiation and turbulence on the diabatic heating and water budget of the stratiform region of a tropical cloud cluster. *J. Atmos. Sci.*, **48**, 903-922.

Cornejo-Garrido, A. G., and P. H. Stone, 1977: On the heat balance of the Walker circulation. *J. Atmos. Sci.*, **34**, 1155-1162.

Cox, S. K., and K. T. Griffith, 1979: Estimates of radiative divergence during phase III of the GARP Atlantic Tropical Experiment: Part II. Analysis of phase III results. *J. Atmos. Sci.*, **36**, 586-601.

Deser, C., and J. M. Wallace, 1990: Large-scale atmospheric ciuculation features of warm and cold episodes in the tropical Pacific. *J. Climate*, **3**, 1254-1281.

Deser, C., 1994: Daily surface wind variations over the equatorical Pacific Ocean. *J. Geophys. Res.*, **99**, 23071-23078.

Deser, C., and C. A. Smith, 1997: Diurnal and semidiurnal variations of the low-level wind field over the tropical Pacific Ocean. *J. Climate,* submitted.

Dewart, J. M., 1978: Diurnal variability in the GATE region. Atmos. Sci. Paper No. 298, Colorado State University, 80 pp.

Donner, L. J., C. J. Seman, and J. P. Sheldon, 1997: Cloud-radiative interactions in high-resolution cloud-resolving models. Preprints, *9th Conference on Atmospheric Radiation*, Long Beach, published by AMS, Boston, MA, 47-48.

Dopplick, T. G., 1972: Radiative heating of global atmosphere. *J. Atmos Sci.*, **20** 5-22.

Dorman, C. E., and R. G. Bourke, 1979: Precipitation over the Pacific Ocean, 30°S to 60°N. *Mon. Wea. Rev.*, **107**, 896-910.

Dudhia, J., 1989: Numerical study of convection observed during the Winter Monsoon Experiment using a mesoscale two-dimensional model. *J. Atmos. Sci.*, **46**, 3077-3101.

Duvel, J. P., R. S. Kandel, 1985: Regional-scale diurnal variations of outgoing infrared radiation observed by METEOSAT. *J. Clim. Appl. Meteor.*, **24**, 335-349.

Duvel, J. P., 1989: Convection over tropical Africa and the Atlantic Ocean during northern summer. Part I: Interannual and diurnal variations. *Mon. Wea. Rev.*, **117**, 2782-2799.

Evans, J. L., and R. E. Shemo, 1996: A procedure for automated satellite-based identification and climatology development of various classes or organized convection. *J. Appl. Meteor.*, **35**, 638-652.

Falvey, R. J., 1992: A composite study of the Madden-Julian oscillation. Atmos. Sci. Paper No. 494, Colorado State University, 140pp.

Fingerhut, W. A., 1978: A numerical model of a diurnally varying tropical cloud cluster disturbance. *Mon. Wea. Rev.*, **106**, 255-264.

Finkelstein, J., 1964: Diurnal variation of rainfall amount on tropical Pacific islands. *Symposium on Tropical Meteor.*, Rotura, N.Z., *Proc.* New Zealand Meteorology Services, Wellington, 286-294.

Foltz, G. S., 1976: Diurnal variation of the tropospheric energy budget. Atmos Sci. Paper No. 262, Colorado State University, 141 pp.

Foltz, G. S., and W. M. Gray, 1979: Diurnal variation in the troposphere's energy balance. *J. Atmos. Sci.*, **36**, 1450-1466.

Frank, N. L., 1969: Atlantic tropical systems of 1969. *Mon. Wea. Rev.*, **98**, 307-314.

Frank, W. M., 1978: The life cycles of GATE convective systems. *J. Atmos. Sci.*, **35**, 1256-1264.

Fu, R., A. D. Del Genio, and W. B. Rossow, 1990: Behavior of deep convective clouds in the tropical Pacific deduced from ISCCP radiances. *J. Climate*, **3**, 1129-1152.

Fu, R., S. K. Krueger, and K.-N. Liou, 1995: Interactions of radiation and convection in simulated tropical cloud clusters. *J. Atmos. Sci.*, **52**, 1310-1328.

Gamache, J. F., and R. A. Houze, 1982: Water budget in a mesoscale convective system in the Tropics. *J. Atmos. Sci.*, **40**, 1835-1850.

Garstang, M., 1958: Some meteorological aspects of low latitude tropical western Atlantic: Results of *Crawford* Cruise No. 15. Woods Hole Oceanographic Institution Woods Hole, Mass. Rep. No. 58-42, 97 pp.

Gray, W. M., 1972: The magnitude and character of the radiation induced vertical circulation of the troposphere. Preprint volume, *Conf. of Atmospheric Radiation*. 7-9 Aug., published by AMS, Boston, MA, 255-259.

Gray, W. M., 1973: Cumulus convection and larger scale circulations. I. Broadscale and mesoscale considerations. *Mon. Wea. Rev.*, **101**, 839-855.

Gray, W. M., 1976: Diurnal variation of oceanic deep cumulus convection. Paper II. Physical hypothesis. Atmos. Sci. Paper No. 243, Colorado State University, 106 pp.

Gray, W. M., and R. W. Jacobson, Jr., 1977: Diurnal variation of deep cumulus convection. *Mon. Wea. Rev.*, **105**, 1171-1188.

Gray, W. M., 1995: Tropical cyclones. *Invited lecture to WMO Congress*, Geneva, Switzerland, 164 pp. Being Published.

Gray, W. M., J. D. Sheaffer, and W. Thorson, 1994: On the fundamental role of tropospheic radiational cooling on the diurnal cycle of intense tropical convection. Proceedings of the *Fourth Atmospheric Radiation Measurement (ARM) Science Team Meeting*, 28 Feb.-3 Mar., Charleston, SC, published by U. S. Dept. of Energy, CONF-940277, 161-165.

Gray, W. M., and J. D. Sheaffer, 1995: Cloud-radiative forcing of the diurnal cycle of intense convection in the tropical Pacific. Proceedings of the *Fifth Atmospheric Radiation Measurement (ARM) Science Team Meeting*, 19-23 Mar., San Diego, CA, published by U. S. Dept. of Energy, CONF-9503140, 125-127.

Gray, W. M., and J. D. Sheaffer, 1996: On the fundamental role of day versus night radiation differences in forcing nocturnal convective maxima and in assessing global warming prospects. Proceedings of the *Sixth Atmospheric Radiation Measurement (ARM) Science Team Meeting*, 4-8 Mar., San Antonio, TX, published by U. S. Dept. of Energy, in press.

Griffith, C. G., W. L. Woodley, P. G. Grube, D. W. Martin, J. Stout, and D. N. Sikdar, 1976: *Rainfall Estimation from Geosynchronous Satellite Imagery during Daylight Hours*. NOAA Tech. Rep. ERL 356-WMPO 7, Boulder, CO, 106 pp.

Grossman, R. L., and O. Garcia, 1990: The distribution of deep convection over the ocean and land during the Asian summer monsoon. *J. Climate*, **3**, 1032-1044.

Grube, P. G., 1979: Convection induced temperature change in GATE. Atmos. Sci. Paper No. 305, Colorado State University, 128 pp.

Gruber, A., 1976: An estimate of the daily variation of cloudiness over the GATE A/B area. *Mon. Wea. Rev.*, **104**, 1036-1039.

Guan, H., R. Davies, and M. K. Yau, 1995: Longwave radiative cooling rates in axially symmetric clouds. *J Geophys. Res.*, **100**, 3213-3220.

Guan, H., M. K. Yau, and R. Davies, 1996: The effects of longwave radiation in a small cumulus cloud. *J. Atmos. Sci.*, submitted.

Guichard, F., J.-L. Redersperger, and J.-P. Lafore, 1996: The behavior of a cloud ensemble in response to external forcings. *Quart. J. Roy. Meteor. Soc.*, **122**, 1043-1073.

Hall, T. J., and T. H. Vonder Haar, 1997: Diurnal cycle and morphology of deep tropical convection examined with a high resolution satellite data set. Preprints, *22nd Conference on Hurricanes and Tropical Meteorology*, Fort Collins, published by AMS, Boston, MA, 184-185.

Hann, J., 1901: *Lehrbuch der Meteorologie*, 1st ed. Leipzig, Chr. Herm. Tauchnitz, 338-346.

Hartmann, D. L., H. H. Hendon, and R. A. Houze, Jr., 1984: Some implications of the mesoscale circulations in tropical cloud clusters for large-scale dynamics and climate. *J. Atmos. Sci.*, **41**, 114-121.

Hartmann, D. L., and E. E. Recker, 1986: Diurnal variation of outgoing longwave radiation in the tropics. *J. Clim. Appl. Meteor.*, **25**, 800-812.

Hendon, H. H., and K. Woodbery, 1993: The diurnal cycle of tropical convection. *J. Geophys. Res.*, **98**, 16623-16637.

Hendon, H. H., and B. Liebmann, 1994: Organization of convection within the Madden-Julian oscillation. *J. Geophys. Res.*, **99**, 8073-8083.

Holle, R. L., 1968: Some aspects of tropical oceanic cloud populations. *J. Appl. Meteor.*, **7**, 173-183.

Holland, J. Z., 1970: Preliminary report on the BOMEX sea-air interaction program. *Bull. Amer. Meteor. Soc.*, **51**, 809-820.

Holton, J. R. , 1992: *An Introduction to Dynamic Meteorology*. Academic Press, 511 pp.

Houze, R. A., Jr., 1977: Structure and dynamics of a tropical squall-line system observed during GATE. *Mon. Wea. Rev.*, **105**, 1540-1567.

Houze, R. A., Jr., S. G. Geotis, F. D. Marks, Jr., and A. K. West, 1981: Winter monsoon convection in the vicinity of North Borneo. Part I: Structure and time variation of the clouds and precipitation. *Mon. Wea. Rev.*, **109**, 1595-1614.

Houze, R. A., Jr., 1982: Cloud clusters and large-scale vertical motions in the tropics. *J. Meteor. Soc. Japan.*, **60**, 396-409.

Houze, R. A., Jr., 1989: Observed structure of mesoscale convective systems and implications for large-scale heating. *Quart. J. Roy. Meteor. Soc.*, **115**, 425-461.

Inchauspe', J., 1970: Diurnal precipitation variations over atolls of Frech Polynesia. *La Meteorologie*, Ser. 5, No. 16, 83-95.

Jacobson, R. W., Jr., 1976: Diurnal variation of deep cumulus convection. Paper I. Observational evidence. Atmos. Sci. Paper No. 243, Colorado State University, 106 pp.

Janowiak, J. E., and P. A. Arkin, 1991: Rainfall variations in the tropics during 1986-1989, as estimated from observations of cloud-top temperature. *J. Geophys. Res.*, **96**, 3359-3373.

Janowiak, J. E., P. A. Arkin, and M. Morrissey, 1994: An examination of the diurnal cycle in oceanic tropical rainfall using satellite and in situ data. *Mon. Wea. Rev.*, **122**, 2296-2311.

Jeandidier, G., and Rainteau, P., 1957: Prevision du temps sur le bassin du Congo. *France Meteor. Nat. Monor.*, No. 9.

Kidder, S. Q., and T. H. Vonder Haar, 1977: Seasonal oceanic precipitation frequencies from Nimbus 5 microwave data. *J. Geophys. Res.*, **82**, 2083-2085.

Kidder, S.Q., and T.H. Vonder Haar, 1995: *Satellite Meteorology: An Introduction*. Academic Press, 456 pp.

Kondragunta, C. R., and A. Gruber, 1996: Seasonal and annual variability of the diurnal cycle of clouds. *J. Geophys. Res.*, **101**, 21337-21390.

Kraus, E. B., 1963: The diurnal precipitation change over the sea. *J. Atmos. Sci.*, **20**, 552-556.

Lau, K. M., T. Nakazawa, and C.-H. Sui, 1991: Observations of cloud cluster hierarchies over the tropical western Pacific. *J. Geophys. Res.*, **96**, 3197-3208.

Lajoie, F. A., and I. J. Butterworth, 1984: Oscillation of high-level cirrus and heavy precipitation around Australian region tropical cyclones. *Mon. Wea. Rev.*, **112**, 535-544.

Lavoie, R. L., 1963: Some aspects of the meteorology of the tropical Pacific viewed from an atoll. Rep. No. 27, Institute of Geophysics, University of Hawaii, 76 pp.

Lilly, D. K., 1988: Cirrus outflow dynamics. *J. Atmos. Sci.*, **45**, 1594-1605.

Lin, X., 1997: Multiscale Variability Associated with the Intraseasonal Oscillation over the Western Pacific Warm Pool. Ph.D. Dissertation, Colorado State University, 199 pp.

Lindzen, R. S., 1978: Effect of daily variations of cumulonimbus activity on the atmospheric semidiurnal tide. *Mon. Wea. Rev.*, **106**, 526-533.

Lindzen, R. S., and S. Nigam, 1987: On the role of sea surface temperature gradients in forcing low-level winds and convergence in the tropics. *J. Atmos. Sci.*, **44**, 2418-2436.

Liou, K.-N., 1986: Influence of cirrus clouds on weather and climate processes: A global perspective. *Mon. Wea. Rev.*, **114**, 1167-1199.

Liu, G., J. A. Curry, and R.-S. Sheu, 1995: Classification of clouds over the western equatorial Pacific Ocean using combined infrared and microwave satellite data. *J. Geophys. Res.*, **100**, 13811-13826.

London, J., 1957: A study of the atmospheric heat balance. Final Report, Contract AF 19(122)-165, Dept. of Meteor. Oceanogr. New York University, 99 pp.

Lopez, R. E., 1973: Cumulus convection and larger scale circulations. II. Cumulus and mesoscale interactions. *Mon. Wea. Rev.*, **101**, 856-870.

Lopez, R. E., 1977: The lognormal distribution of cumulus cloud populations. *Mon. Wea. Rev.*, **105**, 865-880.

Loranger, D. C., E. A. Smith, and T. H. Vonder Haar, 1978: Initial estimates of GATE atmospheric radiaton budgets with atmospheric heating considerations. Preprints, *3rd Conf. on Atmospheric Radiation*, Davis, CA, Amer. Meteor. Soc., 174-178.

Lukas, R., 1991: The diurnal cycle of sea surface temperatures in the western equatorial Pacific. TOGA Notes, **2**, 1-5.

Machado, L. A. T., M. Desbois, and J.-P. Duvel, 1992: Structural characteristics of deep convective systems over tropical Africa and the Atlantic Ocean. *Mon. Wea. Rev.*, **120**, 392-406.

Machado, L. A. T., J.-P. Duvel, and M. Desbois, 1993: Diurnal variations and modulation by easterly waves of the size distribution of convective cloud clusters over West Africa and the Atlantic Ocean. *Mon. Wea. Rev.*, **121**, 37-49.

Machado, L. A. T., and W. B. Rossow, 1993: Structural characteristics and radiative properties of tropical cloud clusters. *Mon. Wea. Rev.*, **121**, 3234-3260.

Madden, R. A., and P. Julian, 1972: Description of global scale circulation cells in the tropics with a 40-50 day period, *J. Atmos. Sci.*, **29**, 1109-1123.

Maddox, R. A., 1980: Mesoscale convective complexes. *Bull. Amer. Meteor. Soc.*, **61**, 1374-1387.

Malkus, J. S., 1964: Convective processes in the tropics. *Proceedings of Symposium.On Tropical Meteorology*, Rotorua, New Zealand, 247-277.

Mapes, B. E., and R. A. Houze, Jr., 1992: An integrated view of the 1987 Australian monsoon and its mesoscale convective systems. Part I: Horizontal structure. *Quart. J. Royal. Meteor. Soc.*, **118**, 927-963.

Mapes, B. E., and R. A. Houze, Jr., 1993: Cloud clusters and superclusters over the oceanic warm pool. *Mon. Wea. Rev.*, **121**, 1398-1415.

Martin, D. W., and V. E. Suomi, 1972: A satellite study of cloud clusters over the tropical North Atlantic Ocean. *Bull. Amer. Meteor. Soc.*, **53**, 135-156.

Martin, D. W., and A. J. Schreiner, 1981: Characteristics of West African and east Atlantic cloud clusters: A survey from GATE. *Mon. Wea. Rev.*, **109**, 1671-1688.

Matsumoto, S., K. Ninomiya, and T. Akiyama, 1967: Cumulus activities in relation to the mesoscale convergence field. *J. Meteor. Soc. Japan*, **45**, 292-305.

McBride, J. L., and W. M. Gray, 1978: Mass divergence in tropical weather systems. Atmos Sci. Paper No. 299, Colorado State University, 109 pp.

McBride, J. L., and W. M. Gray, 1980: Mass divergence in tropical weather systems. Paper I: Diurnal variation. Paper II: Large scale controls on convection. *Quart. J. Roy. Meteor. Soc.*, **106**, 501-538.

McClatchey, F. A: 1972: *Optical Properties of the Atmosphere* (Third Edition). Distributed by National Technical Information Service, U. S. Dept. of Commerce.

McGarry, M. M., and R. J. Reed, 1978: Diurnal variations in convective activity and precipitation during phases II and III of GATE. *Mon. Wea. Rev.*, **106**, 101-113.

Meinardus, W., 1941: Die Meteorologishchen Ergebnisse der "Meteor" Expedition 1925-1927 (Summary). *Ann d. Hydrog., Mar. Meteor.*, **69**, 37-49.

Meisner, B. N., and P. A. Arkin, 1987: Spatial and annual variations in the diurnal cycle of large-scale tropical convective cloudiness and precipitation. *Mon. Wea. Rev.*, **115**, 2009-2032.

Miller, D., and J. M. Fritsch, 1991: Mesoscale convective complexes in the western Pacific region. *Mon Wea. Rev.*, **119**, 2978-2992.

Miller, R. A., and W. M. Frank, 1993: Radiative forcing of simulated tropical cloud clusters. *Mon. Wea. Rev.*, **121**, 482-498.

Minnis, P., and E. F. Harrison, 1984: Diurnal variability of regional cloud and clear-sky radiative parameters derived from GOES data. Part II: November 1978 cloud distribution. *J. Clim. Appl. Meteor.*, **23**, 1012-1031,

Murakami, M., 1983: Analysis of deep convective activity over the western Pacific and southeast Asia. Part I: Diurnal variation. *J. Meteor. Soc. Japan*, **61**, 60-75.

Muramatsu, T., 1983: Diurnal variations of satellite-measured T_{BB} areal distribution and eye diameter of mature typhoons. *J. Meteor. Soc. Japan*, **61**, 77-90.

Nakazawa, T., 1988: Tropical superclusters within intraseasonal variations over the western Pacific. *J. Meteor. Soc. Japan*, **66**, 823-839.

Negri, A. J., R. F. Adler, and P. J. Wetzel, 1984: Rain estimation from satellites: An examination of the Griffith-Woodley technique. *J. Clim. Appl. Meteor.*, **23**, 102-116.

Nelkin, E. J., A. J. Negri, and R. F. Adler, 1996: Analysis of the diurnal rainfall cycle over the equatorial western Pacific via satellite infrared and microwave techniques. *J. Appl. Meteor.*, submitted.

Nitta, T., and S. Esbensen, 1974: Diurnal variations in the western Atlantic trades during the BOMEX. *J. Meteor. Soc. Japan*, **52**, 254-257.

Panofsky, H. A., and G. W. Brier, 1968: *Some Applications of Statistics to Meteorology*. Pennsylvania State University, University Park, PA, 224 pp.

Pedgley, D. E., 1969: Diurnal variation of the incidence of monsoon rainfall over the Sudan (Part I). *Meteor. Mag.*, **98**, 97-107.

Pedgley, D. E., 1969: Diurnal variation of the indicence of monsoon rainfall over the Sudan (Part II). *Meteor. Mag.*, **98**, 129-135.

Pedgley, D. E., 1971: Diurnal incidence of rain and thunder at Asmara and Addis Ababa, Ethiopia. *Meteor Mag.*, **100**, 66-71.

Purdom, J. F. W., 1976: Some uses of high-resolution GOES imagery in the mesoscale forecasting of convection and its behavior, *Mon. Wea. Rev.*, **104**, 1474-1483.

Ramage, C.S., 1952: Diurnal variation of summer rainfall over East China, Korea, and Japan. *J. Meteor.*, **9**, 83-86.

Ramage, C. S., 1971: *Monsoon Meteorology*. Academic Press, 295 pp.

Randall, D. A., J. A. Abeles, and T. G. Corsetti, 1985: Seasonal simulations of the planetary boundary layer and boundary-layer stratocumulus clouds with a general circulation model. *J. Atmos. Sci.*, **42**, 641-674.

Randall, D. A., Harshvardhan, and D. A. Dazlich, 1991: Diurnal variability of the hydrologic cycle in a general circulation model. *J. Atmos. Sci.*, **48**, 40-61.

Randall, D. A., K.-M. Xu, R. J. C. Somerville, and S. Iacobellis, 1996: Single-column models and cloud ensemble models as links between observations and climate models. *J. Climate*, **9**, 1683-1697.

Rao, P. K., S. J. Holmes, R. K. Anderson, J. S. Winston, and P. E. Lehr, 1990: *Weather Satellites: Systems, Data, and Environmental Applications*. AMS, Boston, 503 pp.

Rasmusson, E. M., 1971: Diurnal variation of summertime thunderstorm activity over the United States. USAF Environmental Technical Applications Center, USAFETAC TN 71-4, 13 pp.

Reed, R., and K. D. Jaffee, 1981: Diurnal variation of summer convection over West Africa and East Atlantic in 1974 and 1978. *Mon. Wea Rev.*, **109**, 1081-1093.

Reid, G. C., and K. S. Gage, 1981: On the annual variation in height of the tropical tropopause. *J. Atmos. Sci.*, **38**, 1928-1938.

Reid, G. C., K. S. Gage, and J. R. McAfee, 1989: The thermal response of the tropical atmosphere to variations in equatorial Pacific sea surface temperature. *J. Geophys. Res.*, **94**, 14705-14716.

Reinke, D. L., C. L. Combs, S. Q. Kidder, and T. H. Vonder Haar, 1992: Satellite cloud composite climatologies: A new high resolution tool in atmospheric research and forecasting. *Bull. Amer. Meteor. Soc.*, **73**, 278-285.

Reinke, D. L., T.H. Vonder Haar, K.E. Eis, 1995: Climatological and Historical ANalysis of Cloud for Environmental Simulations: Applications to Battlefield Atmospherics. Presented at the *Battlefield Atmospherics Conf.*, White Sands, NM.

Refsdal, A., 1930: Der Feuchtlabile Niederschlag. *Geofys. Publ.*, **5**, No. 12, 71 pp.

Reynolds, D. W., T. H. Vonder Haar, and S. K. Cox, 1973: The effect of solar radiation absorption in the tropical atmosphere. Atmos. Sci. Paper No. 210, 43 pp.

Reynolds, D. W., T. H. Vonder Haar, and S. K. Cox, 1975: The effect of solar radiation absorption in the tropical troposphere. *J. Appl. Meteor.*, **14**, 433-444.

Reynolds, R. W., and D. C. Marsico, 1993: An improved real-time global sea surface temperature analysis. *J. Climate*, **6**, 114-119.

Rickenbach, T. M., and S. A. Rutledge, 1996: The diurnal variation of tropical oceanic rainfall: Dependence on convective organization. *J. Atmos. Sci.*, submitted.

Richards, F., and P. Arkin, 1981: On the relationship between satellite-observed cloud cover and precipitation. *Mon. Wea. Rev.*, **109**, 1081-1093.

Riehl, H., 1947: Diurnal variation of cloudiness over the subtropical Atlantic Ocean. *Bull. Amer. Meteor. Soc.*, **28**, 37-40.

Riehl, H., 1954: *Tropical Meteorology*. McGraw-Hill, 392pp.

Riehl, H., and J. S. Malkus, 1958: On the heat balance in the equatorial trough zone. *Geophysica*, **6**, 503-538.

Riehl, H., and A. H. Miller, 1978: Differences between morning and evening temperatures of cloud tops over tropical continents and oceans. *Quart. J. Roy. Meteor. Soc.*, **104**, 757-764.

Riehl, H., and J. Simpson, 1979: The heat balance of the equatorial trough zone, revisited. Contributions to *Atmos. Physics.*, **52**, 287-304.

Roca, R., L. Picon, M. Desbois, and H. L. Treut, 1997: Direct comparison of Meteosat water vapor channel data and general circulation model results. *Geophys. Res. Letters*, **24**, 147-150.

Rogers, C. D., 1967: The radiative heat budget of the troposphere and lower stratosphere. MIT, Dept. of Meteor., Planetary Circulations Project, Report No. A2, 99 pp.

Ruprecht, E., and W. M. Gray, 1974: Analysis of satellite-observed cloud clusters. Atmos Sci. Paper No. 219, Colorado State University, 91 pp.

Ruprecht, E., and W. M. Gray, 1976: Analysis of satellite-observed tropical cloud clusters. I.Wind and dynamic fields. II. Thermal, moisture and precipitation. *Tellus*, **28**, 391-413.

Schmetz, J., and Q. Liu, 1988: Outgoing longwave radiation and its diurnal variation at regional scales derived from Meteosat. *J. Geophys. Res.*, **93**, 11192-11204.

Schiffer, R. A., and W. B. Rossow, 1983: The International Satellite Cloud Climatology Project (ISCCP): The first project of the World Climate Research Programme. *Bull. Amer. Meteor. Soc.*, **64**, 779-784.

Sellers, W. D., 1965: *Physical Climatology*. The University of Chicago Press, 272 pp.

Sharma, A. K., A. T. C. Chang, and T. T. Wilheit, 1991: Estimation of the diurnal cycle of oceanic precipitation from SSM/I data. *Mon. Wea. Rev.*, **119**, 2168-2175.

Shin, K.-S., G. R. North, Y.-S. Ahn, and P. A. Arkin, 1990: Time scales and variability of area-averaged tropical oceanic rainfall. *Mon. Wea. Rev.*, **118**, 1507-1516.

Short, D. A., and J. M. Wallace, 1980: Satellite-inferred morning-to-evening cloudiness changes. *Mon. Wea. Rev.*, **108**, 1160-1169.

Silva Dias, P. L., J. P. Bonatti, and V. E. Kousky, 1987: Diurnally forced tropical tropospheric circulation over South America. *Mon. Wea. Rev.*, **115**, 1465-1478.

Simpson, J., 1990: Global circulation and tropical cloud activity. Proceedings of the *International Symposium on Aqua and Planet*, 25-26 June, Tokai University, Tokyo, 77-90.

Slingo, A., Wilderspin, R. C., and S. J. Brentnall, 1987: Simulation of the diurnal cycle of outgoing longwave radiation with an atmospheric GCM. *Mon. Wea. Rev.*, **115**, 1451-1457.

Smith, E. A., 1980: The modulation by tropical cloud systems of the bulk radiative heat budget. Volume of extended abstracts, *International Radiation Symposium*, 11-16 Aug., Fort Collins, CO, 352-354.

Spencer, R. W., and W. D. Braswell, 1996: How dry is the tropical free troposphere? Implications for global warming theory. *Bull. Amer. Meteor. Soc.*, submitted.

Steranka, J., E. B. Rodgers and R. C. Gentry, 1984: The diurnal variation of Atlantic Ocean tropical cyclone cloud distribution inferred from geostationary satellite infrared measurements. *Mon. Wea. Rev.*, **112**, 2338-2343.

Sui, C.-H., X. Li, and K.-M. Lau, 1996: Radiative-convective processes in simulated diurnal variations of tropical oceanic convection. *J. Atmos. Sci.*, submitted.

Sui, C.-H., Y. N. Takayabu, and D. A. Short, 1997: Diurnal variations in tropical oceanic cumulus convection during TOGA COARE. *J. Atmos. Sci.*, **54**, 639-655.

Takayabu, Y. N., K.-M. Lau, and C.-H. Sui, 1996: Observation of a quasi-2-day wave during TOGA COARE. *Mon. Wea. Rev.*, **124**, 1892-1913.

Takeuchi, T., and M. Nagatani, 1974: Oceanic thunderstorms in the tropical and subtropical Pacific. *J. Meteor. Soc. Japan*, **52**, 509-511.

Tao, W.-K., S. Lang, J. Simpson, C.-H. Sui, B. Ferrier, and M.-D. Chou, 1996: Mechanisms of cloud-radiation interaction in the tropics and midlatitudes. *J. Atmos. Sci.*, **53**, 2624-2651.

Thompson, R. M., Jr., S. W. Payne, E. E. Recker and R. J. Reed, 1979: Structure and properties of synoptic-scale wave disturbances in the intertropical convergence zone of the eastern Atlantic. *J. Atmos. Sci.*, **36**, 53-72.

Tsay, S.-C., P. M. Gabriel, M. D. King, and G. L. Stephens, 1996: Spectral reflectance and atmospheric energetics in cirrus-like clouds. Part II: Applications of a Fourier-Riccati approach to radiative transfer. *J. Atmos. Sci.*, **53**, 3450-3467.

Vonder Haar, T. H., D. L. Reinke, K. E. Eis, J.L. Behunek, C.R. Chaapel, C.L. Combs, J.M. Forsythe, M.A. Ringerud, 1995: Climatological and Historical ANalysis of Clouds for Environmental Simulations (CHANCES) Database. *Final Report*. Science and Technology Corp., Hampton, VA (USAF Phillips Lab Technical Report PL-TR-95-2101), 71pp.

Waliser, D. E., and C. Gautier, 1993: A satellite-derived climatology of the ITCZ. *J. Climate*, **6**, 2162-2174.

Wallace, J. M., and F. R. Hartranft, 1969: Diurnal wind variations, surface to 30 kilometers. *Mon. Wea. Rev.*, **97**, 446-455.

Wallace, J. M., 1975: Diurnal variations in precipitation and thunderstorm frequency over the conterminous United States. *Mon. Wea. Rev*, **103**, 406-419.

Watanabe, K., 1959: Hygrokinematical analysis and it's application in weather forecasting. *J. Meteor. Soc. Japan*, **37-5**, 164-189.

Webster, P. J., and G. L. Stephens, 1980: Tropical upper-tropospheric extended clouds: Inferences from Winter MONEX. *J. Atmos. Sci.*, **37**, 1521-1541.

Webster, P. J., and R. Lukas, 1992: TOGA COARE: The coupled ocean-atmosphere response experiment. *Bull. Amer. Meteor. Soc.*, **73**, 1377-1416.

Webster, P. J., 1994: The role of hydrological processes in ocean-atmosphere interactions. *Rev. Geophys.*, **34**, 427-476.

Webster, P. J., C. A. Clayson, and J. A. Curry, 1996: Clouds, radiation, and the diurnal cycle of sea surface emperature in the tropical western Pacific. *J. Climate*, **9**, 1712-1730.

Weickmann, H. K., A. B. Long, and L. R. Hoxit, 1977: Some examples of rapidly growing oceanic cumulonimbus clouds. *Mon. Wea. Rev.*, **105**, 469-476.

Williams, K. T., and W. M. Gray, 1973: Statistical analysis of satellite-observed trade wind cloud clusters in the western north Pacific. *Tellus*, **15**, 313-334.

Williams, M., and R. A. Houze, Jr., 1987: Satellite-observed characteristics of winter monsoon cloud clusters. *Mon. Wea. Rev.*, **115**, 505-519.

Woodley, W. L., C. G. Griffith, J. S. Griffin, and S. C. Stromatt, 1980: The inference of GATE convective rainfall from SMS-1 imagery. *J. Appl. Meteor.*, **19**, 388-408.

Wong, T., and G. Stephens, 1994: On the radiative processes associated with the tropical mesoscale convection system. Dept. of Atmos. Sci. Paper No. 547, Colorado State University, 235 pp.

Wong, T., and G. Stephens, 1994: A numerical study on the interactions between tropical cloud clusters, radiation, and dynamics. Preprint volume, *Sixth Conf. on Climate Variations*, 23-28 Jan., Nashville, TN, published by AMS, Boston, MA, 307-312.

Yanai, M., S. Esbensen, J-H. Chu, 1973: Determination of bulk properties of tropical cloud clusters from large-scale heat and moisture budgets. *J. Atmos. Sci.*, **30**, 611-627.

Xu, K.-M., and D. A. Randall, 1995: Impact of interactive radiative transfer on the macroscopic behavior of cumulus ensembles. Part I: Radiation parameterization and sensitivity tests. Part II: Mechanisms for cloud-radiation interactions. *J. Atmos. Sci.*, **52**, 785-817.

Zehr, R. M., 1987: The diurnal variation of deep convective clouds and cirrus with tropical cyclones. Preprints, *17th Conf. of Hurricanes and Tropical Meteorology*, Miami, published by AMS, Boston, MA, 276-279.

Zehr, R. M., 1992: Tropical Cyclogenesis in the Western North Pacific. Ph.D. Dissertation, Colorado State University, 213 pp.

Zhang, C., 1993: Large-scale variability of atmospheric deep convection in relation to sea surface temperature in the tropics. *J. Climate*, **6**, 1898-1913.

Zisper, E. J., and C. Gautier: 1978: Mesoscale events within a GATE tropical depression, *Mon. Wea. Rev.*, **106**, 789-805.